ENGINEERING RESEARCH INSTITUTE
UNIVERSITY OF MICHIGAN
ANN ARBOR

ANALYSIS OF

DYNAMIC CHARACTERISTICS OF THE MAGNETRON SPACE CHARGE

PRELIMINARY RESULTS

Technical Report No. 5
Electron Tube Laboratory
Department of Electrical Engineering

BY

H. W. WELCH, JR.

S. RUTHBERG

H. W. BATTEN

W. PETERSON

Approved by: W. G. DOW

G. HOK

Project M762

CONTRACT NO. W-36-039 sc-35561
SIGNAL CORPS, DEPARTMENT OF THE ARMY
DEPARTMENT OF THE ARMY PROJECT NO. 399-13-022
SIGNAL CORPS PROJECT NO. 112B-0

January, 1951

ABSTRACT

The electronic space charge in the oscillating magnetron is considered with emphasis on the study of maximum-current boundary, frequency pushing, and voltage tuning. Possible causes of maximum-current boundary are enumerated. A new method for calculation of space-charge-limited current in the oscillating magnetron is presented. Transit time and cathode temperature effects are discussed semiquantitatively. General methods for calculation of the induced current due to given space-charge distributions are developed and applied to the magnetron. The results are compared with calculations of r-f current in the anode structure made from experimental measurement. Experimental and theoretical results from several sources are combined with the results from this report to present explanation of the frequency pushing and voltage tuning phenomena with approximate quantiative calculation.

ACKNOWLEDGEMENTS

The authors wish to acknowledge with thanks the assistance to development of ideas presented in this report which was obtained from discussion with the following people: Mr. W. C. Brown and Mr. Edward Dench of Raytheon Manufacturing Company, Dr. D. A. Wilbur and Mr. P. H. Peters of General Electric Research Laboratories, and Mr. J. F. Hull of Evans Signal Laboratory. Also, all of the personnel in the University of Michigan Electron Tube Laboratory were in one way or another helpful to the preparation of this report, particularly Professor W. G. Dow who made specific suggestions relative to the method for calculation of space-charge-limited current and induced r-f current. Other personnel of the laboratory are the following:

J. R. Black	Research Engineer
J. S. Needle	Instructor of Electrical Engineering
G. Hok	Research Engineer
G. R. Brewer S. Ruthberg	Research Associates
V. R. Burris	Machine Shop Foreman
R. F. Steiner J. W. Van Natter	Assembly Technicians
R. F. Denning D. L. McCormick T. G. Keith E. A. Kayser	Laboratory Machinists
N. Navarre	Draftsman
S. Spiegelman	Stenographer

TABLE OF CONTENTS

LIST OF FIGURES

MAJOR REPORTS ISSUED TO DATE

Contract No. W-36-039 sc-32245. Subject: Theoretical Study, Design and Construction of C-W Magnetrons for Frequency Modulation.

Technical Report No. 1 --

H. W. Welch, Jr. "Space-Charge Effects and Frequency Characteristics of C-W Magnetrons Relative to the Problem of Frequency Modulation", November 15, 1948.

Technical Report No. 2 --

H. W. Welch, Jr., G. R. Brewer. "Operation of Interdigital Magnetrons in the Zero-Order Mode", May 23, 1949.

Technical Report No. 3 --

H. W. Welch, Jr., J. R. Black, G. R. Brewer, G. Hok. "Final Report", May 27, 1949.

Contract No. W-36-039 sc-35561. Subject: Theoretical Study, Design and Construction of C-W Magnetrons for Frequency Modulation.

Interim Report --

H. W. Welch, Jr., J. R. Black, G. R. Brewer. December 15, 1949.

Quarterly Report No. 1 --

H. W. Welch, Jr., J. R. Black, G. R. Brewer, G. Hok. April, 1950.

Quarterly Report No. 2 --

H. W. Welch, Jr., J. R. Black, G. R. Brewer, J. S. Needle, W. Peterson. July, 1950.

Quarterly Report No. 3 --

H. W. Welch, Jr., J. R. Black, J. S. Needle, H. W. Batten G. R. Brewer, W. Peterson, S. Ruthberg. September, 1950.

Technical Report No. 4 --

H. W. Welch, Jr. "Effects of Space Charge on Frequency Characteristics of Magnetrons", Proc. IRE, 38, 1434-1449, December, 1950.

DEFINITION OF SYMBOLS

Units are in the rationalized MKS system except where noted in experimental data given in this report.

Symbol	Definition	Units
A_1	first Fourier coefficient in expansion of ψ_k for magnetron	
A_n	nth Fourier coefficient in expansion of ψ_k for magnetron	
B	magnetic field	webers/m^2
B_1	first even Fourier coefficient in expansion for spoke charge distribution in magnetron	coulombs/m^3
B_a	ath even Fourier coefficient in expansion for spoke charge distribution in magnetron	coulombs/m^3
B_n	nth even Fourier coefficient in expansion for spoke charge distribution in magnetron	coulombs/m^3
B_n	value of magnetic field for which outermost electrons are synchronous with the r-f field	webers/m^2
B_o	value of magnetic field for which electrons just reach synchronous angular velocity at the magnetron anode	webers/m^2
C	capacitance in equivalent circuit for magnetron	farads
C_a	ath odd Fourier coefficient in expansion for spoke charge density in magnetron	coulombs/m^3
C_1	first odd Fourier coefficient in expansion for spoke charge density in magnetron	coulombs/m^3
C_n	nth odd Fourier coefficient in expansion for spoke charge density in magnetron	coulombs/m^3
c-w	continuous wave	
d_{ca}	distance from cathode to anode in diode used to approximate transit time behavior in spokes	m

Symbol	Definition	Units
E	potential	volts
E_a or E_b	anode potential	volts
E_{an}	potential on magnetron anode for which outermost electrons attain synchronism	volts
E_h	Hartree potential: voltage at which magnetron space charge should be able to support oscillation	volts
E_H	Hull potential or cutoff voltage: voltage at which anode current begins in static magnetron	volts
E_n	potential at the radius for which electrons become synchronous	volts
E_o	potential which represents energy of synchronous electron at the anode	volts
E_{rf}	r-m-s radio-frequency potential at magnetron anodes	volts
E_T	r-m-s radio-frequency potential across tank circuit equivalent to magnetron resonant circuit	volts
f	frequency	cycles/sec
G_L	conductance of load transformed to magnetron anode terminals	mhos
G_T	total conductance at magnetron anode terminals	mhos
G_m	symbol used by Doehler to represent electronic conductance in the magnetron (Section 3)	mhos
I_A	Allis current in magnetron defined at radius r	amps
I_{Aa}	Allis current in magnetron defined at anode radius r_a	amps
I_{An}	Allis current in magnetron defined at synchronous radius r_n	amps
I_b	d-c anode current	amps
I_g	r-m-s current from current generator equivalent to magnetron space charge	amps

Symbol	Definition	Units
I_{La}	Langmuir current defined at the anode radius with E_H on anode	amps
I_{Ln}	Langmuir current defined at the synchronous radius	amps
I_{Lo}	Langmuir current defined at the anode radius for E_o on the anode	amps
I_m	circulating current in magnetron used by Doehler (Section 3)	amps
k	mode number in magnetron	
L	length of magnetron interaction space	m
n	N/2 = mode number for π mode; or used as summation index	
N	number of anodes in magnetron	
P_L	power delivered to the load	watts
q	charge delivered per half cycle	coulombs
Q	total charge circulating in the spokes of the magnetron space charge	coulombs
Q_e	2π x ratio of energy stored in internal circuit to energy lost in external circuit	
Q_L	2π x ratio of energy stored in internal circuit to energy lost in combined external and internal circuit	
Q_o	2π x ratio of energy stored in internal circuit to energy lost in internal circuit	
r_a	radius of magnetron anode	m
r_c	radius of magnetron cathode	m
r_n	radius of space-charge cloud in oscillating magnetron for edge in synchronism with r-f field	m
r_H	radius of space-charge cloud in static magnetron	m
R	ratio of r/r_c	
R_n	ratio of r_n/r_c	

Symbol	Definition	Units
R_m	reciprocal of G_m	ohms
R_o	position of equivalent point charge in approximation calculations of induced current in magnetron in terms of r/r_c	
S_k	surface of the kth electrode	m^2
t	time	sec
T	transit time	sec
T_c	cyclotron period $= 2\pi/\omega_c$	sec
v_a	velocity of electron at the anode of the magnetron	m/sec
Y_{oc}	characteristic admittance of resonant circuit $= \omega_o C$ or $\sqrt{C/L}$ in equivalent circuit	mhos
Y_e	$\lvert I_g/E_T \rvert$: magnitude of electronic admittance vector	mhos
Y_T	total equivalent circuit admittance	mhos
α	one-half angular width of anode segment	deg
α	ratio of space-charge-limited current of magnetic diode to that of ordinary diode (Allis current to Langmuir current)	
α_a	ratio of space-charge-limited current of magnetic diode to that of ordinary diode (Allis current to Langmuir current) defined at anode	
α_n	ratio of space-charge-limited current of magnetic diode to that of ordinary diode (Allis current to Langmuir current) defined at synchronous radius	
β	one-half angular width of space-charge spoke	deg
β	constant in Langmuir's diode equation	
β_a	Langmuir's constant evaluated at $r = r_a$	
β_n	Langmuir's constant evaluated at $r = r_n$	

Symbol	Definition	Units
δ	$(\lambda_o - \lambda)/\lambda_o$	
η	overall oscillator efficiency = $\eta_c \eta_e$	per cent
η_c	circuit efficiency	per cent
η_e	electronic efficiency	per cent
θ	angle between space-charge spoke and zero of r-f voltage wave on anode	deg
θ'	angular measure in coordinate system rotating with velocity of r-f wave	deg
θ_1	$\omega_n t$	deg
λ	wavelength of oscillation = c/f	m
λ_o	resonant wavelength of circuit	m
ρ	space-charge density	coulombs
$(\rho v)_n$	normal component of convection-current density	amps/m^2
τ	total space charge in hub of space-charge swarm	coulombs
ϕ	phase angle of current-generator output (I_g) in equivalent circuit	deg
ψ	potential function defined by Twiss relative to tangential energy parabola (Section 3)	
ψ_k	scalar potential function defined in Section 10 for use in induced-current calculation	
ω	angular velocity of electron	radians/sec
ω_c	cyclotron angular frequency (Be/m)	radians/sec
ω_f	$2\pi f$: angular frequency	radians/sec
ω_k	angular velocity synchronous with r-f wave in mode k	radians/sec
ω_L	Larmor angular frequency (Be/2m)	radians/sec
ω_n	angular velocity synchronous with r-f wave of mode number n	radians/sec
ω_o	angular frequency of resonance in circuit	radians/sec

PHYSICAL CONSTANTS AND CONVERSIONS

Symbol	Definition
c	velocity of radiation in free space = 2.99×10^{8} m/sec
e	electronic charge = 1.6×10^{-20} e.m.u.
	= 1.6×10^{-19} coulombs
m	electronic mass = 9.1×10^{-31} kg
e/m	specific charge of electron = 1.759×10^{7} e.m.u./g
	= 1.759×10^{11} coulombs/kg
ϵ_o	dielectric constant of free space = $\frac{1}{36\pi} \times 10^{-9}$ farads/m

$$1 \text{ weber/m}^2 = 10^4 \text{ gauss}$$

ANALYSIS OF

DYNAMIC CHARACTERISTICS OF THE MAGNETRON SPACE CHARGE

PRELIMINARY RESULTS

1. Purpose of Study (H. W. Welch, Jr.)

The purpose of this report is to present the results of an analysis of space-charge behavior in the oscillating magnetron. This analysis has been carried on in the University of Michigan Electron Tube Laboratory during the past year and, although not complete, the results of the analysis are sufficiently conclusive to merit discussion at this time. The analysis is based on concepts introduced in earlier reports on the magnetron space charge which have been issued by this laboratory.[1,2*]

These reports and other treatments of the subject** have dealt primarily with space charge in the static magnetron. The picture of the space charge resulting from the analysis of the static magnetron can be extended by hypothesis to give a mechanistic picture of the space charge in the oscillating magnetron, which has been generally accepted as correct, at least in general form. This is the picture (given in Fig. 4.1) of a hub of relatively dense space charge surrounding the cathode with a number of spokes extending to the anode. These spokes are considered the mechanism which excites r-f currents in the anodes which are attached to a resonant circuit.

---

* Numbered footnotes refer to the Bibliography.

** Other treatments will be discussed in Section 3 and are listed in the Bibliography.

In Technical Report No. 1 issued by this laboratory a method was given for calculation of the radius for which hub-boundary electrons are synchronous and of the space-charge density in the spokes. The space charge in the spokes is called the synchronous space charge, while the space charge in the subsynchronous swarm or hub is called the static magnetron space charge.

The purpose of the analysis and experimental investigations which are presented in the following pages can now be stated. It is assumed that the hub boundary and synchronous-space-charge density are calculable by the use of relationships just mentioned and that the behavior within the hub is approximately that to be expected from the theory of the static magnetron. With these assumptions and the other concepts associated with the mechanistic picture of the space-charge swarm given in Fig. 4.1, our purpose is to develop methods for calculation of operating characteristics associated with magnetron behavior. These include primarily frequency pushing, maximum-current boundary, electronic efficiency, starting voltage, and slope of the volt-ampere characteristic. All these factors in the operating magnetron are definitely related to the load through the r-f current and r-f voltage. It is this relationship, in particular, which is interesting for reasons mentioned in the next section.

The emphasis in this discussion is on the study of frequency pushing and maximum-current boundary. The results are quite promising in that they can be used to make quantitative predictions of magnetron behavior. Approximate methods for calculating electronic efficiency and starting voltage are well known. At this time only qualitative suggestions of the form of a more exact treatment can be made. No satisfactory method for calculation of slope of the volt-ampere characteristic (i.e., d-c operating currents

and voltages) has been developed. Knowledge of the relationship of this slope to magnetron r-f performance would be useful, since the experimental data are easily obtained.

The quantity of information in existence, both theoretical and experimental, which pertains to the problem at hand is quite extensive. Much of this information, however, is not useful, or it is inadequate because of the omission of important details. A brief survey of the work which has been done is given in Section 3 of this report. The next few sections are devoted to the development of hypotheses which furnish a description of space-charge behavior. The remainder of the report contains development of relationships, based on the hypothesis, which furnish quantitative results to be compared with the available experimental results.

Results of the various treatments of static magnetron space-charge behavior are used without much discussion of how the results were obtained. On the other hand, the relationships involved in the induced-current calculations are presented in some detail in order to make clear certain points in the theory which are of particular importance in the case of the magnetron. Also, the method of induced-current calculation as developed here is a little more generally applicable than other treatments of the subject.

2. Low-Q Operation of Magnetrons; Voltage Tuning (H. W. Welch, Jr.)

The need for the analysis presented in the following pages has been emphasized by the desirability of achieving operation of the magnetron under very heavily loaded conditions. The fact that this is possible in the 500 to 1000-mc range was demonstrated in the General Electric Laboratories by W. H. Wilbur and P. H. Peters.[6] Typical data are shown in

Figs. 8.1 and 8.2. The desirable feature of this type of operation is that extremely large frequency deviations can be produced by changing the anode voltage. The deviation may be obtained at relatively constant power level so that the prospects of frequency modulation by this method are good. In order to design for this particular type of operation at microwave frequencies, it was felt necessary to have an improved understanding of the magnetron behavior under the special conditions imposed. As the lumped-constant circuits usable below 1000 mc gradually must be replaced by distributed-constant circuits at about 2000 mc, it becomes increasingly difficult to have the resonant circuit outside the vacuum envelope. It thus becomes more difficult to make adjustments in loading conditions and, consequently, more essential to predict the magnetron behavior before assembly.

The most apparent features of the operation obtained at General Electric are the following:

a) The Q_L is undoubtedly very low. Although no direct measurements of Q are available, it is probable that Q_L's of the order of 10 or less are being used.

b) The voltage-tuning phenomenon is similar to the usually observed frequency pushing, but is much more pronounced because of the low Q_L.

c) The low current dropout usually experienced when a magnetron is loaded heavily is conspicuously absent.

d) The temperature of the cathode must be limited to achieve satisfactory operation. This requires use of a tungsten cathode giving a definite emission boundary. This limitation of emission seems to be intimately related to the maximum-current boundary and a required criterion for obtaining oscillation.

e) Efficiency is reduced as band width is increased. This must be due to decreased electronic efficiency, since circuit efficiency is obviously high.

f) Loading is accomplished right at the tube anode terminals (i.e., almost directly across the capacitive portion of the resonant circuit). Loads farther from the tube may cause trouble with the long-line effect.

As is suggested in d) and e) above, an understanding of frequency pushing and maximum-current boundary is particularly needed. Conventional microwave magnetrons usually give trouble with current dropout when the Q is reduced below 50. The effect of temperature, which seems to be important, is not at all clear and, although it is discussed briefly and qualitatively in the following pages, it still remains a point in question which will require additional study.

Although the ideas presented in this report are generally applicable to an understanding of magnetron behavior, the emphasis in the discussion will be on aspects particularly necessary to the understanding of low-Q operation or voltage tuning.

3. Survey of Recent Developments Pertinent to the Study of Magnetron Space-Charge Behavior (H. W. Welch, Jr.)

The available literature on analysis of magnetron characteristics is rather extensive. However, the essentials of the theory as developed prior to 1946 are covered in Chapter 13 of Microwave Electronics by Slater[7] and the papers by Brillouin[14,15,16] and Page and Adams[12,13]. The three papers by Brillouin which are mentioned arrive at answers of the same general nature as the work of Allis, Hartree, and Stoner (which is discussed in Slater's book). They are interesting because the method of approach makes possible a more straightforward solution. Brillouin also demonstrates the importance of using the plane magnetron solution as an approximation of of the large-cathode cylindrical magnetron. The approach used by Brillouin is essentially that used by Llewellyn in which the anode voltage is found as a function of the assumed current. This method proves to be much simpler than the inverse problem. Analytical solutions are obtained, whereas the work of Allis, Hartree, and Stoner involved numerical integration.

Brillouin divides magnetrons into three types:

I. Plane Magnetrons

II. Cylindrical Magnetrons $r_a/r_c \lesssim 2$

III. Cylindrical Magnetrons $r_a/r_c \gtrsim 2$

where r_a/r_c = the ratio of anode radius to cathode radius. Actually, the difference in the static characteristics of magnetrons in Class I and those of magnetrons in Class II is so small that it can be neglected for all practical purposes. Two different types of solution are found below the cutoff voltage. These are: a double-stream solution, for which electrons are steadily flowing to and from the cathode, and a single-stream solution, for which all electrons are moving parallel to the cathode surface. A useful fact to have in mind is that the electron energy corresponding to the potential distribution in the single-stream solution (the Hull parabola) exists approximately in all solutions. This might be called the "tangential energy" since it corresponds to energy of motion of the electrons tangential to the cathode surface. It represents a condition of balance between the Lorentz force of the magnetic field and the force of the electric field existing between cathode and anode. The additional centrifugal force which exists in the cylindrical magnetron is insignificant. The "radial energy", representing kinetic energy flow of electron to and from the cathode, is always small compared to the tangential energy in a magnetron near or below cutoff.

Slater suggests that other solutions exist for which there are many swarms or layers of electrons, one within the other running parallel to the cathode. Within each swarm or layer there is a double-stream solution. The current which streams in and out is greatest in the single-swarm

double-stream solution. The type of solution which will exist is not determinate from the initial conditions as used by Slater. However, it has been shown by Allis, Brillouin, and others that for $r_a/r_c \lesssim 2$, the double-stream solution cannot exist.

In a very recent study of the problem by Twiss[10] it is pointed out that these difficulties are removed when initial velocities of the electrons at the cathode are considered. Twiss defines cutoff as the anode voltage below which electron flow is everywhere double-stream. This new definition is necessary because, when a statistical distribution of initial velocities is assumed, there are always some electrons with enough energy to reach the anode. Twiss measured potential relative to the tangential energy parabola. This potential is called ψ in his notation.* Thus, if ψ is everywhere zero, the potential distribution is the single-stream distribution. For the double-stream solution radial energy exists in addition to the tangential energy; therefore ψ must be greater than zero. If there exists a minimum in ψ between cathode and anode, all electrons which pass the minimum will reach the anode. Between the minimum and the cathode, by Twiss' definition, a double-stream solution exists. If the value of ψ at the anode is less than the minimum value between cathode and anode, then a double-stream solution will exist everywhere and cutoff is defined. The value of cutoff defined in this way is usually less than one per cent different from the usual definition.

The significant result to be emphasized in this discussion is the behavior of the Twiss solution when the initial velocity or absolute

---

* ψ is actually a potential divided by kT, where k is the Boltzmann constant and T is the cathode temperature in °K.

temperature is required to go to zero. As is pointed out by Twiss, the ambiguity is removed from the Slater solution since:

a) When initial velocities are assumed entirely normal to the cathode surface, and cathode absolute temperature is allowed to go to zero, the limiting solution is the Brillouin steady-state solution.

b) When initial velocities are assumed entirely tangential to the cathode surface, and cathode absolute temperature is allowed to go to zero, the limiting solution is the Slater double-stream solution.

Two other points which are important to the present discussion are made in the Twiss paper. They are the following:

c) Multiple-layer, double-stream solutions are possible, but only in a very small range of voltages near cutoff (of the order of one to three per cent of anode potential).

d) The solution is no longer restricted to single-stream for $r_a/r_c \lesssim 2$.

Twiss also assumes that:

e) In order that a swarm distribution be maintained, the total outward moving current must be supplied from the cathode. The inward moving, returning electrons are not used twice but, of course, may give rise to secondaries.

This last statement implies that rather large cathode emission is required to maintain any swarm, since the double-stream flow is usually much greater than the anode current. If emission is not sufficient, some very different swarm distribution may exist. This possibility will be discussed briefly in Sections 8 and 9.

Most of the work just discussed relates particularly to theory of the static magnetron. It is, however, important as a basis for theory of the dynamic magnetron. It cannot be overemphasized that the static magnetron potential distribution in any solution differs very little from the Hull or tangential energy distribution and that the <u>total</u> electronic

space charge within a static swarm is essentially unchanged by the nature of the solution.

Theories of the dynamic magnetron are not so plentiful and are less conclusive than static magnetron theories. Most magnetron design has been carried out by means of dimensional scaling from working models. This technique has been discussed thoroughly by Slater and others.[7,8,9] It is possible to design a magnetron for normal operation, using the Hartree relationship for the starting voltage,

$$\frac{E_a}{E_o} = 2\frac{B}{B_o} - 1 , \qquad (3.1)^*$$

the relationship for maximum electronic efficiency,

$$\eta = 1 - \frac{E_o}{E_a} , \qquad (3.2)$$

and limitations imposed by requirements of power output, cathode emission, and heat dissipation. It is not possible, however, to design for "abnormal" operation where, for example, unusual currents, frequency ranges, or loading may be used. The problem of abnormally heavy loading is the chief concern of this report, although the theory presented is not restricted to use in this case.

A good summarizing treatment of dynamic magnetron characteristics has been presented by Doehler.[3,4] Part I of this series of articles[3] is devoted primarily to static characteristics, while Part II[4] is primarily a discussion of dynamic characteristics. The third part of the articles[5]

---

* See the Definition of Symbols, pages vi-x.

is less general, being primarily a discussion of a magnetron amplifier. Some of the material in Part II of these articles is better covered by Fiske, Hagstrum, and Hartman[9] and was probably extracted from their work. However, the treatment by Doehler is more complete in certain respects which are to be emphasized in this report. Therefore, it will be discussed here in some detail.

Doehler makes a distinction between two types of oscillation in the magnetron. These are the following:

f) Electronic oscillations are those oscillations sustained by the natural frequencies of the electron motion in their double-stream orbits. These oscillations do not require a multianode structure, since they are primarily due to radial motion in the electron swarm. If the electric field is neglected, the frequency of this oscillation is

$$\omega = B\frac{e}{m} . \qquad (3.3)$$

When the electric field is taken into account,

$$\omega \cong \frac{Be}{m}\left(1 - \frac{2E_a}{r_a^2(e/m)B^2}\right) . \qquad (3.4)$$

g) Resonance oscillations are those oscillations sustained by synchronism of the angular velocity of the rotating swarm as a whole with a particular characteristic angular velocity of the electromagnetic wave around a multianode system. These are the usually observed magnetron oscillations and the primary concern of this report.

Brillouin discusses a third type of oscillation which arises from the negative resistance in the static characteristic.

h) Negative resistance oscillations* are those oscillations sustained near cutoff in a magnetron by portions of the static characteristic having negative slope.

Fig. 3.1a shows a static characteristic for a plane one-anode magnetron. The negative resistance branches occur between P_1 and Q_2, P_2

---

* Oscillations supported by negative resistance between segments of a split-anode magnetron have been discussed by G. R. Kilgore, Proc.I.R.E. 24, 1140 (1936).

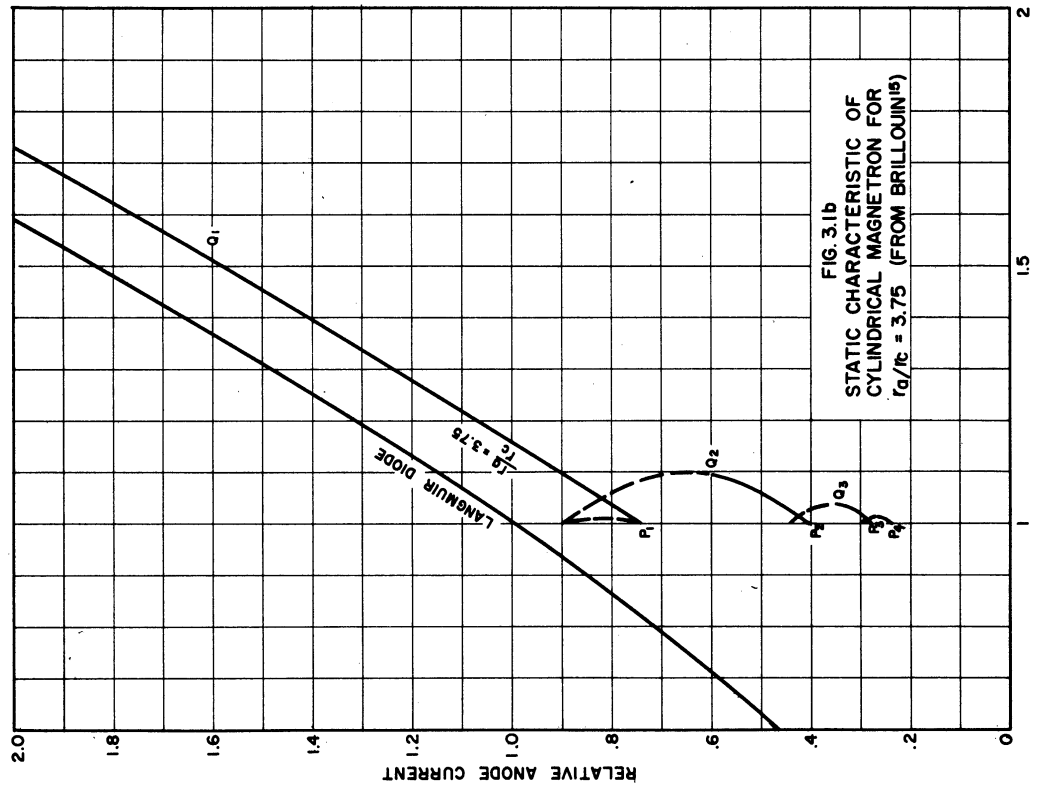

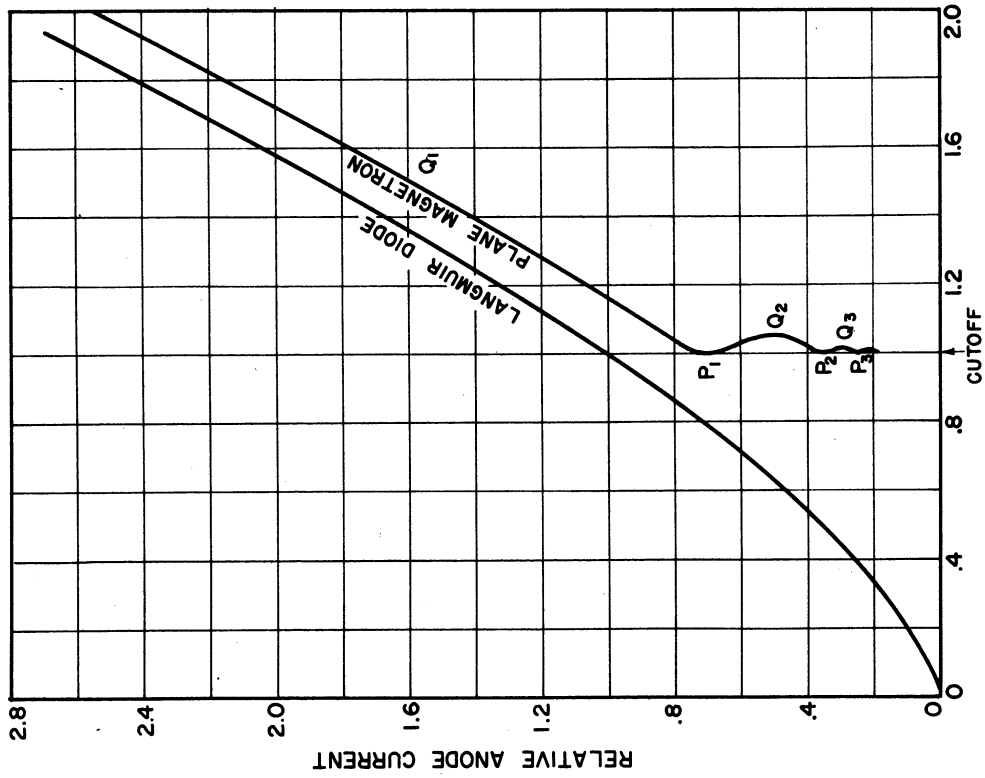

FIG. 3.1a STATIC CHARACTERISTIC OF PLANE MAGNETRON (FROM BRILLOUIN[15])

and Q_3, and P_3 and Q_4. Fig. 3.1b shows a similar curve for a cylindrical magnetron with r_a/r_c of 3.75. The curve is similar to the plane magnetron curve in form, but Brillouin shows by calculation of the trajectories that the branches P_1 and Q_2, P_2 and Q_3, and P_3 and Q_4 have no physical meaning for $r_a/r_c \gtrsim 2$. For $r_a/r_c \lesssim 2$ the static curve is hardly distinguishable from the curve for the plane magnetron. Probably the most important point to be made in the present discussion is that negative-resistance oscillations occur only in the immediate vicinity of the cutoff field and bear no immediate relationship to the synchronous resonance (g above).

Doehler identifies the electronic oscillations with what he calls inverted cyclotron operation. In this type of operation the balance of forces is between the Lorentz force and the centrifugal force, the electric field force being negligible. This gives the cyclotron resonance of Eq 3.3. Eq 3.4 is a first-order correction of the frequency when the radial field is taken into account.

In the conventional magnetron geometry, oscillation of this type could be produced by injecting a beam of electrons parallel to the anode and cathode surfaces and perpendicular to the magnetic field. The injection velocity would have to be that determined by the balance between the Lorentz and centrifugal forces; otherwise the electron would proceed at once to the anode or the cathode. In a multianode magnetron, the frequency of the mode excited would be the frequency of Eq 3.3 or 3.4 multiplied by a mode number, k, which depends on the properties of the anode structure and the resonant circuit. The cyclotron resonance can be observed in the conventional magnetron.[2] Eq 3.4 has been confirmed, according to Doehler,

by Gutton and Ortusi.* A recent paper by Mourier** describes a travelling wave tube based on this principle.

Doehler distinguishes resonance oscillations of synchronism from electronic oscillations by stating that the force balance in the case of resonance oscillations is primarily between the electric field force and the Lorentz force rather than between the centrifugal force and the Lorentz force. The important basis for this distinction is in the difference in the phase focussing of the electrons in the two types of operation when r-f fields exist in the magnetron. This difference may be illustrated by reference to Fig. 3.2. In the case of electronic oscillations, an electron present at point A, where the field is radially accelerating to an electron, is retarded in the tangential direction (Eq 3.4), whereas an electron at point B, where the field is radially decelerating, is accelerated in the tangential direction. The electrons tend to focus at point C in a region of acceleration or in an unfavorable phase for transfer of energy. Also, electrons in a region of tangential acceleration tend to move outward into a stronger field region because of the increased centrifugal force, while electrons in a tangentially decelerating region tend to move inward, where fields are weaker. Thus, the electrons in the decelerating region, which are in a favorable phase for transfer of energy, are moved to a region where the energy transfer takes place least efficiently.

On the other hand, if the balance is between the electric force and the Lorentz force, as it is in resonance oscillations, the angular

---

* H. Gutton and J. Ortusi, Conference de la Societé des Électriciens francais, January, 1947.

** G. Mourier, "L'Anticyclotron, un nouveau type de tube á propagation d'ondes, á champ magnetique", Annales de Radioélectricité, tome V, no.21, July, 1950.

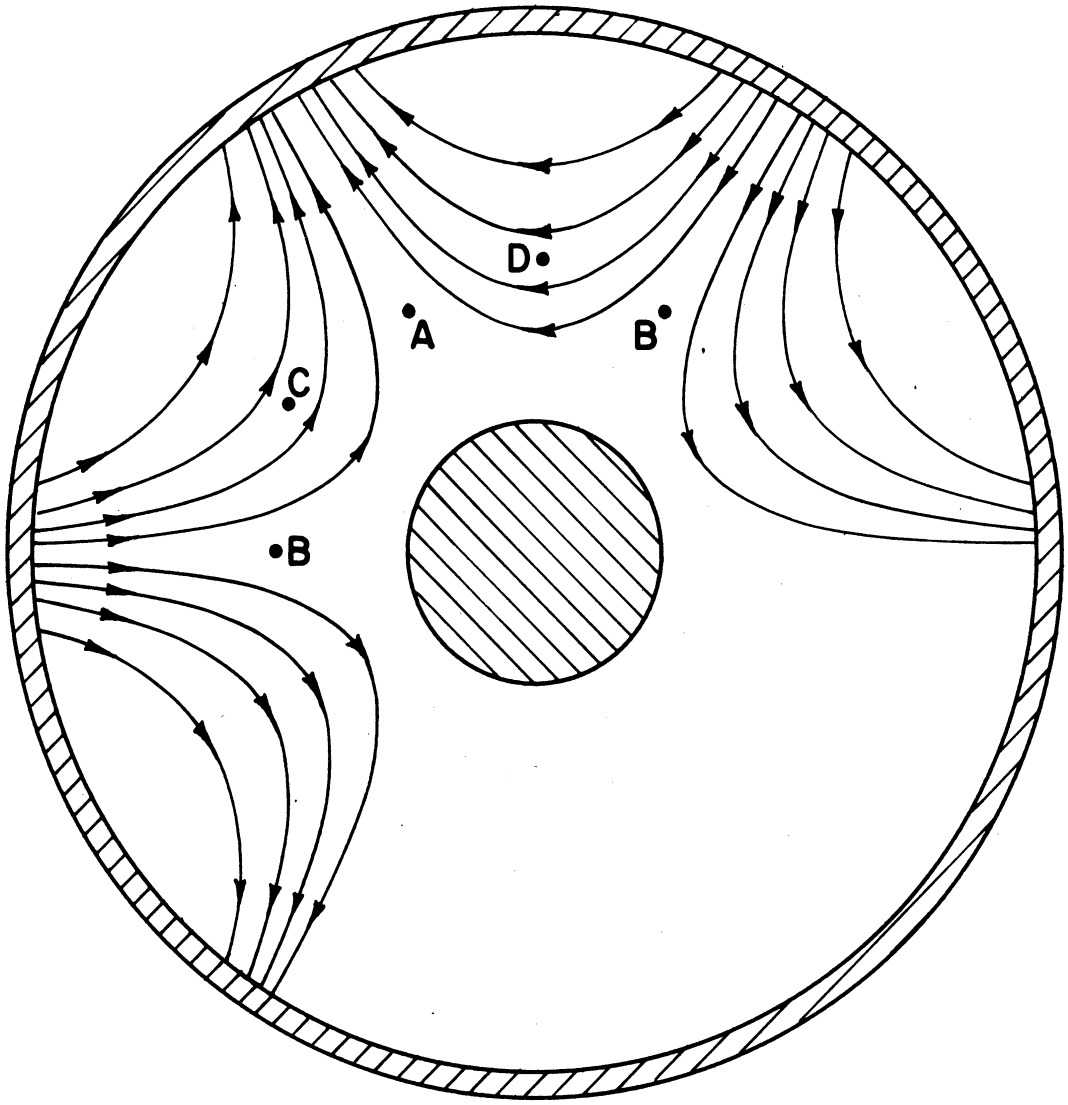

FIG. 3.2

EFFECT OF PHASE FOCUSSING FOR SYNCHRONOUS RESONANCE OSCILLATION (focussing at D) AND ELECTRONIC OSCILLATION (focussing at C)

ARROWS REPRESENT DIRECTION OF FORCE ON ELECTRON

DRIFT MOTION OF THE ELECTRONS IS IN CLOCKWISE DIRECTION

FROM DOEHLER[4]

velocity of the electrons is increased by a strengthened electric field. Thus an electron at point A is accelerated in the tangential direction and an electron at point B is retarded. There is, therefore, a phase focussing at point D which is a favorable phase for the transfer of energy. Electrons which are slowed down in the tangential direction move outward due to the decrease of the Lorentz force relative to the electric field force. Conversely, electrons which are accelerated move inward. Thus, working electrons move into the stronger field region and nonworking electron move into a weaker field region, as is desired.

This discussion forms the basis for both qualitative and quantitative ideas of the space charge in the operating magnetron. Doehler obtains a relationship for starting voltage similar to Eq 3.1 and a relationship for electron efficiency identical with Eq 3.2. Both these equations depend on the idea of synchronism of the electrons with the travelling wave of the r-f field at the anode. Doehler places considerable emphasis on the importance of a correction factor $F(r_c/r_a)$ by which the right-hand side of Eq 3.1 is multiplied in his treatment. Several calculations of starting voltage (or "optimum" voltage, as he calls it), using his corrected formula, are made on the tubes listed in the article by Fiske, Hagstrum, and Hartman in the Bell System Technical Journal (25, 1946). Based on a comparison of these calculations with the experimental values, Doehler draws the conclusion that multianode magnetrons usually do not oscillate in the π mode. This conclusion does not seem to be justified without further evidence. The evidence of recent work in this country at Raytheon and MIT*, where modes are being carefully identified in multivane tubes, and at

---

* Privately communicated by Mr. W. C. Brown of Raytheon and Mr. R. R. Moats of MIT.

Michigan, where the zero-order mode in interdigital magnetrons is being studied,* is contrary to Doehler's conclusions. The latter example is particularly interesting because this mode does not have the complex mode spectrum that can exist in the vane tubes, so that less ambiguity is possible.

Doehler also compares the formula for efficiency, Eq 3.2, with the experimental result of the article by Fiske, Hagstrum, and Hartman. This formula represents the maximum efficiency, since it does not account for the losses due to radial velocities of electrons at the anode, which can be quite high in pulsed magnetrons, or losses due to back heating of the cathode. Thus, the calculated efficiency generally is higher than the observed efficiency.

By an approximate method Doehler arrives at a formula for the electronic impedance in a magnetron with small gaps between anodes and a small cathode. It is assumed that in the radial plane which passes through a gap the potential undergoes a discontinuity given by $2\Delta E_a(r/r_a)^2$ and that everywhere else the potential does not depend on the radius. He also assumes that the total circulating current density I_m is given by the total value resulting from static considerations. But, since the electrons are only found in the negative phase of the alternating field, the current density must be doubled in this phase to give the required total current. Thus, the current density as a function of time is given by the graph of Fig. 3.3.

---

* H. W. Welch, Jr., G. R. Brewer, Operation of Interdigital Magnetrons in the Zero-Order Mode, Technical Report No. 2, University of Michigan Electron Laboratory, May, 1949.

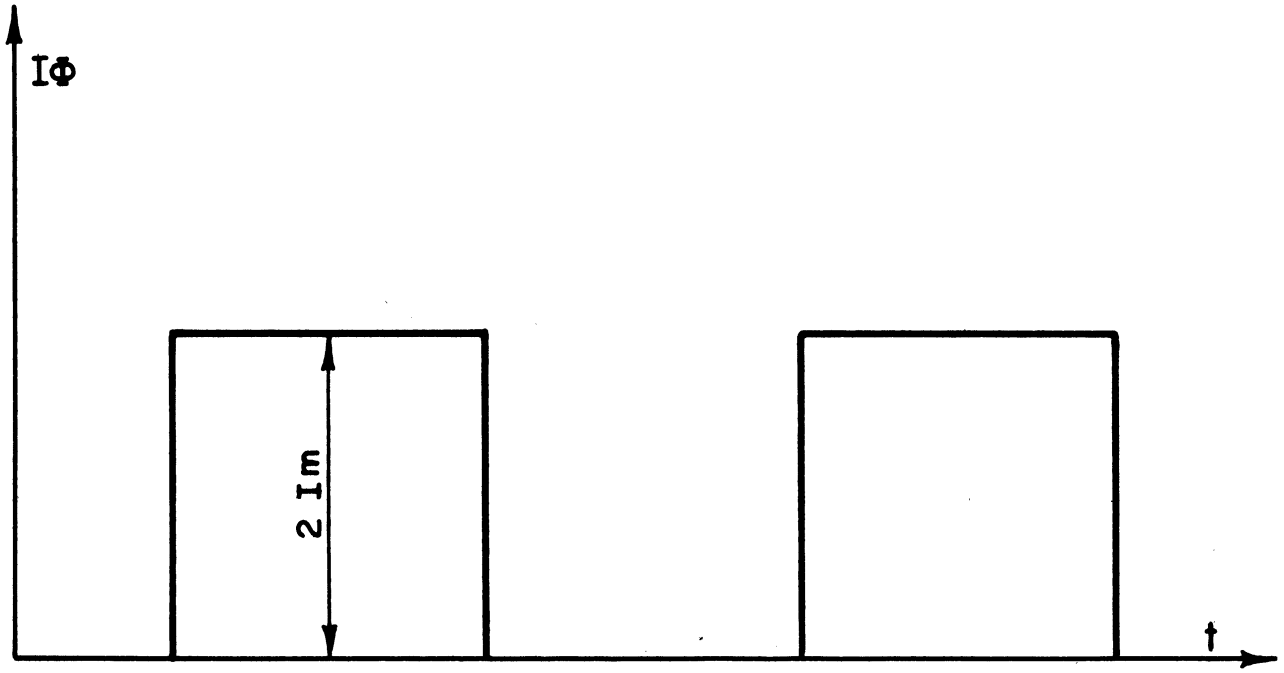

FIG. 3.3

MAGNETRON CIRCULATING CURRENT AS A FUNCTION OF TIME. (FROM DOEHLER[4])

Doehler's method for calculation of the circulating current is based on the semi-empirical conclusion that the electron density is constant for B $\gtrsim$ 1.2 to 1.5 B_{cutoff}, and that the distribution of constant space charge is valid for any r_a/r_c. For a magnetron with small cathode, this gives, from Poisson's equation,

$$\rho = \frac{4\epsilon_o}{r_a^2} E_a \quad . \tag{3.5}$$

The total circulating current is

$$I_m = \int_{r_c}^{r_a} \rho \omega r \, dr \quad . \tag{3.6}$$

With these two fundamental relationships and the assumptions mentioned above, the following value for the negative resistance of the electrons is obtained by Doehler:

$$R_m = \frac{1}{G_m} = -\frac{\pi}{2} \frac{\Delta E_a}{\omega_f E_a \epsilon_o L} \tag{3.7}$$

ω_f = $k \cdot \omega$ = angular frequency of oscillation .

The assumption of constant space-charge density and the force-balance condition between electric field force and Lorentz force give

$$\omega = \frac{2E_a}{r_a^2 B} \quad . \tag{3.8}$$

Therefore we have

$$G_m \sim \frac{1}{\Delta E_a} \sim \frac{1}{E_{rf}} \tag{3.9}$$

and

$$G_m \sim \frac{1}{B} . \qquad (3.10)$$

These proportionalities are checked by measurements of Jaenke and Harvey which are reproduced in Fig. 3.4 from Doehler's paper.

Jaenke has also studied experimentally the admittance of a 4-slot magnetron not in resonance by making hot impedance tests. His results support the discussion which will be presented in the following pages. These measurements are reproduced in Fig. 3.5. It is notable that almost the complete circle of resonance is covered, including both inductive and capacitive branches and that the conductance is always negative. The difference of the experimental curves from circles is easily explained, since the circles would represent constant current magnitude. This must not be the case, since the focussing forces which form the spokes of space charge are changing as the frequency is changed.

The impedance with large cathode has not yet been calculated, although it is hoped that this calculation will result from an extension of the work which follows in this report.

A large quantity of experimental work, which has not been completely interpreted, has resulted from post-1945 magnetron research. Some of this has been made available to the University of Michigan Laboratory Staff and will be mentioned in the following pages as it is used.

4. Basic Physical Picture of the Space-Charge Behavior (H. W. Welch, Jr.)

As has been stated in Section 1, the method of analysis which is used in this report is based on a hypothetical mechanistic picture of the space charge in the oscillating magnetron. The effect of the assumed

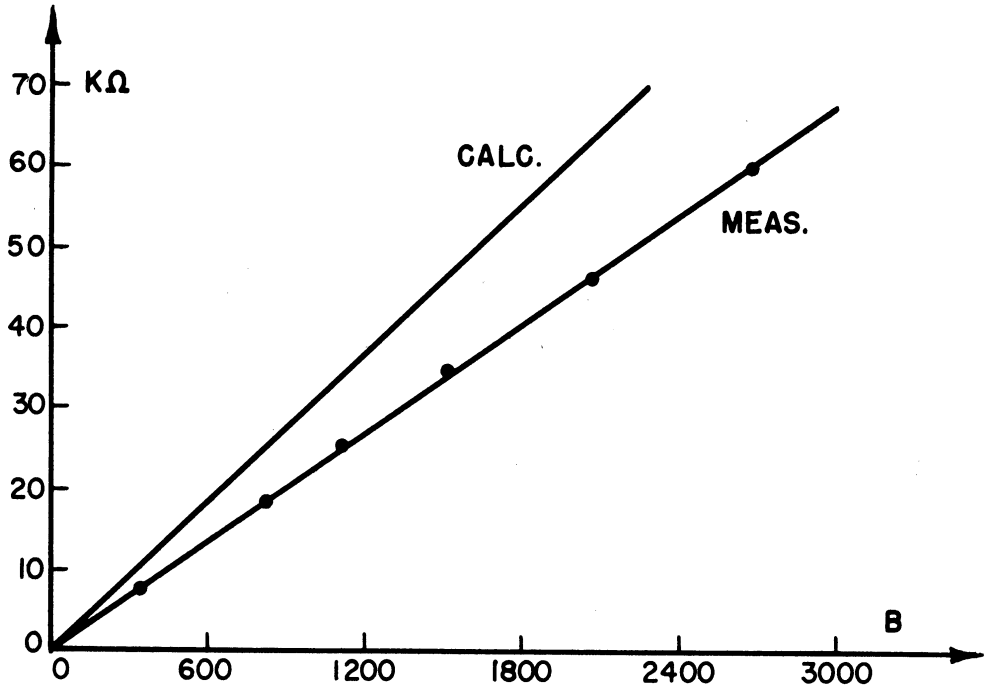

FIG. 3.4a

IMPEDANCE OF THE MAGNETRON AS A FUNCTION OF B. (MEASURED BY HARVEY, FROM DOEHLER[4])

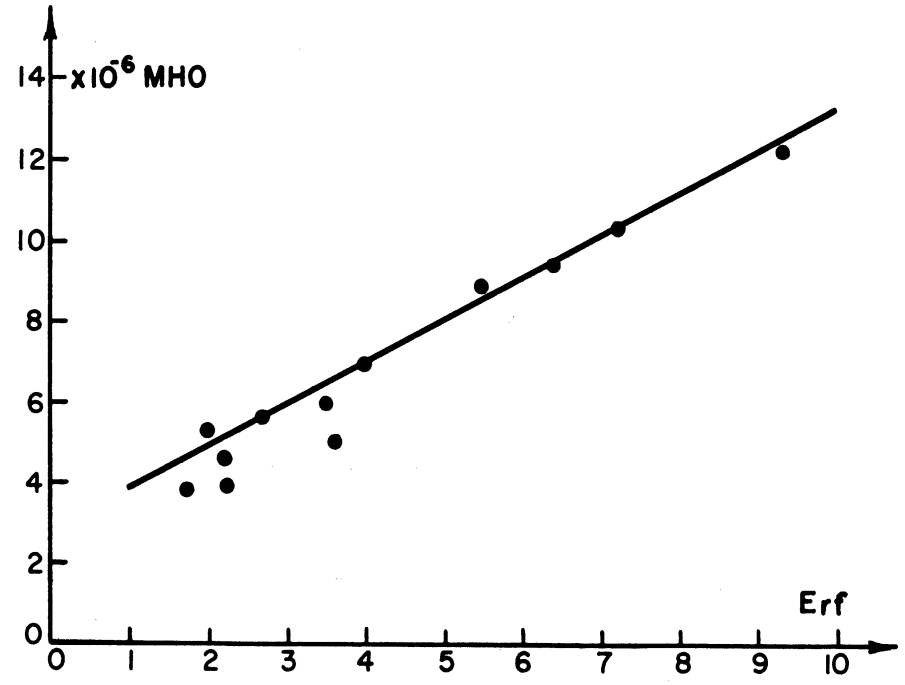

FIG. 3.4b

ADMITTANCE OF A MAGNETRON AS A FUNCTION OF R-F AMPLITUDE. (MEASURED BY JÄNKE, FROM DOEHLER[4])

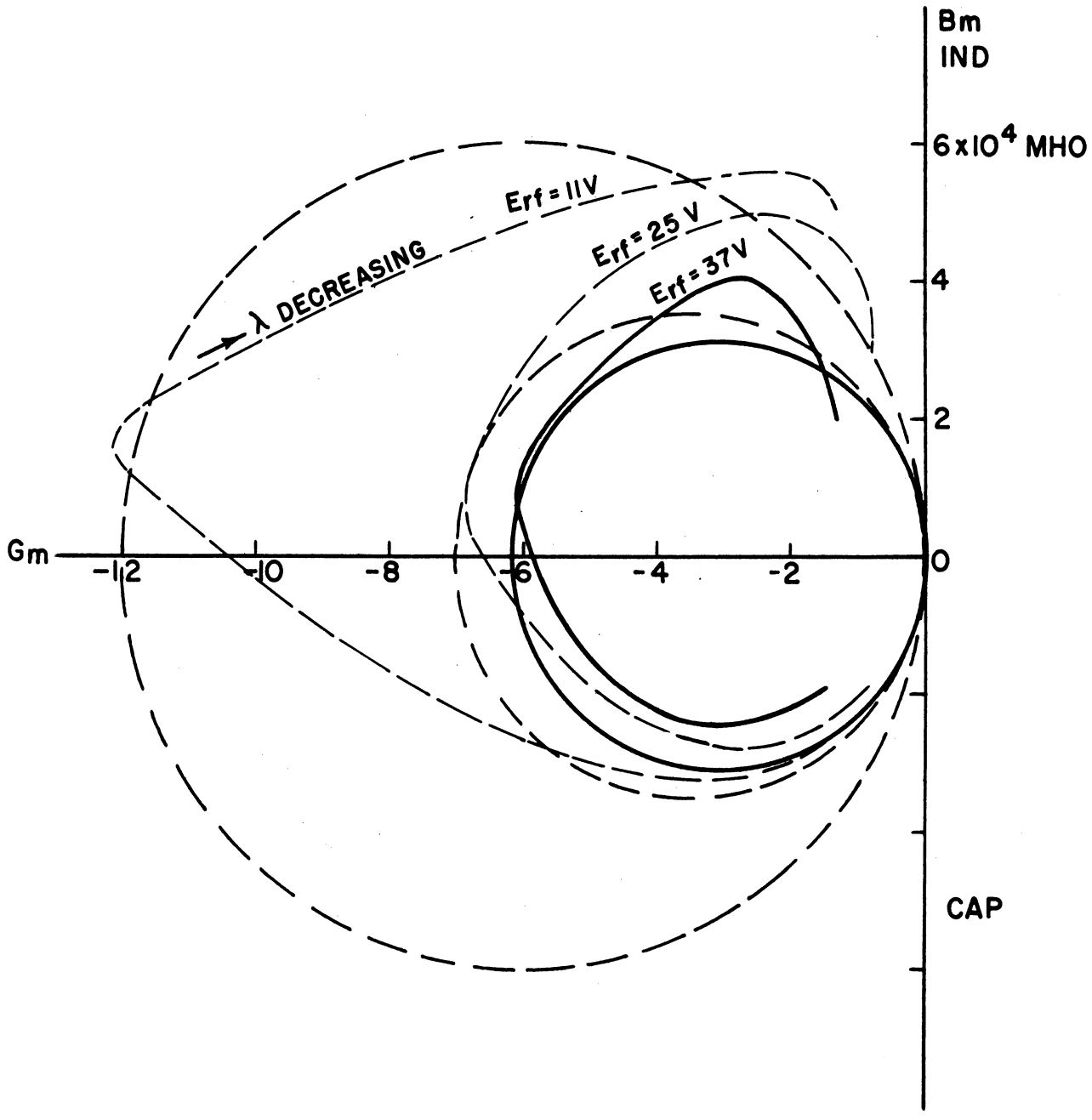

FIG. 3.5
ADMITTANCE OF A 4 SLOT MAGNETRON (MEASURED BY JÄNKE, FROM DOEHLER[4])

configuration on the external circuit is calculable by methods described in the following pages. Experimental observations indicate the accuracy of the assumed configuration. If by successive corrections of the mechanistic picture it becomes possible to predict accurately results for an arbitrary (within limits) magnetron geometry, then the picture is sufficiently accurate from an engineering point of view. This procedure is always necessary in problems involving space charge and self-excited oscillation (the method of self-consistent field calculation, for example). The methods described in this report are an attempt to bypass involved calculations of the behavior of individual electrons by assuming the complete space-charge picture at the outset.

Fig. 4.1 shows the general form of the space-charge distribution which is assumed on the basis of the previously developed theories and concepts. This picture is different from the one used by Doehler in the assumed existence of the subsynchronous swarm. The angular velocity of the electrons in the subsynchronous swarm is the following function of radius:

$$\omega = \frac{Be}{2m}\left(1 - \frac{r_c^2}{r^2}\right) \quad . \qquad (4.1)^*$$

Between the synchronous radius and the anode the angular velocity is a constant:

$$\omega_n = \frac{2\pi f}{n} \quad , \qquad (4.2)$$

where n is the mode number.

We will usually consider the π mode, in which case,

---

* Ref. 1, page 28.

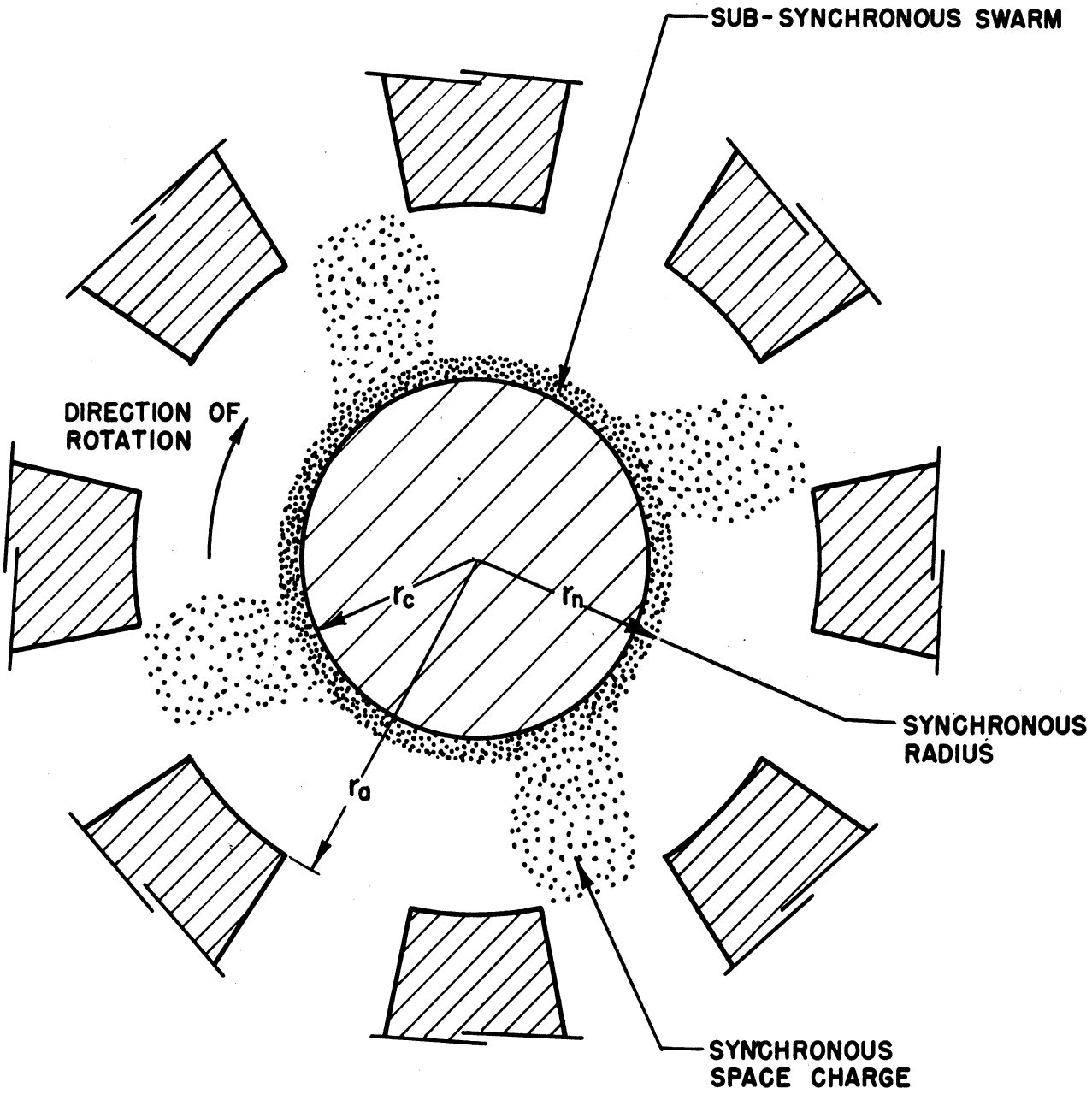

FIG. 4.1

BASIC PHYSICAL PICTURE OF THE MAGNETRON SPACE CHARGE DESCRIBED IN SECTION 4

$$n = \frac{N}{2} = \text{one-half the total number of anode sectors.}^{*}$$

The radius of the subsynchronous swarm at the boundary of which $\omega = \omega_n$ is determined by the magnetic field or the anode potential by either of the following relationships:

$$\frac{Bn}{B_o} = \frac{1 - r_c^2/r_a^2}{1 - r_c^2/r_n^2} \qquad (4.3)^{**}$$

$$\frac{E_{an}}{E_o} = \frac{r_n^2}{r_a^2}\left[2\,\frac{1 + r_c^2/r_n^2}{1 - r_c^2/r_n^2}\,\ln\frac{r_a}{r_n} + 1\right]. \qquad (4.4)^{**}$$

In the derivation of 4.4 it is assumed that the total space charge within the subsynchronous swarm is given by

$$\tau = -\pi\epsilon_o\,\frac{B^2e}{2m}\,r_n^2\left(1 - \frac{r_c^4}{r_n^4}\right). \qquad (4.5)^{***}$$

Eq 4.5 in turn depends on the gradient of the potential at r_n being correctly given by the gradient of the tangential energy, or Hull, parabola. This will be nearly the case, even if initial velocities and current crossing the subsynchronous swarm boundary are considered.

The potential at the edge of the swarm is given by the following:

$$\frac{E_n}{E_o} = \frac{r_n^2}{r_a^2} \qquad (4.6)^{****}$$

---

* An excellent discussion of the mode number (usual symbol, k) is given in Ref. 9, pages 182 to 192.

** Ref. 1, pages 36 and 37.

*** Ref. 1, page 32.

**** Ref. 1, page 38.

if we assume that radial velocities are small compared to angular velocities at the boundary.

If it is assumed that all space charge outside the synchronous radius is moving in synchronism, it is implied that an r-f field is present to slow the electrons to synchronism. The synchronous space charge will form into spokes, the exact phase and shape of which, relative to the r-f field configuration, are yet to be determined. The shape of the spokes shown in Fig. 4.1 is arbitrary. Discussion of various possibilities of phasing and shape, and their relative usefulness in predicting results, will be given in Sections 5, 11, 12, 13, and 14.

The average density of the space charge in the spoked region remains to be given. The following relationship is used in this report:

$$\rho = -2\epsilon_o \frac{m}{e} \omega_n(\omega_c - \omega_n) \quad . \qquad (4.7)^*$$

This density is a constant independent of radius, as was deduced by Doehler[3,4] by a semi-empirical method. The value is not quite the same, since the inner boundary of the constant density is assumed to be the subsynchronous swarm rather than the cathode. This imposes different boundary conditions on the field and potential than those used in Doehler's development. Also, in order to compare with Doehler's value, it is necessary to assume the Hartree voltage on the anode.

5. Frequency Pushing (H. W. Welch, Jr.)

The phenomenon of frequency pushing can be discussed in terms of two sets of fundamental concepts, one involving an approximate picture of

---

* Ref. 1, page 40.

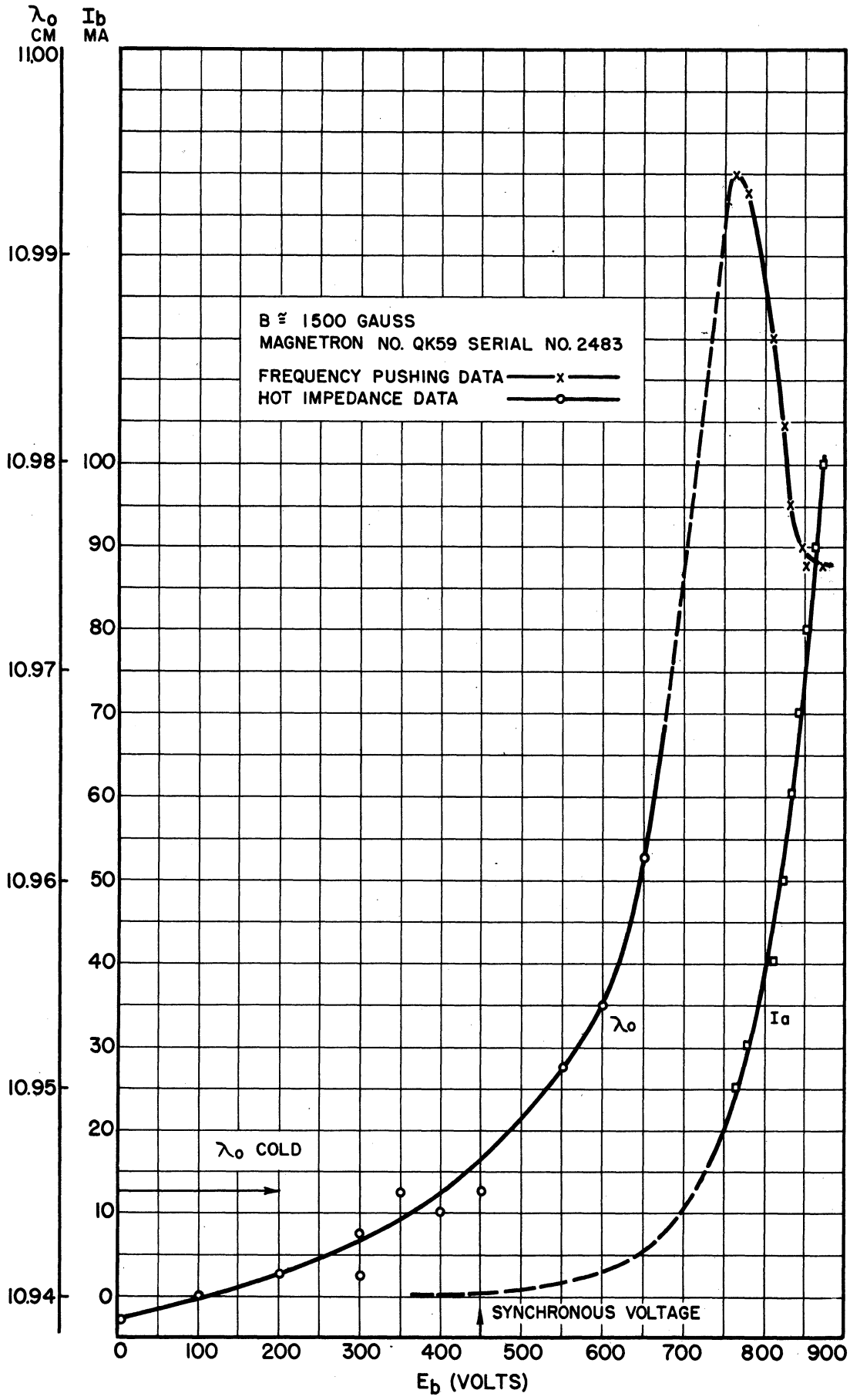

FIG. 5.1

CHANGE OF MAGNETRON RESONANT WAVELENGTH WITH PLATE VOLTAGE

COMPARISON OF FREQUENCY PUSHING AND HOT IMPEDANCE TEST RESULTS

the magnetron space charge, and the other involving the equivalent circuit of the magnetron. The space-charge behavior will be discussed in this section. In Section 13, after the introduction of some concepts which make possible an estimate of magnitudes of the induced r-f current in the magnetron, an equivalent circuit will be introduced which is useful in relating space-charge swarm properties to the generated power output and frequency. In Fig. 5.1 a set of data is reproduced from Technical Report No. 1 which illustrates nicely the effects to be described. These data are the result of hot-impedance measurements carried continuously into pushing measurements on a QK-59 magnetron. In the hot-impedance measurements resonant wavelength is measured by feeding in an external signal and by making the usual standing-wave-ratio and position-of-minimum measurements to determine resonance. When oscillation starts, pushing is measured as the oscillatory wavelength as a function of plate voltage instead of plate current (which is, however, also measured) in order that comparison with the hot-impedance test may be made on the same scale.

These data may be interpreted in the following manner, with reference to the conceptual picture of the space charge in Fig. 5.2. As anode voltage is increased from zero, the resonant wavelength increases slowly because of the increase in capacitance caused by the increase in diameter of the dense hub. The electrons in this hub are proceeding around the cathode at subsynchronous angular velocities; i.e., the angular velocity of the boundary space-charge swarm is less than the angular velocity of the travelling electromagnetic wave arising from the impressed radio frequency which goes around the interaction space in the same direction as the rotating swarm. At about 450 volts, these two velocities become synchronous, and

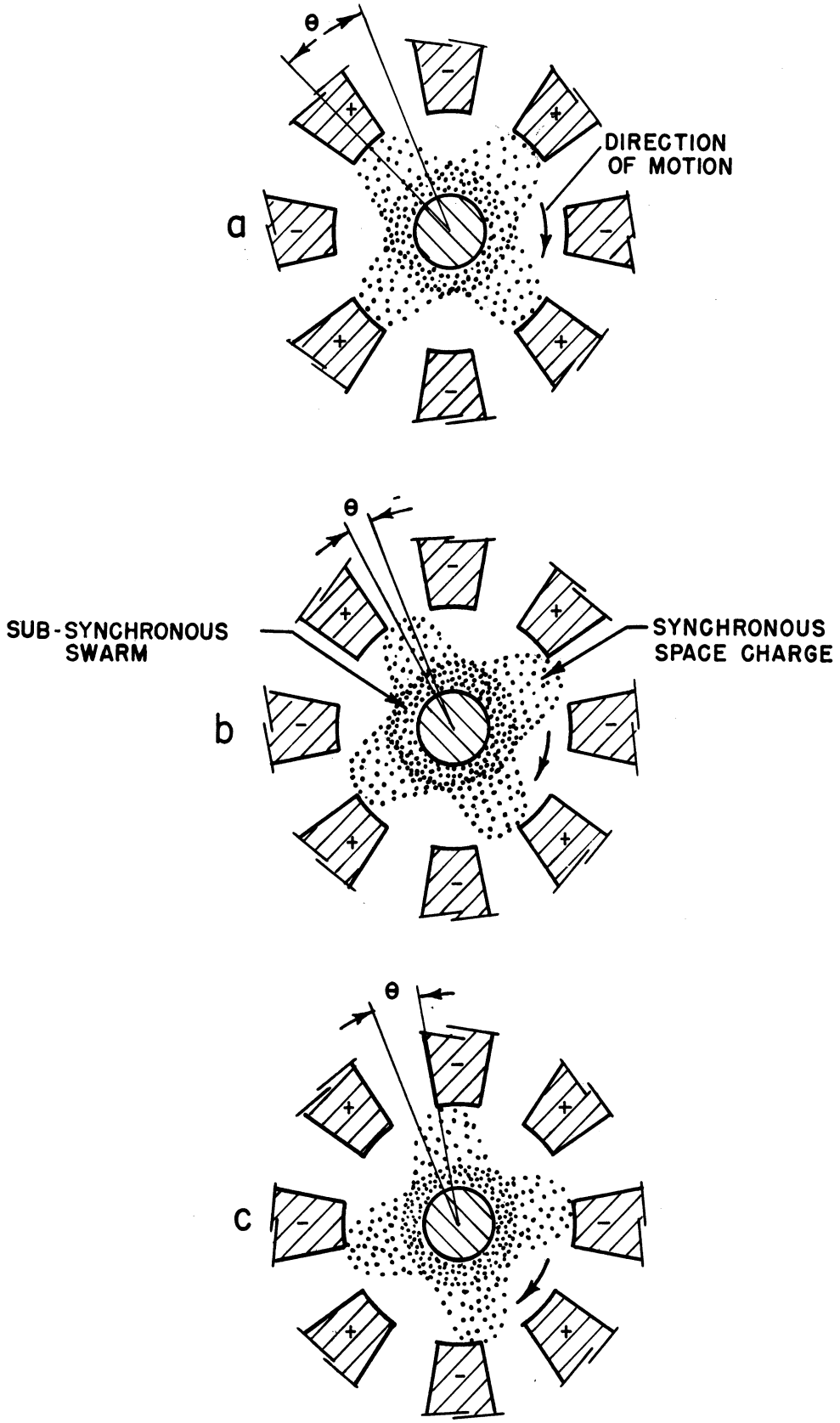

FIG. 5.2
PICTORIAL REPRESENTATION OF SPACE CHARGE WITHIN INTERACTION SPACE AT AN INSTANT WHEN ANODES ARE AT A MAX. POTENTIAL DIFFERENCE IN THE π MODE

above 450 volts, the electrons would normally be going faster than synchronism. However, if the impressed r-f signal is strong enough, which is apparently the case, the normally faster-than-synchronous electrons will be slowed to synchronism, forming a synchronous swarm of space charge. The synchronous space-charge swarm will form in spokes, because electrons will be slowed down only in regions of retarding field and thus drift outward and back to a position of equilibrium in the positive potential region of the travelling wave.* In regions of accelerating field the electrons will be speeded up and sent back toward the cathode by the Lorentz force. As anode voltage is raised, the spoke will grow outward, still maintaining the same phase relationship with the wave, provided no power is continuously transferred by the space-charge swarm to the r-f field. At approximately the Hartree voltage the space-charge spoke will just reach out to the anode. The effect of the presence of the spoke is to cause an induced current to appear in the anodes. The magnitude of this current will be discussed in Sections 10, 11, and 12. The maximum value of the fundamental component of this current leads the maximum positive potential by 90 degrees if the spoke is in the position shown in Fig. 5.2A. This follows from the observation that when a spoke passes under an anode at maximum positive potential, the current changes from positive to negative. Thus, the expanding spoke should increase the effective capacitance of the system, since it contributes a leading current.

The extension of the spoke occurs more rapidly with voltage than the expansion of the cloud, which accounts for the relatively rapid increase of the resonant wavelength after the synchronous voltage is reached (see

---

* Note: There is no continuous delivery of energy at the point.

Fig. 5.1). Also, the fact that the effect is capacitive is not dependent on the density of the space charge but on the position at which the spoke is formed. The effect of the hub, as has been pointed out in previous reports,[1,2] may be either to increase or to decrease the resonant wavelength, depending on the density of the space charge. Curves illustrating this point were given in Technical Report No. 4 and more extensively in Quarterly Report No. 1, on this contract.

As soon as the spoke reaches out to the anode, there can be a transport of electrons through the spokes and consequently a net delivery of power from the spokes to the r-f field. It will thus be necessary for the current induced by the rotating spoke to have a component in phase with the r-f voltage. Since output power is in general increased by raising the anode voltage, the electrons in the spoke will tend to speed up relative to the motion of the swarm so that the spoke will tend to advance in phase. This is indicated in Fig. 5.2b. The angle θ between the spoke and the position of maximum r-f field is now smaller, an appreciable current exists in phase with the r-f voltage, and power is delivered. The capacitive effect of the spokes is decreased, and the resonant wavelength is changing back toward the cold resonant frequency of the tank circuit (corresponding to E_a = 825 volts in Fig. 5.1). As the angle θ goes to zero, the space-charge swarm will deliver maximum power, since the electrons are moving in the maximum decelerating field. The resonant frequency will then be the resonant frequency of the tank circuit, since the current is in phase with the r-f voltage. If the anode voltage is increased beyond this point, the spoke will still tend to speed up and the angle θ will become negative. Power delivery will fall off and the resonant wavelength will be below the cold

resonant wavelength of the tank circuit. This position of the spoke is indicated in Fig. 5.2c. According to Wilbur,[6] this type of behavior has been noticed on the G.E. magnetrons (see Fig. 8.6 of this report). That is, the frequency is pushed through the cold resonant frequency of the tank circuit, and power output goes through a maximum.* The measurements of Jaenke, which were reproduced in Section 3, also indicate that both capacitive and inductive reactance are possible.

The above speculation involving behavior of the space-charge swarm intimates that the observed effects are caused by the shifting in phase of the space-charge spokes relative to the r-f voltage maximum. In other words, the configuration and density of the spoke remains constant and is independent of the magnitude of the r-f voltage. This is conceivable, though it is probably not so. However, if it is not quite so, the qualitative description of the behavior just given will still hold, with modification. The modifications which must be introduced are of four types, change of shape of the spokes, change of space-charge density, effect of induced current from radial motion, or change of phase angle by the effect of the collection current. The change in form of the spokes will change the magnitude of the current to the space-charge swarm and thus its value relative to the capacitive current in the circuit. It will be shown in Section 12 that this effect is not particularly important on an order-of-magnitude basis. The induced current is directly proportional to space-charge density for a given spoke geometry. The correct value of space-charge density is still a point in question. Radial velocities in

---

* Note that the condition for $\theta = 0$ may not be quite the cold resonant frequency of the magnetron due to effects of the hub of space charge and temperature effects.

most c-w magnetrons are easily shown to be much smaller than the tangential velocities, so this correction is not likely to be important. The effect of collection current, on the other hand, should be a first-order correction since, as will be shown in Section 13, the d-c current is of the same order of magnitude as the r-f current. If the spoke mechanism is assumed, it is quite obvious that collected current is a maximum when a spoke is opposite an anode segment, whereas the induced current is maximum when the spoke is between two anode segments. The phase difference between the two currents would, therefore, be approximately 90 degrees. The deviation from 90 degrees might be considerable if, for example, most of the current were collected on the leading edge of the anode segment.

A more quantitative treatment of the phenomena discussed in this section will be introduced in Sections 11 to 14.

6. Maximum-Current Boundary — General (H. W. Welch, Jr.)

There are several factors which are known to be involved in the determination of maximum-current boundary for magnetrons. In the problem of obtaining operation at very low Q's, the maximum-current boundary is apt to be the limiting factor. Therefore, it seemed advisable to study in some detail the underlying causes of the maximum-current boundary in c-w magnetrons in order to find the proper way to design them without this limitation.

The initial study has been carried on with the intent that a general understanding of the factors involved will be obtained, after which each factor will be studied until it is understood well enough to be subject to control. Discussions with engineers from other laboratories, particularly Mr. Edward Dench and Mr. W. C. Brown of Raytheon, have been

extremely helpful. Extensive experimental data on maximum-current boundary were provided by Mr. Dench. As a result of this initial study, the following five factors are suggested as being particularly important in determination of maximum-current boundary in c-w magnetrons.

a). Cathode limitation of available current. This is usually a thermionic emission limitation but may be made more complex by enhanced emission such as that observed by Mr. Jepson of Columbia Radiation Laboratory.[17]

b). Space-charge limitation of available current. This is the current which, assuming no saturation at the cathode, may be passed through the space-charge swarm in the magnetron as determined by the voltage at the edge of the swarm.

c). Transit-time limitation of current through the spokes. In order to supply the conduction current necessary to supply power to the system, a certain number of electrons must be collected during each cycle of operation. This requires that the average radial velocity have a certain minimum value, dependent on the average space-charge density in the spokes. If the minimum radial velocity reaches the value roughly determined by the radial length of the spoke divided by the minimum time of transit through the spoke, the conduction current will be a maximum. Further increase in voltage will then be expected to cause current drop-out.

d). Induced-current limitation placed by the maximum possible density and extent of space charge in the spokes. This is actually not a maximum-current boundary but a maximum-power boundary. However, it is possible that as the maximum-power boundary is reached something would

happen to the focussing action of the fields in the spokes to cause current dropout.

e). Mode competition, causing current dropout in one mode when another mode is more favorable to the magnetron oscillation.

f). Debunching due to insufficient focussing action by the r-f field as the spoke changes in position and the current increases.

Power-supply regulation is also a factor in determining current dropout; it has been considered in some detail by Raytheon engineers (Mr. E. Dench and Mr. W. C. Brown have supplied information on this point). This was not considered in the study at Michigan, since it is more of a circuit problem than a tube problem.

The method of control of two of the above factors is immediately obvious. Cathode limitation of current can be rectified by provision of adequate emission, and mode competition can be eliminated by provision of adequate mode separation. The question which arises is how much is adequate. According to Mr. Brown of Raytheon, experience indicates that a voltage mode separation of greater than 17 per cent is sufficient. This separation depends on loading, however, and should be investigated further.* The problem of the cathode is also not completely obvious, since it is frequently experimentally observed in c-w magnetrons that, when the measured diode emission is from three to six times the average current drawn by the magnetron, the temperature begins to have an effect on the maximum-current boundary.

---

* Mr. R. R. Moats of MIT has recently completed a doctoral thesis on this subject. The results are to be presented at the National I.R.E. Convention in March, 1951.

The space-charge limitation, transit-time limitation, and induced-current limitation are all considered in some detail in the following sections. No detailed discussion of the debunching phenomenon is offered, although we feel sure that it may cause trouble in some magnetrons. This should be true especially under heavily-loaded conditions when large currents are demanded, and thus an understanding would be helpful in the determination of optimum design for low-Q operation. In particular, it would be expected that a defocussing effect would occur when the spoke has advanced to the position of 5.2c, where the current is lagging the voltage. The resonant frequency has passed through the tank-circuit frequency, and, if the spoke continues to advance in phase as power input is increased, power output must decrease unless the very large out-of-phase inductive current is allowed. The focussing action of the fields which was discussed briefly in Section 3 does not act in favor of this result, so it is expected that the magnetron will either stop operating or jump to another, more favorable, mode. This action was suggested to the author by Gunnar Hok in 1945.*

The action just described has been discussed by Moats,[18] who attributes to this cause maximum-current boundary in a conventional magnetron (similar to the one used in obtaining the data of Fig. 5.1). This is doubtful and could be checked by careful measurement of the magnetron resonant frequency coincident with oscillatory measurements (such as those shown in Fig. 5.1). Moats apparently did not make such a measurement and assumed in his work that the magnetron started oscillating at the resonant

---

* See Very High Frequency Techniques, McGraw-Hill Book Company, New York, 1947, Chapter 21 by Gunnar Hok, p. 508.

frequency (thus, the spoke in position of 5.2b) and, as power increased, was carried by pushing to a higher frequency. This is not in agreement with experience, since a normally operating magnetron always operates at frequencies below the tank resonant frequency.* The low-Q operation described by Wilbur[6] is, according to him, one of the exceptions to this rule. In this case the Q is so low that a measurement of tank resonant frequency is not easily accomplished by any of the usual methods. In order to obtain operation at all the filament temperature must be reduced. (A tungsten cathode is used.) This indicates an effect of temperature other than the effect of current limitation.

Some of the experimental observations and theoretical possibilities relative to the temperature-limited behavior are treated in Section 8 after the discussion of space-charge-limited current which appears in the next section.

7. Space-Charge-Limited Current in the Oscillating Magnetron (H. W. Welch, Jr., and W. Peterson)

Measurements at the MIT Radiation Laboratory led Slater[7] and others to suggest the empirical space-charge-limitation current of half the Allis current in the oscillating magnetron. The Allis current is the space-charge-limited current at the cutoff voltage in the static magnetron. The following analysis results in a method for theoretical calculation of the space-charge-limited current in an oscillating magnetron.

---

* Care must be taken to measure this frequency while the magnetron is hot. The ideal data are a complete set of the type shown in Fig. 5.1. A number of such measurements are included in the data supplied by Raytheon.

The physical assumptions are based on the picture of the space-charge swarm presented in Fig. 4.1. It is assumed that the radius of the hub of the space-charge swarm is that radius at which the electrons first reach angular velocities synchronous with the electromagnetic wave travelling around the interaction space. The following relationship, giving the synchronous radius determined by the magnetic field, was introduced in Section 4:

$$\frac{B}{B_o} = \frac{1 - r_c^2/r_a^2}{1 - r_c^2/r_n^2} \quad . \tag{7.1}$$

Also, it was stated that, under certain simplifying assumptions, the potential at the edge of the swarm is given by the following

$$\frac{E_n}{E_o} = \frac{r_n^2}{r_a^2} \quad . \tag{7.2}$$

In these equations

r_n = radius of swarm where electrons reach synchronism with r-f field

E_n = potential at edge of synchronous swarm corresponding to the energy of the electron attributable to angular velocity.

It is convenient to use as a reference the space-charge-limited current as derived by Langmuir for a nonmagnetic diode. This current is defined as follows for E_o on the anode.

$$I_{Lo} = 2\pi\,(2.331)\,\frac{L}{r_a}\,\frac{E_o^{3/2}}{\beta_a^2} \quad , \tag{7.3}$$

where

β_a = a function of the ratio r_a/r_c defined by Langmuir.*

---

* W. G. Dow, Engineering Electronics, Wiley, New York, 1937: see page 535 for table of values for β^2.

If we define further

E_H = voltage corresponding to the energy of an electron just reaching the anode under static conditions (Hull voltage)

I_{La} = Langmuir current with E_H applied,

we have the following relationships for the static magnetron:

$$\frac{I_{La}}{I_{Lo}} = \left(\frac{E_H}{E_o}\right)^{3/2} , \tag{7.4}$$

and the cutoff equation defining E_H is

$$E_H = \frac{B^2 e}{8m} r_a^2 \left(1 - \frac{r_c^2}{r_a^2}\right)^2 ,$$

which may be written

$$\frac{E_H}{E_o} = \left(\frac{B}{B_o}\right)^2 . \tag{7.5}$$

With the assumption that the potential corresponding to the energy of radial motion of the electrons is very small compared to E_n, so that we may use Eq 7.2, we may write the following:

$$\frac{I_{Ln}}{I_{Lo}} = \left(\frac{E_n}{E_o}\right)^{3/2} \frac{r_a}{r_n} \frac{\beta_a^2}{\beta_n^2} \tag{7.6}$$

$$\beta_a^2 = \beta^2 \left(\frac{r_a}{r_c}\right)$$

$$\beta_n^2 = \beta^2 \left(\frac{r_n}{r_c}\right) .$$

I_{Ln} is the Langmuir current in a diode with anode at r_n and voltage E_n applied. In order to relate these currents to the magnetron, the Langmuir current must be related to the space-charge-limited current for a magnetic

diode. This has been shown by Allis,[7] Page and Adams,[12] and Brillouin,[14,15] with general agreement, to have a value given by

$$I_A = \alpha I_L \ , \tag{7.7}$$

where α is a function of r/r_c, shown in Fig. 7.1. Note that α has the value of 0.72 for a plane magnetron and 0.86 for a cylindrical magnetron with infinitely small cathode. For conventionally used values of r_a/r_c in the magnetron, $\alpha = 0.71$. The space-charge-limited current for the magnetic diode defined by 7.7 is usually called the Allis current.

It becomes apparent that the current we wish to define is given by

$$I_{An} = \alpha_n I_{Ln} \ , \tag{7.8}$$

where I_{An} is the maximum space-charge-limited current which can be drawn through the hub of the rotating space-charge wheel in the oscillating magnetron, and I_{Ln} is given by Eq 7.7. I_{Ln}/I_{Lo} may be conveniently plotted using the two following parametric equations derived from Eqs 7.1, 7.2, and 7.6:

$$\frac{I_{Ln}}{I_{Lo}} = \frac{r_n^2}{r_a^2}\frac{\beta_a^2}{\beta_n^2} = \frac{(r_n/r_c)^2\beta_a^2}{(r_a/r_c)^2\beta_n^2} \tag{7.9}$$

$$\left(\frac{B}{B_o}\right)^2 = \left(\frac{1 - r_c^2/r_a^2}{1 - r_c^2/r_n^2}\right)^2 \ . \tag{7.10}$$

In Fig. 7.2, I_{Ln}/I_{Lo} is plotted as a function of $(B/B_o)^2$ for various values of r_a/r_c.

In the oscillating magnetron the operating voltage is approximately given by the Hartree relationship

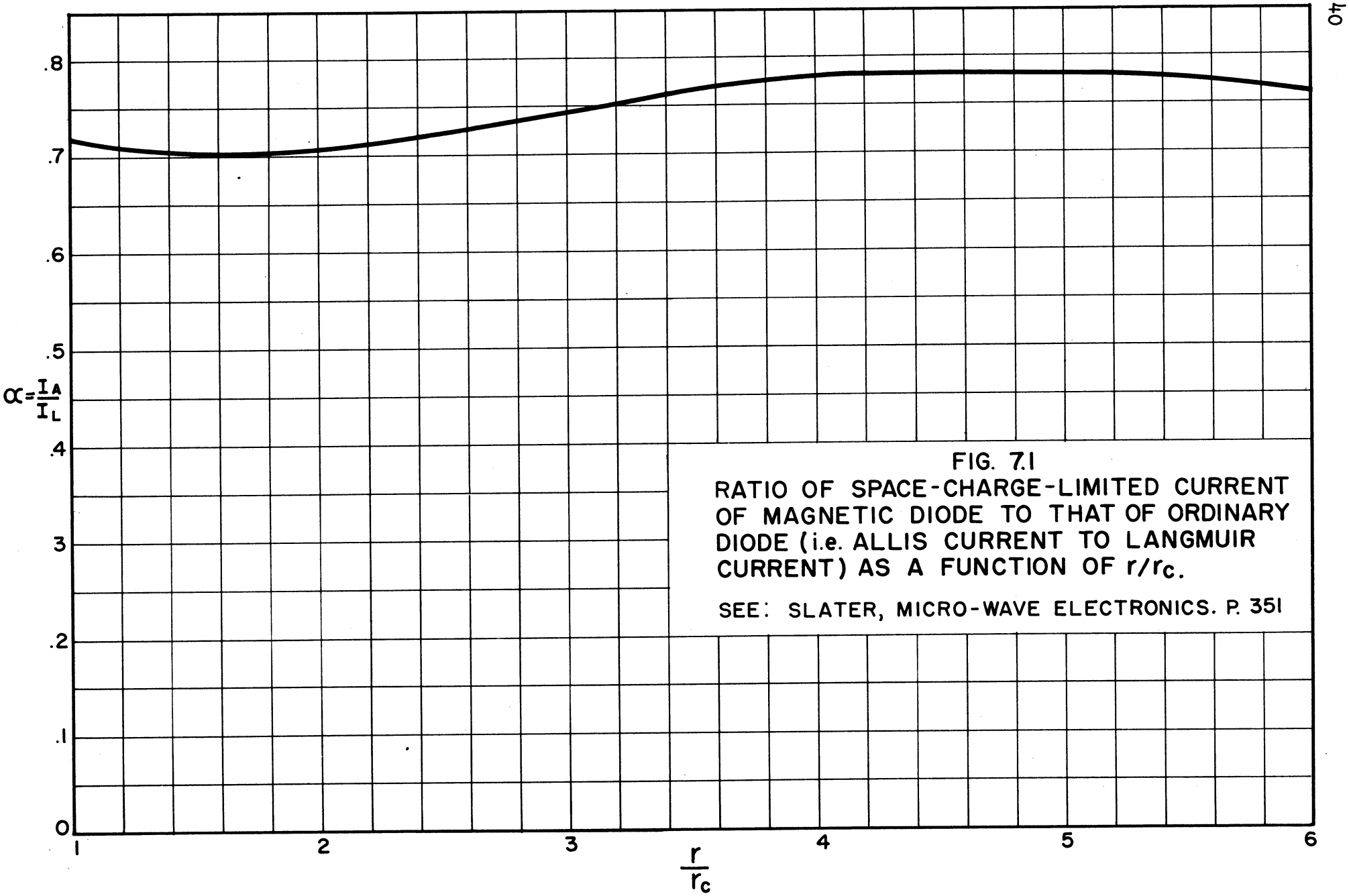

FIG. 7.1
RATIO OF SPACE-CHARGE-LIMITED CURRENT OF MAGNETIC DIODE TO THAT OF ORDINARY DIODE (i.e. ALLIS CURRENT TO LANGMUIR CURRENT) AS A FUNCTION OF r/r_c.

SEE: SLATER, MICRO-WAVE ELECTRONICS. P. 351

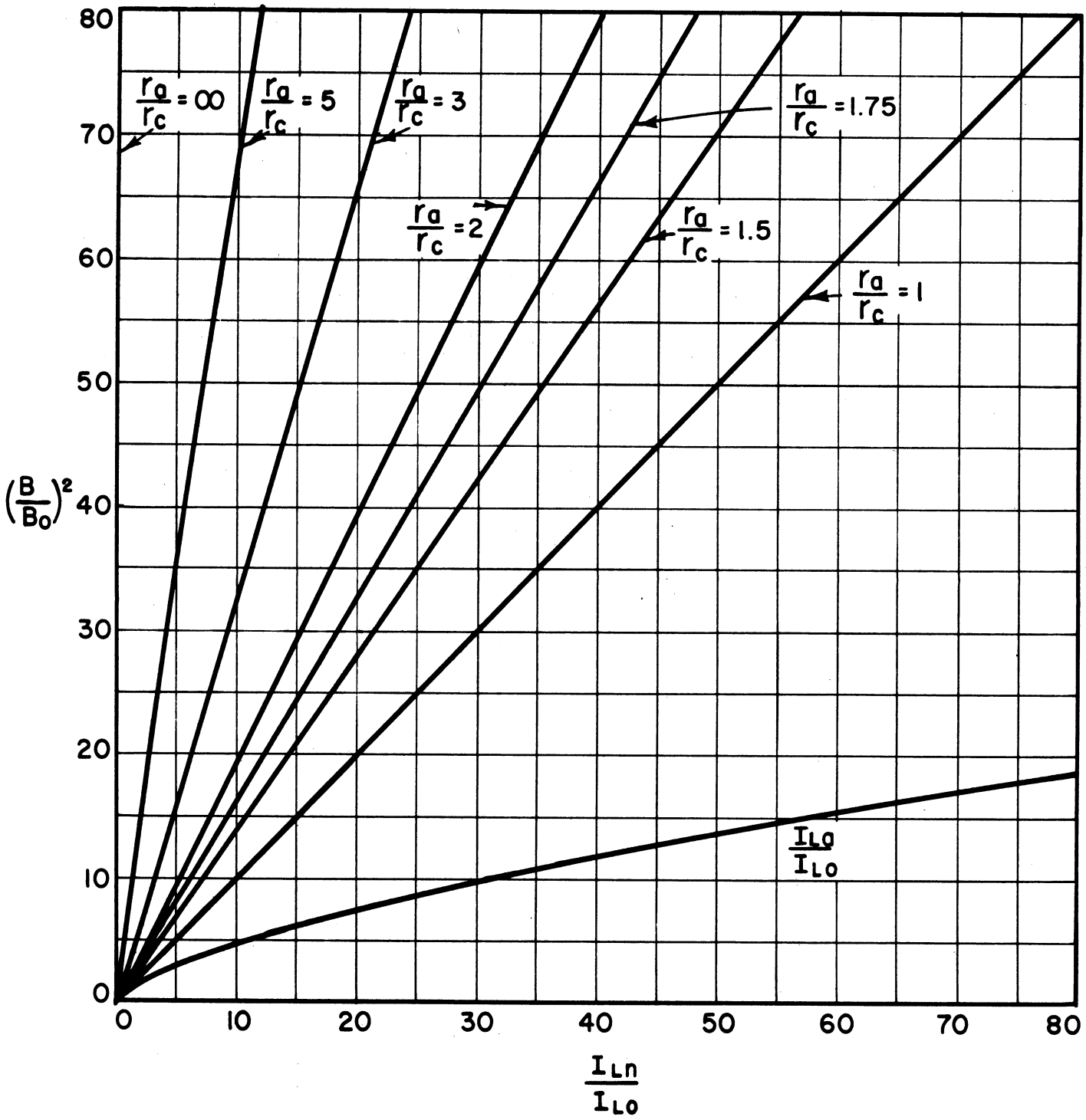

FIG. 7.2 SPACE-CHARGE-LIMITED CURRENT IN OSCILLATING MAGNETRON FROM EQUATIONS 7.9 AND 7.10

$\left(\frac{B}{B_0}\right)^2$ USED AS A VARIABLE

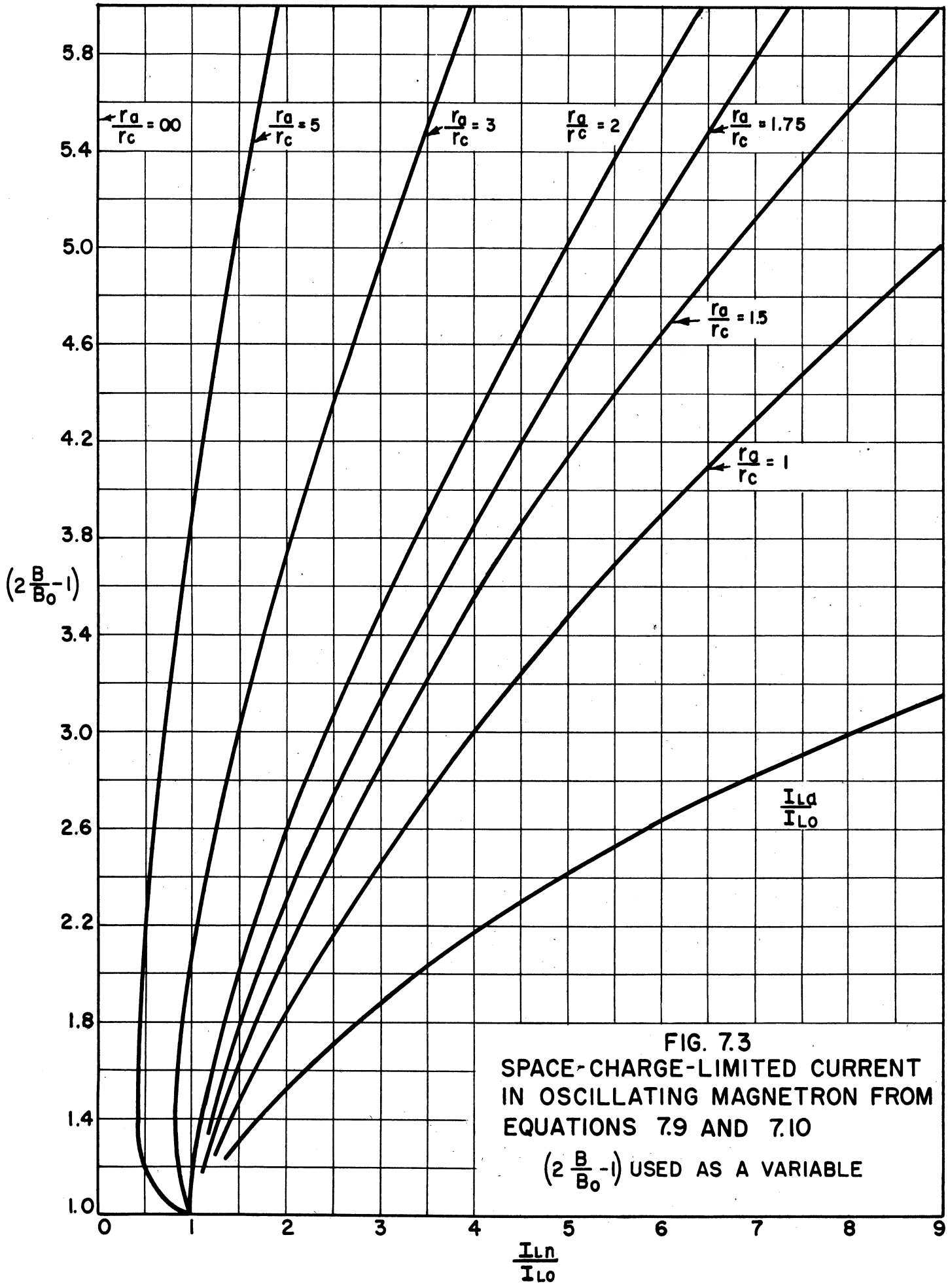

FIG. 7.3
SPACE-CHARGE-LIMITED CURRENT IN OSCILLATING MAGNETRON FROM EQUATIONS 7.9 AND 7.10
$(2\frac{B}{B_0}-1)$ USED AS A VARIABLE

$$\frac{E_a}{E_o} = 2\frac{B}{B_o} - 1 \quad . \tag{7.11}$$

In Fig. 7.3 the values of I_{Ln}/I_{Lo} are plotted as a function of $2(B/B_o) - 1$ to give an idea of the appearance of the maximum-current boundaries on a performance chart. It must be kept in mind that the actual space-charge-limited current is given by $\alpha_n I_{Ln}$, or about 0.71 the values given by the curves.

No experimental data known to be free from other causes of maximum-current boundary have been examined yet to check these results. However, the currents given are somewhat less than the one-half Allis current empirically determined by Slater on the basis of experimental observation of pulsed magnetrons. The Allis current divided by α_a is plotted on the same scale for reference in both figures.

$$\left(\frac{I_{La}}{I_{Lo}} = \frac{1}{\alpha_a}\frac{I_{Aa}}{I_{Lo}}\right).$$

8. Voltage Tuning and Temperature-Limited Operation (H. W. Welch, Jr.)

The effect of temperature limitation on maximum-current boundary insofar as an actual limitation of available current is involved is fairly obvious. There are other effects observed experimentally, however, which are not explained by the theory. The purpose of this section is to present some of the experimental facts and to discuss points in the theory which explain the voltage-tuning phenomena and which indicate the possibility of other types of temperature effects.

There are two fundamental processes by which temperature could affect magnetron operation. One of these is by the limitation of collection

current, and the other is by alteration of the space-charge and potential distributions within the interaction space, thus affecting spoke formation and, therefore, induced current.

The amount of collection current needed is determined by the power input and anode voltage. Under temperature-limited conditions, after the saturation current is reached, an increase in anode voltage cannot increase the d-c anode current. On the other hand, the increase in anode voltage must increase the total individual electron velocity. As a result of the increase in the tangential component of velocity, the frequency will increase, and, as a result of the increase in total velocities of electrons striking the anode, efficiency will decrease. In fact, it might be possible that all the additional energy due to the raised anode voltage would be lost in dissipation so that the added power input would not result in additional power output. This is unlikely. However, if one assumes it to be true, one is led to expect a frequency of oscillation proportional to anode voltage and a power output proportional to anode current (and therefore constant). These are essentially the results observed by Wilbur at G.E. in extremely low-Q operation. It is illustrated by the data of Fig. 8.1.

To illustrate the decrease in electronic efficiency due to the increased velocities of electrons striking the anode, the electronic efficiency calculated from Eq 3.2 is plotted in Fig. 8.1. This shows the decrease in efficiency due to the increase in tangential velocity of the electrons striking the anode. Under temperature-limited conditions there would also be a considerable increase in radial velocities, so that the decrease in efficiency would be greater than that shown in Fig. 8.1.

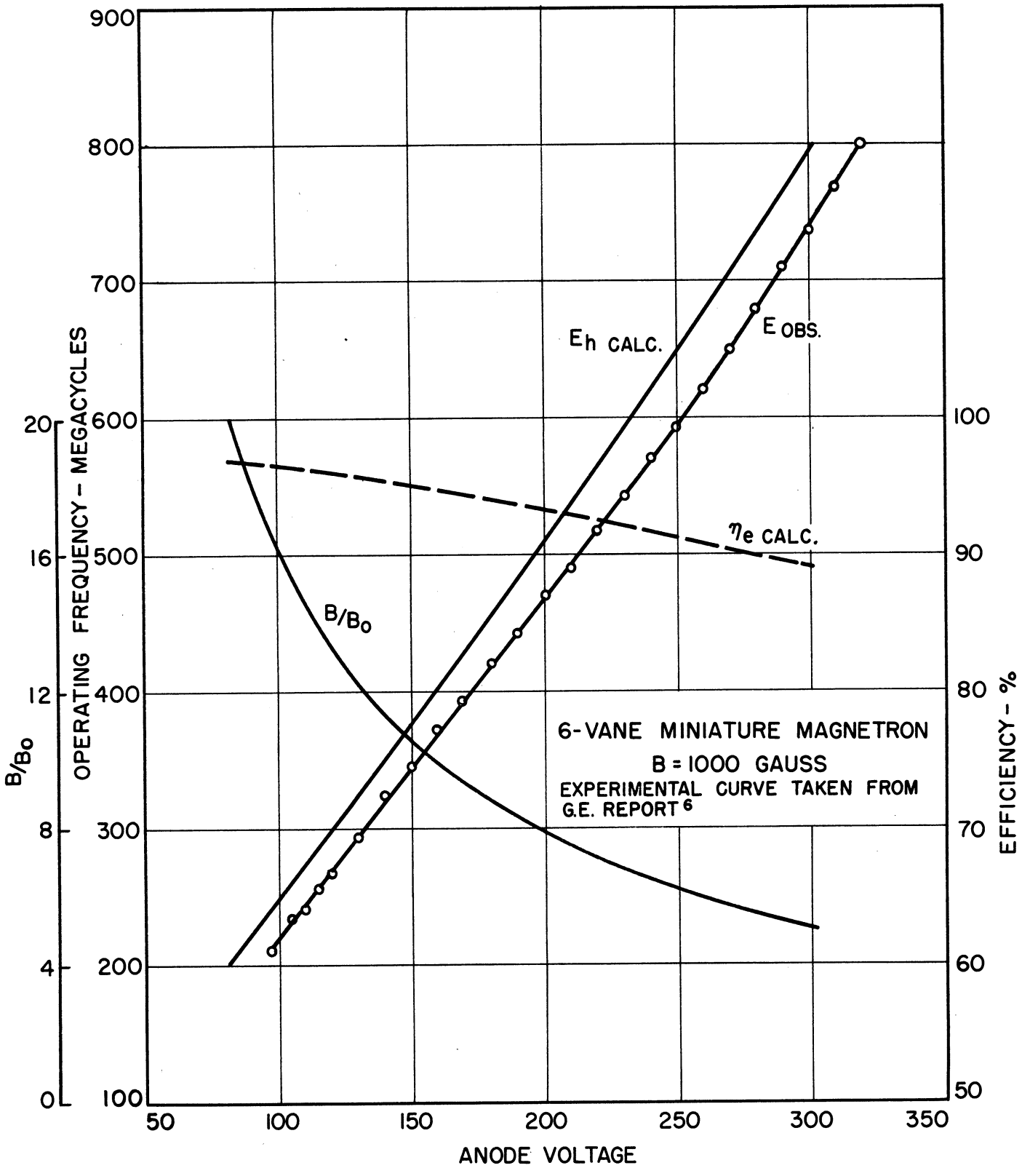

FIG. 8.1 ANODE VOLTAGE TUNING CHARACTERISTICS

The wavelength shift is predicted by the use of Eq 3.1 for the Hartree voltage; this equation may be written in complete form as follows:

$$E_a = \frac{\pi r_a^2}{n} f B \left[1 - \frac{r_c^2}{r_a^2} \right] - \frac{2\pi^2}{n^2} \frac{m}{e} f^2 r_a^2 \quad . \qquad (8.1)$$

If B/B_o is large compared to unity, the second term on the right of Eq 8.1 can be neglected and frequency is proportional to anode voltage. This is almost true in the data of Fig. 8.1. Eq 8.1 and B/B_o are plotted; the comparison between the slopes of the predicted and measured frequency-shift curves is quite good, but the voltage for a given frequency is low. The error introduced by neglecting the second term of Eq 8.1 would be less than 10 per cent over about half of the tuning range.

For moderate loading the power output does not remain constant, but increases to a maximum and then falls off again. This effect is shown in Fig. 8.2, which is a typical set of data reproduced from the G.E. report. This type of variation in power output as frequency is increased can be explained by the arguments presented in Section 5 as a result of the advance in phase of the spoke of space charge.

If, as the anode voltage is raised, the r-f voltage and r-f current are increased to the point that the power output tends to be more than can be supplied with the available d-c current and electronic efficiency, the tube must stop operating. In the operation obtained at G.E., the r-f voltage is substantially constant because, for the very low Q which is used, the load admittance does not vary rapidly with frequency; thus the required balance is maintained under temperature-limited conditions.

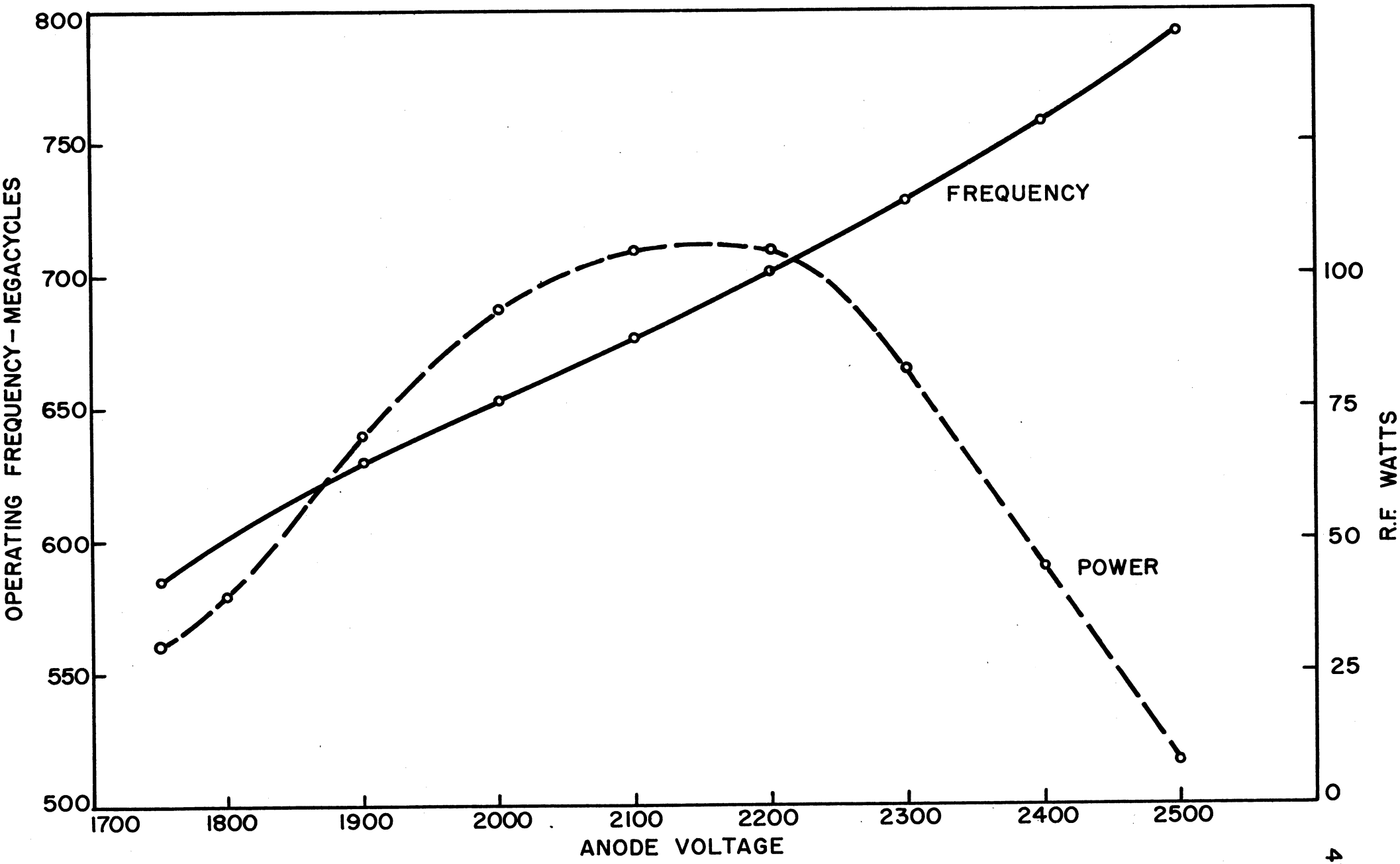

FIG. 8.2 VOLTAGE TUNING CHARACTERISTICS FROM GE REPORT[6] P. 82

There are several possible mechanisms by which the space charge and potential distributions may be affected by a temperature limitation. One of these may be illustrated by discussion of Fig. 8.3.

The curves in this figure apply to the static magnetron. The tangential energy parabola, labelled E_1, represents the potential corresponding to zero radial velocity in a region where space charge exists in the magnetron. Therefore, it must be the potential at the boundary of a space-charge swarm where no current is crossing. It is given by the following equation:

$$E_1 = \frac{B^2 e}{8m} r^2 \left(1 - \frac{r_c^2}{r^2}\right)^2 \qquad (8.2)$$

The curve labelled E_2 is the logarithmic distribution which exists in a space-charge-free diode given by

$$E_2 = E_a \frac{\log (r/r_c)}{\log(r_a/r_c)} \quad . \qquad (8.3)$$

The curve labelled E_3 is the logarithmic curve which would exist in a magnetron between a boundary of the swarm r_H and the anode r_a if the anode potential were E_a. This curve is plotted from the following equation:

$$E_3 = B^2 \frac{e}{8m} r_H^2 \left[2\left(1 - \frac{r_c}{r_H^2}\right) \log \frac{r}{r_H} + \left(1 - \frac{r_c^2}{r_H^2}\right)\right] \quad . \qquad (8.4)$$

If we assume that the anode voltage applied is E_a, it is apparent from these curves that under approximately space-charge-free conditions, individual electrons would be found as far out as the radius r_T, where they have no energy of radial motion and can therefore not cross the boundary. Between r_c and r_T individual electrons have everywhere energy of radial

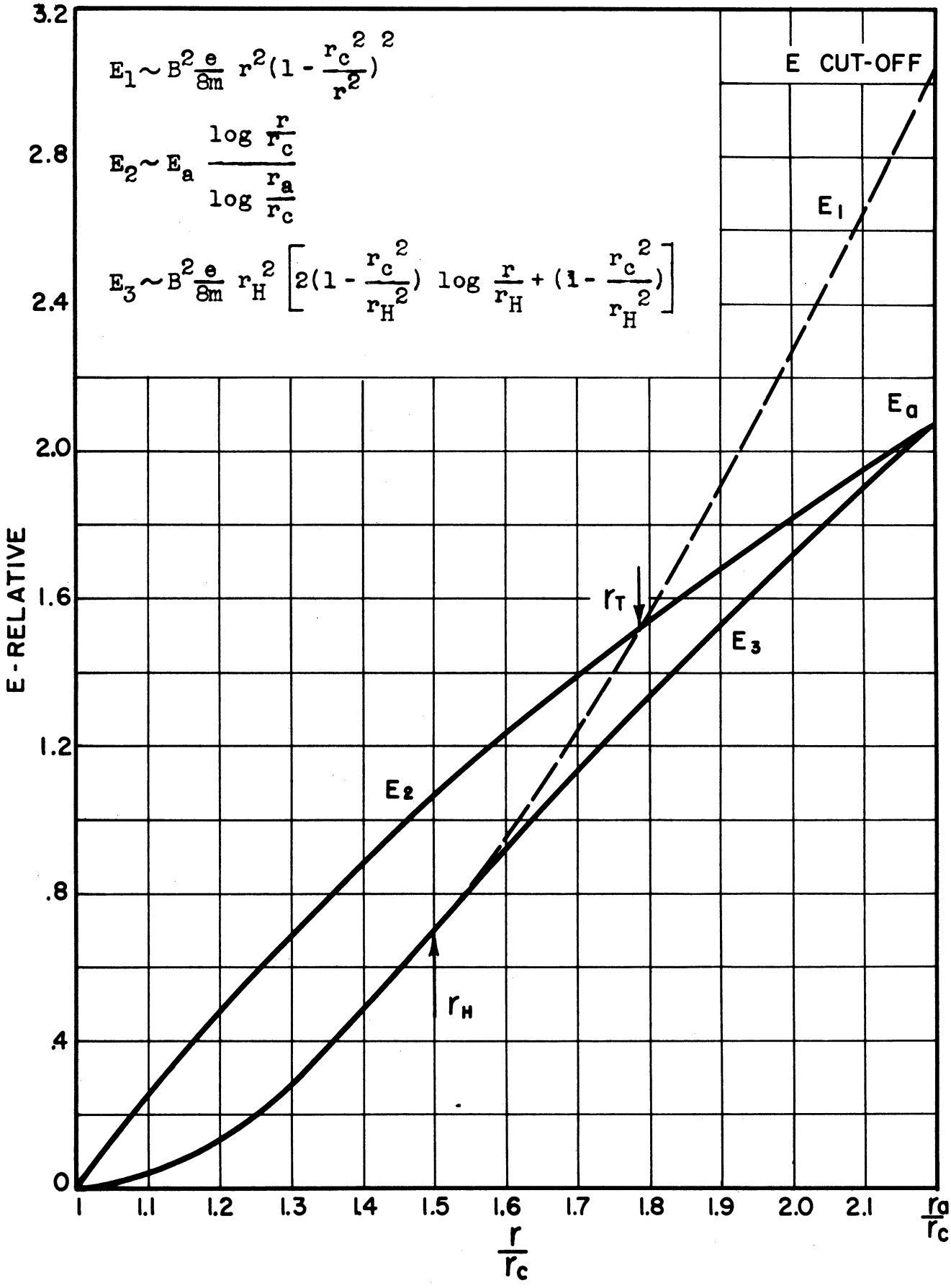

FIG. 8.3 COMPARISON OF SPACE CHARGE FREE AND MAGNETRON SPACE CHARGE CONDITION

motion in addition to the energy of tangential motion (therefore, double-stream radial current exists). This energy could be expressed by the difference in potential between the two curves, $E_2 - E_1$. On the other hand, if space charge exists, and the region between r_c and r_H is filled with a swarm of electrons moving about the cathode (no radial current), the distribution will be that given by curve E_3, and the electrons will only reach the boundary r_H.

The double-stream distribution described by Slater is also bounded at r_H and contains the same total amount of space charge within r_H as the distribution corresponding to the curve E_1. However, higher potentials than E_1 will exist within r_H due to the energy of radial motion. Twiss has shown that r_H is also approximately determined from Eq 8.4 when initial electron velocities are included. We conclude from these results that the only way for a swarm distribution to increase appreciably in extent is for the total amount of space charge to be limited. This limits discussion of temperature-limited behavior for the static magnetron unless we accept Twiss' hypothesis that the outward-moving current in the double-stream flow must be supplied by the cathode (neglecting secondary emission effects). If we accept this latter hypothesis then, as magnetic field is increased, a point is reached above which the cathode cannot supply the needed current, and the space-charge distribution is changed. The gradient at the cathode becomes positive (therefore, there is a surface charge on the cathode), and the possibility of an increase in extent of the space-charge swarm beyond r_H exists. It is hoped that the theoretical development begun by Twiss can be extended to include this point.

Until this theory is developed further, it is only possible to extrapolate the ideas to the oscillating magnetron. In this case current

is being drawn through the swarm* and synchronous space charge will be formed by the r-f fields. However, it is apparent that under a condition of cathode saturation the smaller space-charge density could affect the following:

a) the anode potential required for a given swarm extent (since the angular velocity of electrons at a given radius is independent of the swarm density, this means that electrons travelling at synchronous angular velocities will be available at lower voltages if the amount of space charge in the swarm is limited);

b) the average density of the swarm and, therefore, the magnitude of the rotating current and, possibly, the penetration of the electromagnetic field (these factors are also related to the magnetic field); and

c) the radial velocities through the swarm and, therefore, transit time and consequently, collection current (transit time will be discussed further in the next section).

In conclusion, some experimentally observed facts which have not been discussed will be mentioned with the hope that future extension of the theory will furnish an explanation.

a) Starting voltage may increase as temperature decreases. This is illustrated by the data in Fig. 8.4. Changes of as much as 20 to 30 per cent have been observed.

b) Apparent increases in maximum-current boundary due to filament temperature increases may be due to increased leakage current and not to an increased range of oscillatory current. This is illustrated by the data in Fig. 8.5. Note that the diode emission is from 2 to 10 times the observed maximum-current boundary.

---

* Note: The magnetron current is usually less than the radially circulating current in the swarm which Twiss says the cathode must provide. The latter is given approximately by one-half the currents obtained by use of Figs. 7.2 or 7.3. Thus, even in the oscillating magnetron, if Twiss' hypothesis is correct and if our idea of the existence of the subsynchronous swarm is correct, the subsynchronous swarm may be changed in form if the radial circulating current is not supplied.

c) Maximum-current boundary does not necessarily increase as temperature increases and in fact may decrease after an optimum point is reached. This point is illustrated by the data in Fig. 8.6. This is not an anomalous effect, since similar data were obtained on a number of tubes. According to Wilbur[6] this fact is essential to the low-Q operation as obtained at G.E. There are, however, no data presented in the G.E. reports which clearly show the optimising of maximum-current boundary as a function of temperature; thus, no quantitative conclusion can be made.

d) For a given temperature, maximum-current boundary is dependent on magnetic field and loading. When temperature is changed the current boundary will have a new value still dependent on magnetic field and loading. This is illustrated by the data in Figs. 8.7 and 8.8. The emission figures which are given are for nonmagnetic diode emission and again are from 2 to 10 times the observed maximum-current boundary.

The fact that starting voltage increases as cathode temperature is decreased is not at all important to the practical use of the magnetron. It may be that an explanation of this fact will be helpful in the understanding of other phenomena, however. It is possible that the discrepancy between observed and theoretical voltage-tuning curves in Fig. 8.1 is due to this effect. The very brief discussion in this section of Fig. 8.3 shows that there are certain relationships which must exist between maximum-current boundary, temperature-limited emission, starting voltage, loading, and magnetic field. It is hoped that it will be possible without too many limiting approximations to formulate a more quantitative picture.

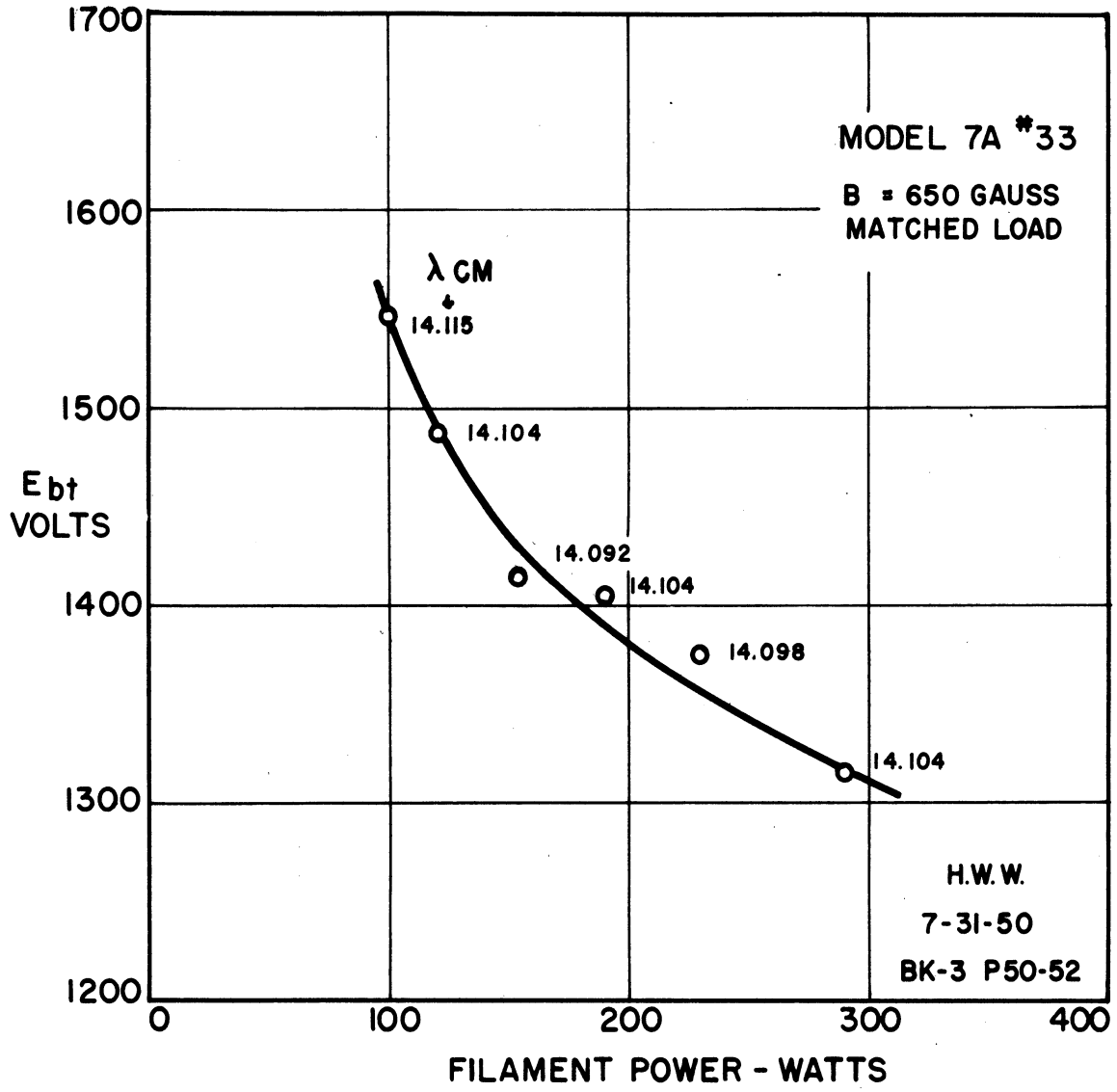

FIG. 8.4
OBSERVED STARTING VOLTAGE AS A FUNCTION OF FILAMENT POWER

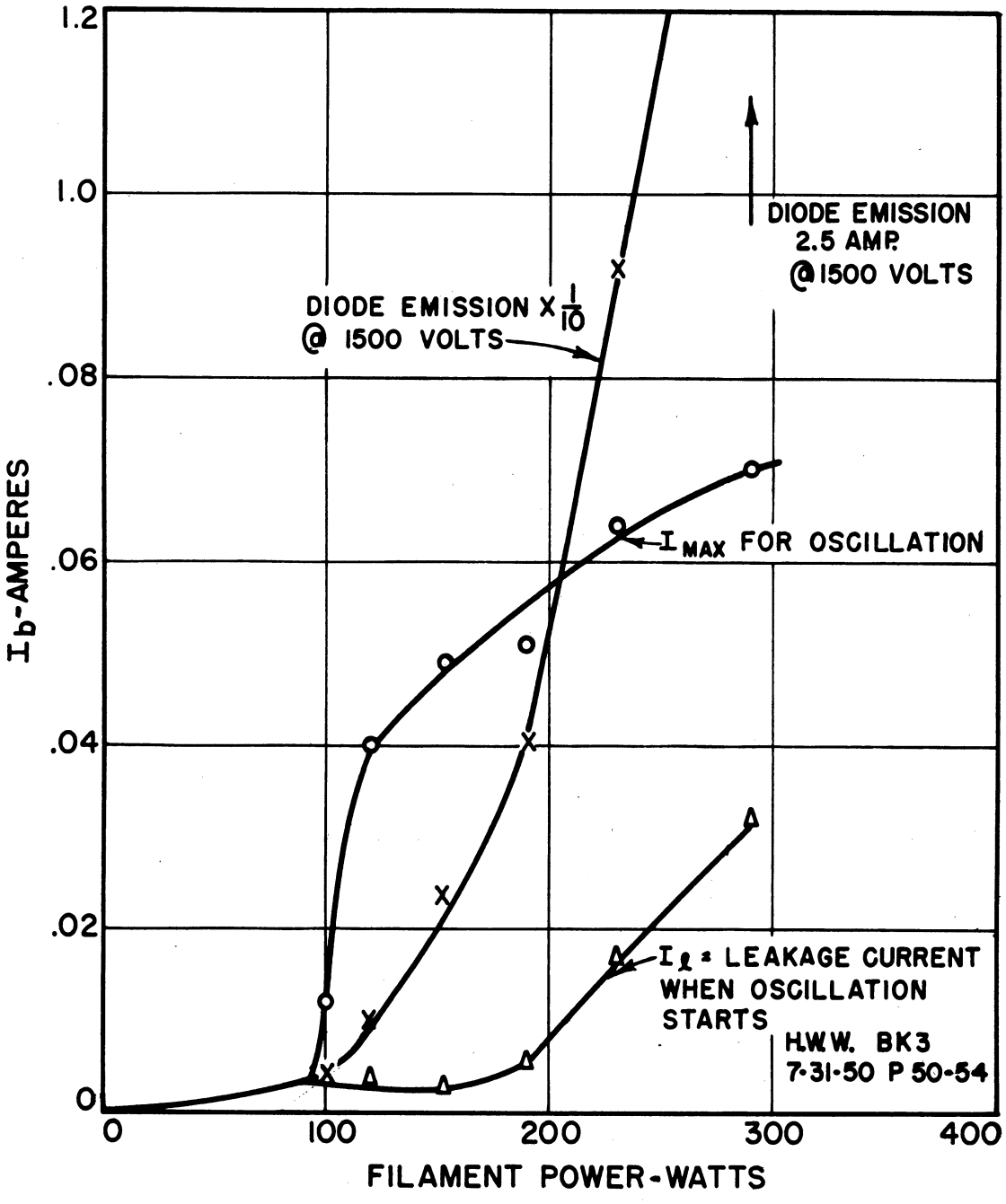

FIG. 8.5
COMPARISON OF MAXIMUM-CURRENT BOUNDARY, LEAKAGE CURRENT AND DIODE EMISSION MODEL 7A #33

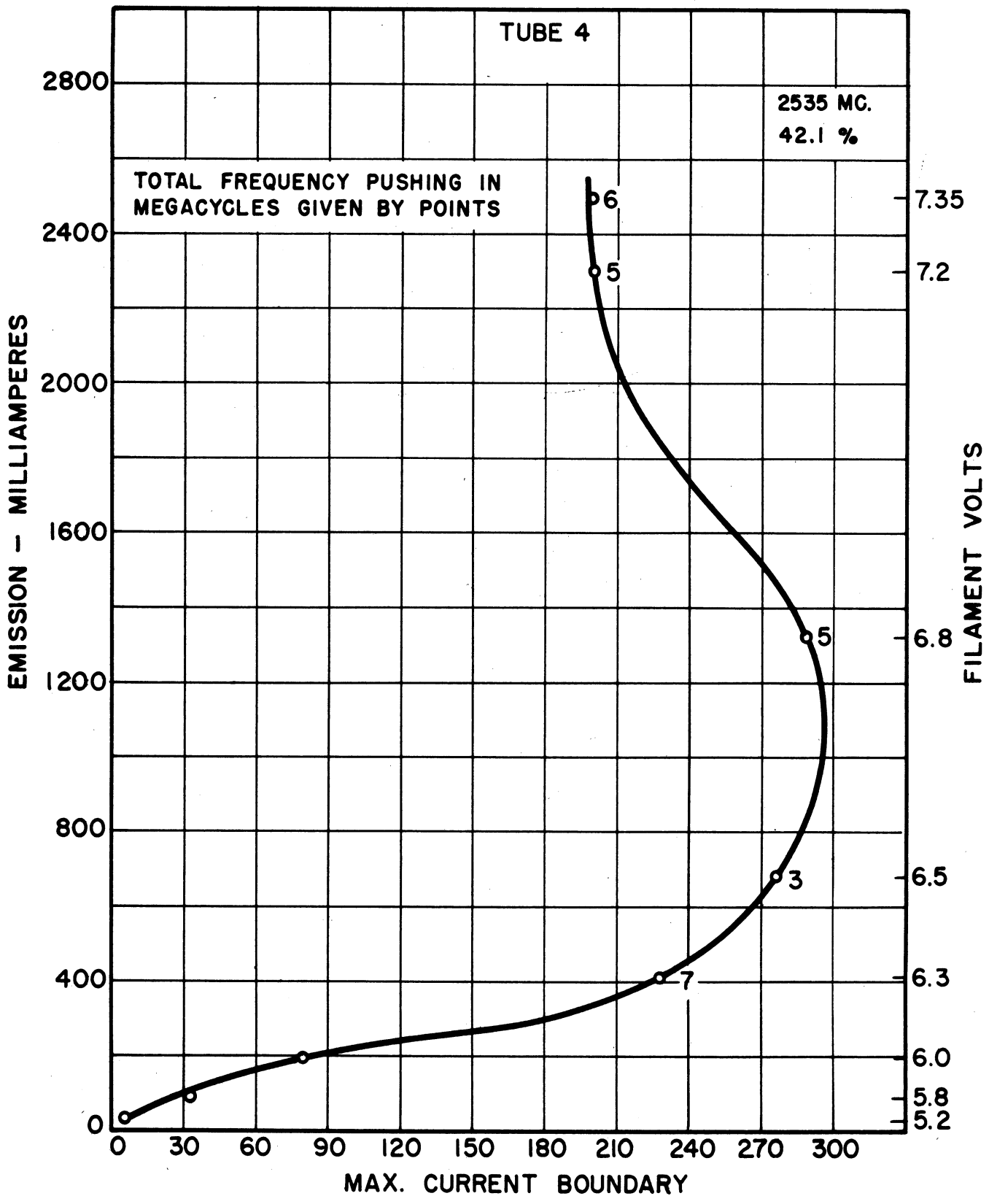

FIG. 8.6 EFFECT OF EMISSION ON MAXIMUM-CURRENT BOUNDARY.- RAYTHEON DATA.

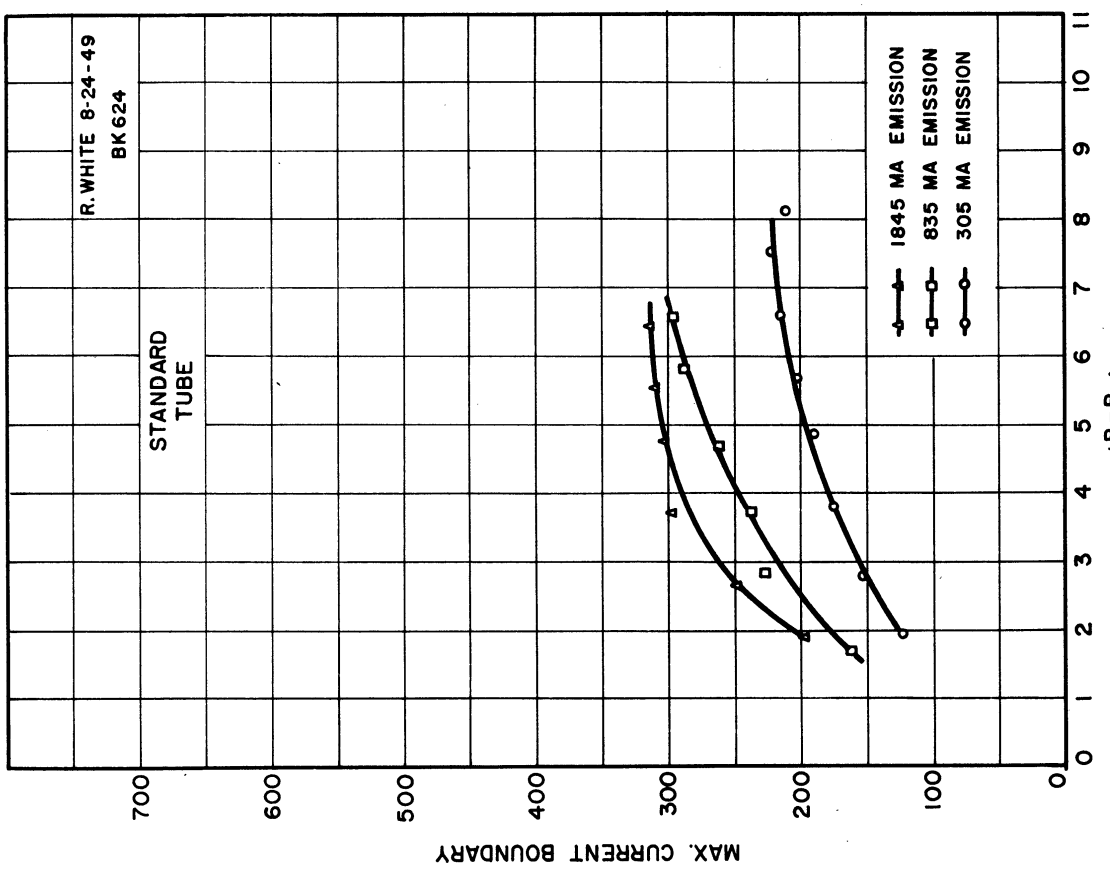

FIG. 8.8 EFFECT OF MAGNETIC FIELD ON MAXIMUM-CURRENT BOUNDARY. RAYTHEON DATA

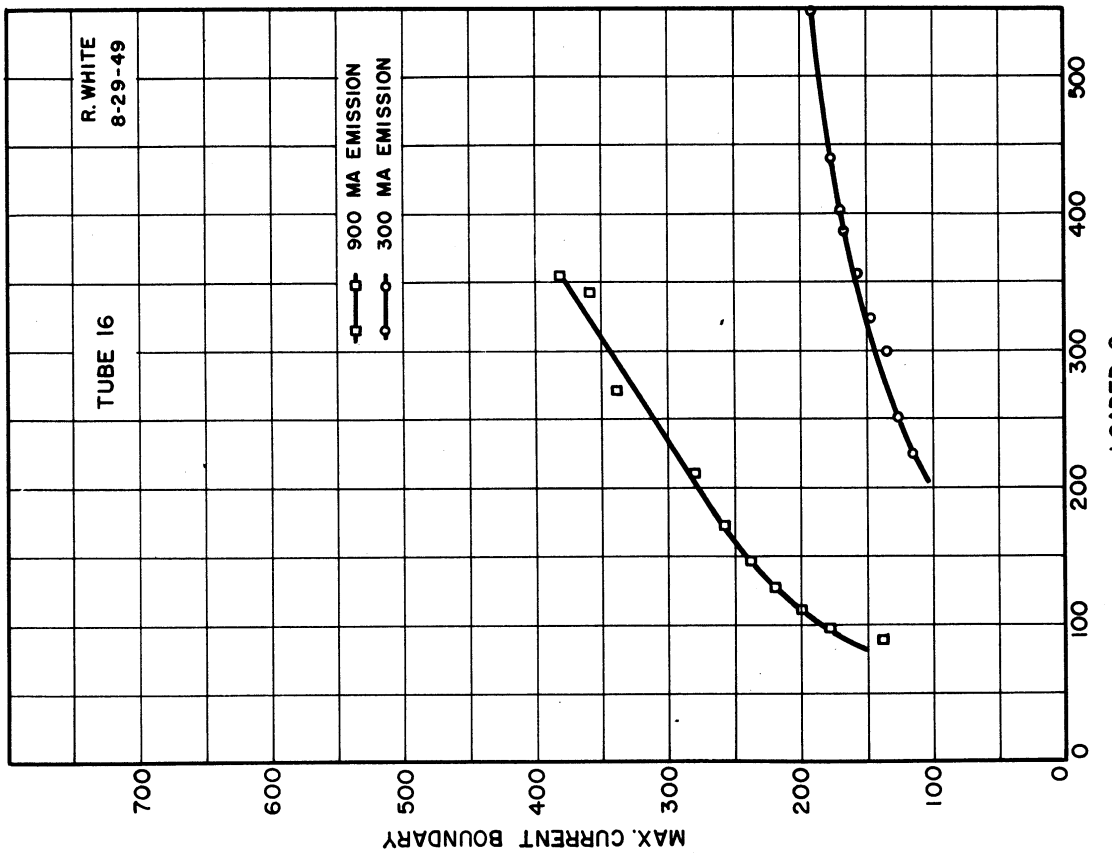

FIG. 8.7 EFFECTS OF LOADING ON MAXIMUM-CURRENT BOUNDARY. RAYTHEON DATA.

9. Transit Time and Maximum-Current Boundary (S. Ruthberg, H. W. Welch,Jr.)

This section contains some calculations from the static magnetron solution which suggest some limitations on the amount of current which can be drawn in an oscillating magnetron. The possibility is indicated that transit time may have some correlation with the maximum-current boundary.

If the striated-type solution discussed by Slater is assumed for the swarm,[7] then the maximum current is found in the single-striated case, where the electrons reach the swarm boundary in one quasi-cycloidal arc. Further, if it is assumed that the plane magnetron solution is similar to the cylindrical case, then the transit time for a particle through the swarm is just the cyclotron period

$$T_c = \frac{2\pi}{\omega_c} = \frac{\pi}{\omega_L} , \qquad (9.1)$$

where ω_c and ω_L are the cyclotron and Larmor angular velocities, respectively. This is the minimum time in which charge can be transported across a striated region, and hence, in this case, to the boundary.

The cyclotron period may be compared to the length in time of the d-c current flow to an anode segment. This time is estimated as follows: Take that mode of operation when the number of wavelengths of r-f in the periphery of the magnetron is one-half the number of anode segments. The r-f wave, advancing one wavelength per period, sweeps through the space occupied by two anode segments; hence, a well defined spoke of the same width as an anode segment and rotating in synchronism with the r-f wave will deliver current to each segment for one-half an r-f cycle. Suppose all the charge in the hub of the space-charge swarm is delivered through the spokes to the anode in a time equal to the larger of the two periods,

cyclotron or half the r-f. This would be a limiting value on the d-c current. Now, the total charge in the hub is given by*

$$\tau = -2\pi\epsilon_o \frac{m}{e} \omega_L^2 r_n^2 \left(1 - \frac{r_c^4}{r_n^4}\right) L \qquad (9.2)$$

This can be shown to be true no matter what distribution exists within the swarm, so long as there is no radial velocity at the boundary and cathode temperature is adequate. The factor r_n may be eliminated from this equation by using the angular-velocity relationship, which is

$$\frac{r_n^2}{r_c} = \frac{\omega_L}{\omega_L - \omega_n} \quad . \qquad (9.3)$$

This in Eq 9.2 gives

$$\tau = -2\pi\epsilon_o \frac{m}{e} \omega_n \omega_L \frac{2\omega_L - \omega_n}{\omega_L - \omega_n} L r_c^2 \quad ; \qquad (9.4)$$

therefore, the current is τ/time.

This is calculated for the Model 3 magnetron of this laboratory, the parameters of which are given in the appendix. The transit time through the hub is found to be 1.8×10^{-10} sec; half the r-f period is 2.82×10^{-10} sec. The transit time through the swarm is, therefore, of the same order as the time of current flow. τ is 10.4×10^{-10} coulomb, so that the current is 3.69 amps. Experimentally, the maximum average current is 0.37 amps.** This is a factor of 10. However, the charge distribution of the hub would surely be destroyed if all charge were delivered in approximately one transit time period.

---

* Ref. 1, page 32, Eq 5.10.

** See Section 14 of this report.

It is assumed that the well differentiated spoke has the same angular width as an anode segment at the anode boundary. It is further assumed that the current drawn by an anode segment from a spoke is constant as long as any portion of the spoke is in contact with the segment. Now, the anode segments are equally spaced, and the space between the segments is equal in size at the boundary to a segment. Thus, the current to a segment versus time is a square pulse of one-half an r-f period in duration; i.e., current is drawn as soon as the front of the spoke contacts the segment and continues until the last part breaks contact. Thus, when the current to one segments ceases, that to the next segment commences. Although each spoke draws one current pulse per r-f cycle and each lasts one-half an r-f period, the current drawn by the tube as a whole is, therefore, a continuous, fixed value. Then, let the total charge in the hub be emptied through the spokes and each half r-f cycle to establish this constant d-c current value. This gives the 3.69 amps d-c calculated.

It is, of course, clear that the assumption is a very bold one, that the same amount of current is drawn no matter how much of the spoke is in contact with an anode segment. It may be more convincing to assume that the amount of charge impinging on a segment is proportional to the amount of spoke in contact with the segment at that instant. Rotating at constant velocity, the portion of the spokes meeting the segments grows linearly in time from the first contact until all of a spoke is at a segment, and then drops off the same way. Thus, the influx of charge and hence the current to the tube is a series of triangular pulses. But how much charge is transported at the instant the whole spoke is in contact? If it is the same as in the first case, the peak current of the triangle

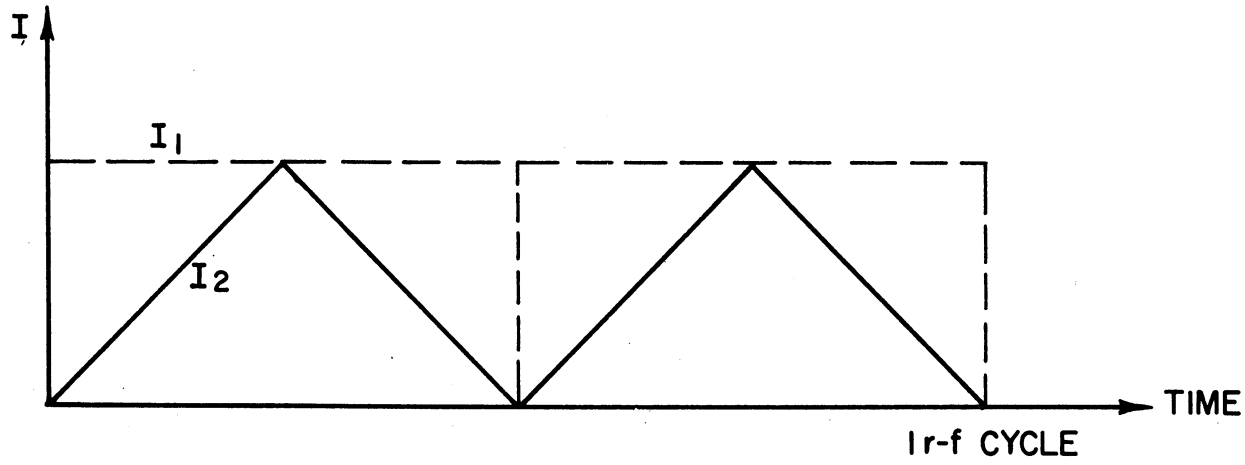

FIG. 9.1 POSSIBLE FORMS FOR COLLECTION CURRENT IN THE MAGNETRON

is that of the first, and hence the average value in the second case is one-half that in the first case, giving the maximum-current boundary as 1.85 amps (see Fig. 9.1).

An estimate of the minimum value of transit time through the spokes may be made by considering current through rectangular spokes as a parallel electrode case, following the Child-Langmuir distribution. In this case the transit time is given by

$$T = k \frac{d_{ca}}{v_a} , \tag{9.5}$$

where k is 2 when no space charge exists and 3 when space charge exists, d_{ca} is the distance between the two electrodes, and v_a is the velocity of the particles at the anode.

If one end of the spoke is taken at the synchronous potential of the swarm hub edge, E_n, and the other at the Hartree potential, E_h, then

$$\frac{1}{2} m v_a^2 = e (E_h - E_n)$$

and

$$v_a = \sqrt{\frac{2e}{m}} (E_h - E_n)^{1/2} .$$

Using 9.5

$$T = k \frac{\sqrt{m/2e}}{(E_h - E_n)^{1/2}} d_{ca} . \tag{9.6}$$

For the case discussed

$$E_n = 102 \text{ volts}$$

$$E_h = (2B/B_o - 1)E_o = 2100 \text{ volts} ,$$

where $E_o = (1/2)(m/e) \omega_n^2 r_a^2$, $E_n = (1/2)(m/e) \omega_n^2 r_n^2$, and ω_n is

the synchronous angular velocity. d_{ca} is taken as 0.164 cm and k = 3. Thus

$$T = 3\sqrt{m/2e}\ \frac{.164 \times 10^{-2}}{(1998)^{1/2}}$$

$$= 1.81 \times 10^{-10} \text{ sec} ,$$

or of the same order as the minimum transit time through the swarm. The time must actually be much greater than this because of the confining effect of the magnetic field. It becomes a question whether this is larger than one-half the r-f cycle.

Section 7 suggests a method for estimating the maximum space-charge-limited current (I_{An}) for the oscillating magnetron. On this estimate the maximum amount of charge which could be tran
spokes to the anodes can be found and compared to the
hub. Now

$$I_{An} = \alpha_n \left(\frac{I_{Ln}}{I_{Lo}}\right) I_{Lo} . \qquad (9.7)$$

α_n, a function of r_n/r_c, is given in Section 7. I_{Ln} and I_{Lo} are also defined there, where I_{Ln} is the Langmuir current at the synchronous radius for a potential of E_n there, and I_{Lo} is that at the anode for a potential of E_o there.

The current from 9.7 combined with half the time of an r-f cycle gives the charge delivered per half cycle as

$$q = -\alpha_n \left(\frac{I_{Ln}}{I_{Lo}}\right) \frac{I_{Lo}}{2f} . \qquad (9.8)$$

Since, by definition

$$I_{Lo} = \frac{8\pi}{9} \epsilon_o \sqrt{2e/m}\ \frac{L}{r_a}\ \frac{E_o^{3/2}}{\beta_a^2} ,$$

which is the Langmuir relationship, since $f = n\omega_n/2\pi$, and with insertion of E_o

$$q = -\frac{4\pi^2}{9}\epsilon_o\frac{\alpha_n}{n}\left(\frac{I_{Ln}}{I_{Lo}}\right)\frac{m}{e}\frac{\omega_n^2 r_a^2}{\beta_a^2}L \quad . \tag{9.9}$$

Therefore, using Eq 9.4 for τ, we have

$$\frac{q}{\tau} = \frac{\alpha_n}{n\beta_a^2}\frac{I_{Ln}}{I_{Lo}}\frac{\omega_n}{\omega_L}\frac{\omega_L - \omega_n}{2\omega_L - \omega_n}\frac{r_a^2}{r_c^2} \quad . \tag{9.10}$$

Using the parameters given in the Appendix for the Model 3 magnetron,

$$B_o = 329 \text{ gauss} = 2(m/e)\omega_n\frac{1}{1 - (r_c/r_a)^2}$$

$$B/B_o = 5.9$$

$$\alpha_n = 0.72 \quad .$$

From Fig. 7.2, $I_{Ln}/I_{Lo} = 22$. Langmuir's constant for $r_a/r_c = 1.66$ is*

$$\beta_a^2 = 0.18 \quad .$$

Then q/τ is 1.45. That is, if the tube were to have this estimate of space-charge-limited maximum-current boundary, for this case the charge drawn over per half cycle is considerably greater than the total contained in the swarm under static conditions. The current by 9.7 is 5.3 amps, a factor of 15 over 0.37. If the current is drawn over in pulses, as, for example, the triangular pulses of Fig. 9.1, I_{An} will have to be supplied at the peaks only. Thus, the maximum-current boundary will, in this particular case, be reduced to one-half I_{An} and q/τ will be one-half of the

---

* See footnote on page 37.

value 1.45. Even so, the space-charge swarm could not be considered as a reservoir.

It is suggested by Slater that one-half Allis current be used as the maximum-current boundary. In the notation used here this is

$$\frac{1}{2} I_{Aa} = \frac{\alpha_a}{2} \left(\frac{B}{B_o}\right)^3 I_{Lo} \quad . \tag{9.11}$$

This value of current is about five times greater than I_{An} for the case considered. In any case the space-charge swarm cannot be considered a reservoir of charge. It is noted that one-half Allis current is assumed for the anode voltage at cutoff value, which for this case is three times greater than the starting voltage.

All these estimates point to the problem of how quickly the swarm configuration can be re-established, or how much charge can be pulled off the hub without destroying the discharge. If it should require several transit time periods, then the maximum-current boundary might be expected to occur at much smaller currents than taken above. If the swarm does not act as a reservoir, the emission current from the cathode must definitely be considered.

The calculations given above are only to be considered as representating upper and lower limits on the quantities involved. These are given, since actual values are limited by the complexity of the problem.

In temperature-limited operation these calculations would have to be revised. The transit time through the swarm would be approximately one-half the value given by Eq 9.1, since the period of the cycloidal path in the absence of space charge is just half the value in the presence of the magnetron space-charge density. The space-charge reservoir will no

longer exist at all in temperature-limited operation. If operation were limited by the time required to get the electrons across the interaction space, as is indicated as a possibility by the calculations of this section, temperature limitations might produce better operation. If, however, operation is limited by the time required to fill the swarm as a reservoir, limitation of temperature cannot help, since the swarm ceases to exist.

Twiss' calculations indicate that transit time is reduced when initial velocities are taken into account. The transit time through the swarm as given by Twiss is

$$T = 0.57 \frac{\pi}{\omega_c} . \qquad (9.12)$$

This is almost a factor of 4 smaller than the value given by Eq 9.1 and if used would make all the conclusions made in this section more favorable.

10. Basic Concepts for Induced-Current Calculation* (W. Peterson, H. W. Batten, S. Ruthberg)

In this section the induced current due to space charge moving in an electrode system is developed in terms of a unit-potential function.

Consider an N-electrode structure of arbitrary geometry, small compared to the wavelengths of any r-f fields, so that the vector potential component of the electric field intensity, E, can be neglected.** Then the total current density, J, and the electric field intensity in the interelectrode space are given by

---

* The material in this section is generally applicable to any induced-current problem. The symbols are standard notation of electromagnetic field theory and are defined as they are introduced. They are not necessarily listed in the table of symbols used in this report, since the symbols in all other sections pertain particularly to the magnetron.

** Ref. 21, page 140.

$$J = \rho v + \epsilon_o \dot{E} \tag{10.1}$$

$$E = - \text{grad } \phi \tag{10.2}$$

$$\text{div } E = \frac{\rho}{\epsilon_o} , \tag{10.3}$$

where ϕ is the actual potential function of the system. It is convenient to take the actual potential as a superposition of two parts: one part, ϕ_1, due to the electrode potentials and a second part, ϕ_2, due to the space charge, where

$$\phi = \phi_1 + \phi_2 . \tag{10.4}$$

Then, on all electrodes

$$\phi_1 = \phi , \qquad \phi_2 = 0 . \tag{10.5}$$

In the interaction space,

$$\nabla^2 \phi_1 = 0 , \qquad \nabla^2 \phi_2 = - \frac{\rho}{\epsilon_o} . \tag{10.6}$$

By Eq 10.2, E is defined as

$$E = - \text{grad } \phi_1 - \text{grad } \phi_2 = E_1 + E_2 . \tag{10.7}$$

This division of the field gives the total current density from 10.1 as

$$J = \rho v + \epsilon_o \dot{E}_1 + \epsilon_o \dot{E}_2 , \tag{10.8}$$

consisting of a space-charge-dependent part and a non-space-charge-dependent part, represented by J_i and J_c respectively, where

$$J = J_i + J_c \tag{10.9}$$

$$\dot{J}_i = \rho v + \epsilon_o \dot{E}_2 \tag{10.10}$$

$$J_c = \epsilon_o \dot{E}_1 \ . \tag{10.11}$$

Also, through Eqs 10.2, 10.3, and 10.7,

$$\text{div } E_1 = 0 \tag{10.12}$$

$$\text{div } E_2 = \frac{\rho}{\epsilon_o} \ . \tag{10.13}$$

Now consider the k'th electrode of the given system, whose surface is specified by S_k. Label the conduction current flowing <u>from</u> this electrode to an external system by i_k. Then, the conservation of charge requires that the time rate of increase of charge, $\dot{Q}$, in S_k be

$$\dot{Q} = - i_k + \int_{S_k} (\rho v)_n \, dS_k \ , \tag{10.14}$$

where the subscript n denotes the normal component into the electrode. Gauss' theorem, which relates the total charge inside a closed surface to the surface integral of the displacement vector, gives

$$\dot{Q} = - \int_{S_k} (\epsilon_o \dot{E})_n \, dS_k \ , \tag{10.15}$$

so that by Eq 10.14,

$$i_k = \int_{S_k} (\rho v + \epsilon_o \dot{E})_n \, dS_k \ , \tag{10.16}$$

$$i_k = \int_{S_k} (J_i)_n \, dS_k + \int_{S_k} (J_c)_n \, dS_k \quad . \tag{10.17}$$

That is, the conduction current from the electrode is simply equal to the total current arriving, as expected. The important part of this current is the space-charge-dependent part, given by

$$i_{ik} = \int_{S_k} (J_i)_n \, dS_k \quad , \tag{10.18}$$

since the rest of the current accounts for no time-average energy interchange in periodic systems except for the Joulian heat loss. This may be stated in another way; namely, the current

$$i_{ck} = \int_{S_k} (J_c)_n \, dS_k \tag{10.19}$$

can be represented entirely by capacitances external to the interaction system from the standpoint of the external circuit.

To relate the induced current at an electrode to the space-charge behavior, an artifice is employed. The divergence theorem suggests itself as a likely tool, since it relates the surface integral of a vector to a volume integral. It is desired that that volume be the interaction space of the system, and, therefore, the device must carry the surface integration over all electrodes and over the surface at infinity, although the current at particular electrodes is sought. To this end, define a dimensionless scalar function, ψ_k, as unity on the k'th surface but zero on all other electrode surfaces, and satisfying Laplace's equation throughout the interaction space. Thus, Eq 10.18 can be written in the form,

$$i_{ik} = \int_S (\psi_k J_i)_n \, dS \quad , \tag{10.20}$$

where the integration is now taken over all electrode surfaces and the surface at infinity. By the divergence theorem

$$i_{ik} = \int_v \text{div} \, (\psi_k J_i) \, d\tau \quad , \tag{10.21}$$

where $d\tau$ is the volume element. With expansion,

$$i_{ik} = \int_v J_i \cdot \text{grad} \, \psi_k \, d\tau + \int_v \psi_k \, \text{div} \, J_i \, d\tau$$

$$= \int_v d\tau \, \rho v \cdot \text{grad} \, \psi_k + \int_v d\tau \, \epsilon_o \dot{E}_2 \cdot \text{grad} \, \psi_k + \int_v d\tau \, \psi_k \cdot \text{div} \, J_i \quad . \tag{10.22}$$

However, the last two terms of this expression vanish. The last term is zero because

$$\text{div} \, J = \text{div} \, J_i + \text{div} \, J_c = 0$$

and from Eqs 10.11 and 10.12, $\text{div} \, J_c = \epsilon_o \, \text{div} \, \dot{E}_1 = 0$, and so $\text{div} \, J_i = 0$.

A theorem will be developed to show that the second term is zero also. Suppose that ξ is a scalar which vanishes on a given closed surface and that the divergence of a vector, P, vanishes everywhere inside that surface. Then the divergence theorem gives the expression

$$\int_S (\xi P)_n \, dS = \int_v \text{grad } \xi \cdot P \, d\tau + \int_v \xi \, \text{div } P \, d\tau$$

and the hypotheses on ξ and P make the left side of this equation and the second term on the right both zero. Hence, if a scalar ξ vanishes on the boundary of a volume, and a vector, P, is divergence-free in that volume,

$$\int_v \text{grad } \xi \cdot P \, d\tau = 0 \, . \tag{10.23}$$

It is now clear that the second term in Eq 10.22 is zero, since $\nabla \psi_k$ is divergence-free and ϕ_2 is zero on S. Thus

$$i_{ik} = \int_v \rho v \cdot \text{grad } \psi_k \, d\tau \, , \tag{10.24}$$

where the contribution to the conduction current by the space-charge behavior is now in terms of the space charge itself and ψ_k, a function depending only on the geometry of the system.

The current i_{ik} can be put in another important form by expanding J_i first and then going to the divergence theorem; that is, with the value of J_i inserted, 10.20 becomes

$$\begin{aligned} i_{ik} &= \int_S (\psi_k J_i)_n \, dS = \int_S \left[\psi_k \rho v + \psi_k \, \epsilon_o \dot{E}_2 \right]_n dS \\ &= \int_S (\rho v)_n \, dS_k + \int_v d\tau \, \text{div} \, (\psi_k \, \epsilon_o \dot{E}_2) \\ &= \int_{S_k} (\rho v)_n \, dS_k + \int_v d\tau \, \psi_k \, \epsilon_o \, \text{div} \, \dot{E}_2 + \int_v d\tau \, \epsilon_o \dot{E}_2 \cdot \text{grad} \, \psi_k \, . \end{aligned}$$

By Eq 10.23 the last term vanishes. Furthermore, $\epsilon_o \operatorname{div} \dot{E}_2 = \dot{\rho}$, so that

$$i_{ik} = \int_{S_k} (\rho v)_n \, dS_k + \int_v d\tau \, \psi_k \, \dot{\rho} \tag{10.25}$$

or

$$i_{ik} = \int_{S_k} (\rho v)_n \, dS_k + \frac{\partial}{\partial t} \int_v \psi_k \, \rho \, d\tau \tag{10.26}$$

or

$$i_{ik} = \int_{S_k} (\rho v)_n \, dS_k + \frac{\partial}{\partial t} \int_v \psi_k \, dq \, , \tag{10.27}$$

where dq represents a charge element. Eqs 10.23, 10.25, and 10.26 are the forms for the current relationships, which were sought.

It is noted that in Eq 10.27 there exist two components: one is merely the arrival current at the terminal; the other is the time rate of change of the induced displacement flux terminating on the electrode. Since the displacement flux to an electrode is equal in magnitude to the induced charge on that electrode, it appears that

$$q_k = - \int_v \psi_k \, dq \, , \tag{10.28}$$

where q_k is the induced charge. This can be proved.

It should be mentioned that the induced-current theory developed could be applied to a part of an electrode surface, or to any conducting or nonconducting surface. Also, the theory is easily adapted to the use of generalized coordinates by writing $\rho \, d\tau = dq$.

Energy Balance. Certain observations on the energy balance naturally follow from the theory developed.* ψ_k was introduced without any reference to the physical significance that might be associated with this scalar function. However, some associated physical properties do appear. ψ_k may be thought of as a coupling factor in view of Eq 10.27. Other interpretations are possible. If Φ_k is the potential on the k'th electrode, then the space-charge-free potential at any point in the interaction space due to the applied potentials is

$$\phi_1 = \sum_k \Phi_k \psi_k , \tag{10.29}$$

with the corresponding field

$$E_1 = - \sum_k \Phi_k \operatorname{grad} \psi_k . \tag{10.30}$$

These relations lead to interesting results. For instance, the power delivered by the space charge to the terminals becomes

$$\sum_k \Phi_k i_{ik} = \sum_k \Phi_k \int_v d\tau \, \rho v \cdot \operatorname{grad} \psi_k$$

$$= - \int_v d\tau \, \rho v \cdot E_1 , \tag{10.31}$$

while

---

* Although these ideas are not necessary to the developments of this report, they will be included here for future reference.

$$\sum_k \Phi_k i_{ck} = \sum_k \Phi_k \int_v d\tau\, \epsilon_o \dot{E}_1 \cdot \text{grad}\, \psi_k$$

$$= -\epsilon_o \int_v d\tau\, \dot{E}_1 \cdot E_1 = -\frac{\epsilon_o}{2} \frac{d}{dt} \int_v E_1^2 d\tau \quad . \quad (10.32)$$

The right-hand member of this expression is the time rate of change of the energy stored in the E_1 field, and so averages zero for periodic processes. Thus, the capacitative current does not contribute on the average to the power transfer.

The following interesting formulae result from Eq 10.23:

$$\int_v E_2 \cdot J_c\, d\tau = \int_v E_2 \cdot E_1\, d\tau = \int_v E_2 \cdot J_i\, d\tau = 0 \quad . \quad (10.33)$$

It is evident that if any of the vectors are differentiated with respect to time, the equations are still true. The last integral is

$$\int_v E_2 \cdot J_i\, d\tau = \int_v \rho v \cdot E_2\, d\tau + \frac{\epsilon_o}{2} \frac{d}{dt} \int_v E_2^2 d\tau = 0 \quad , \quad (10.34)$$

which states that all the work done per unit time by the field established by the space charge goes into kinetic energy of the particles. Other observations of this sort are possible.*

11. Induced Current in the Magnetron (S. Ruthberg, H. W. Batten, W. Peterson, H. W. Welch, Jr.)

In principle, the current due to the space-charge behavior can be obtained by Eq 10.26, provided ψ_k and ρ are known. But, this is just

---

* For associated discussion, see Ref. 19-23.

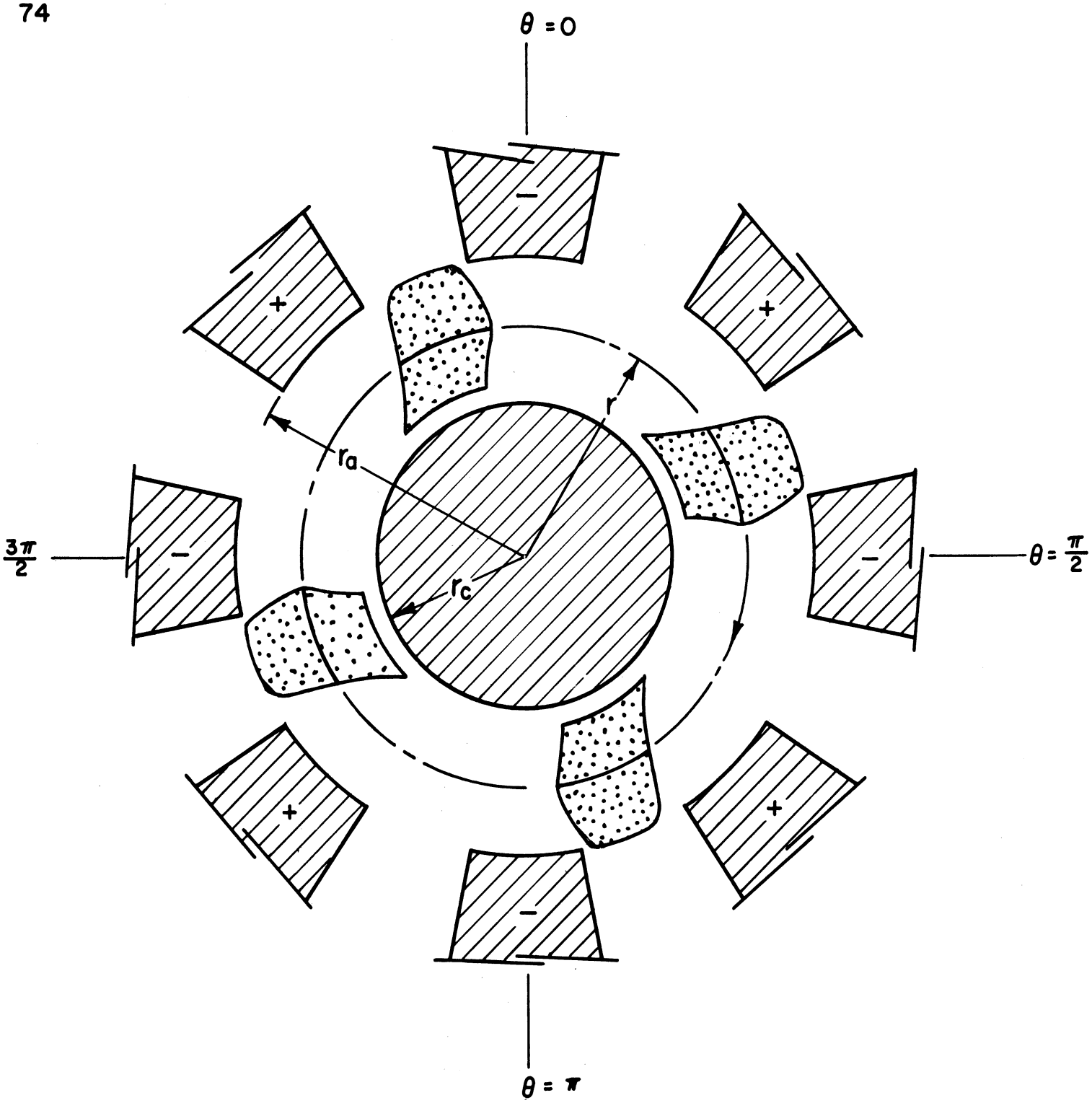

FIG. II.1

SKETCH OF SPACE-CHARGE SPOKES WITH SYMBOLS USED IN THIS SECTION

where the difficulty arises in magnetron theory. ψ_k can be given with reasonable accuracy, but the space-charge distribution is not known. If the space-charge distribution responsible for the induced current is periodic in θ and rotating with constant velocity, a general expression can be given for any component of the induced current. Then, one can make computations based on the hypothetical distributions discussed in Section 4 and compare them with experimental results. This is carried through in this section. Also, an approximate method is given for arbitrary space-charge distribution.

Let the magnetron be operating in the π mode with all space charge in the interaction space rotating synchronously with the r-f field at an angular velocity ω_n. The periodic space charge distribution may be thought of as spokes. Further, this is a steady-state process; i.e., the charge distribution in the spokes is constant, although there is a transport of charge through the spokes to the anodes, contributing to the d-c current. Thus, the time rate of change of the displacement vector on an anode, hence the induced current, is caused by the rotation of the spokes. The value of the induced current is given by the second term of Eq 10.26,

$$i_k = -\frac{\partial}{\partial t} \int_v \psi_k \rho \, d\tau \, . \qquad (11.1)$$

The arrival current,

$$\int_{S_k} (\rho v)_n \, dS_k \, ,$$

is the transport of charge from the spokes to the anodes.

In π-mode operation, alternate anode segments of the magnetron are at the same potential, with the number of spokes in the discharge equal to the number of r-f wavelengths in the periphery, which is half the number of anode segments, or N/2 for N the number of anode segments. ψ_k is chosen as unity at the anodes of one set (unity on every other segment) and zero elsewhere, with the advantage that it then has a periodic value in the interaction space. The space-charge distribution is also periodic. Thus, as a two-dimensional problem, both ψ_k and ρ can be given as Fourier expansions. That is to say, at <u>each</u> value of the radius r in the interaction space, re Fig. 11.1,

$$\psi_k = \sum_n A_n \cos n \frac{N}{2} \theta \quad . \tag{11.2}$$

The A's are now functions of r only; the angular measure is so chosen that ψ_k is symmetric about $\theta = 0$. This is no restriction. The charge distribution is periodic in a system rotating with the spokes, so at each value of r take

$$\rho = \sum_a B_a \cos a \frac{N}{2} (\theta - \theta_1) + \sum_a C_a \sin a \frac{N}{2} (\theta - \theta_1) \quad , \tag{11.3}$$

where $\theta_1 = \omega_n t$ is the angle swept out by the rotating system in time t, $\theta' = \theta - \theta_1$ is the angular measure in the rotating system, and $\theta' = \theta$ at $t = 0$. Note that ρ need not be symmetric.

Then, the instantaneous value of the induced current becomes, after insertion of L as the axial length of the magnetron interaction space

$$i_k = - \frac{\partial}{\partial t} \int_{-\pi}^{\pi} \int_{r_1}^{r_2} \psi_k \rho L r \, dr \, d\theta \quad . \tag{11.4}$$

Substitution of the Fourier expansions into this expression gives

$$i_k = -L\frac{\partial}{\partial t}\sum_{n,a}\int_{-\pi}^{\pi}\int_{r_1}^{r_2} A_n \cos n\frac{N}{2}\theta\left[B_a \cos a\frac{N}{2}(\theta-\theta_1) + C_a \sin a\frac{N}{2}(\theta-\theta_1)\right] r\,dr\,d\theta .$$

Since the coefficients A's, B's, and C's are independent of θ, all terms vanish for $a \neq n$ by orthogonality conditions. Therefore,

$$i_k = -L\frac{\partial}{\partial t}\sum_{n}\left[\int_{-\pi}^{\pi}\cos n\frac{N}{2}\theta\cos n\frac{N}{2}(\theta-\theta_1)\int_{r_1}^{r_2} A_nB_n r\,dr + \int_{-\pi}^{\pi}\cos n\frac{N}{2}\theta\sin n\frac{N}{2}(\theta-\theta_1)\int_{r_1}^{r_2} A_nC_n r\,dr\right]$$

or

$$i_k = -L\pi\frac{\partial}{\partial t}\sum_{n}\left[\cos n\frac{N}{2}\theta_1\int_{r_1}^{r_2} A_nB_n r\,dr - \sin n\frac{N}{2}\theta_1\int_{r_1}^{r_2} A_nC_n r\,dr\right] \quad (11.5)$$

The coefficients B_n and C_n are:

$$B_n = \frac{N}{2\pi}\int_{-2\pi/N}^{2\pi/N}\rho(r,\theta-\theta_1)\cos n\frac{N}{2}(\theta-\theta_1)\,d(\theta-\theta_1) \quad (11.6)$$

$$C_n = \frac{N}{2\pi}\int_{-2\pi/N}^{2\pi/N}\rho(r,\theta-\theta_1)\sin n\frac{N}{2}(\theta-\theta_1)\,d(\theta-\theta_1) . \quad (11.7)$$

The A_n's come from the solution of Laplace's equation for ψ_k.

The important component of the induced current is the fundamental.

$$i_{k1} = L\pi \frac{N}{2} \omega_n \left[\sin \frac{N}{2} \theta_1 \int_{r_1}^{r_2} A_1 B_1 r dr + \cos \frac{N}{2} \theta_1 \int_{r_1}^{r_2} A_1 C_1 r dr \right] \quad (11.8)$$

with amplitudes

$$I_{k1} = L \pi \frac{N}{2} \omega_n \int_{r_1}^{r_2} A_1 B_1 r dr$$

and (11.9)

$$I'_{k1} = L \pi \frac{N}{2} \omega_n \int_{r_1}^{r_2} A_1 C_1 r dr \ .$$

If the total charge in the interaction space is introduced, then since $(N/2)\omega_n = \omega = 2\pi f$,

$$I_{k1} = 4 Q f \int_{r_1}^{r_2} \frac{\pi A_1}{2} \cdot \frac{\pi B_1}{Q} L r dr \ , \quad (11.10)$$

with similar form for I'_{k1}. This last form has a significant interpretation because $\pi A_n/2 \leq 1$ and the root of the sum of the squares of $\int(\pi B_1/Q)Lrdr$ and $\int(\pi C_1/Q)Lrdr \leq 1$, as will be shown later. Thus, $4Qf$ is the maximum r-f induced current obtainable. It is realized by N/2 point charges of value $Q/(N/2)$, equally spaced, rotating at the anode radius with extremely small spacing between anode segments. The factor F, which follows, represents a sort of "figure of merit" for the induced current under these circumstances.

$$F = \left[\left(\int_{r_1}^{r_2} \frac{\pi A_1}{2} \cdot \frac{\pi B_1}{Q} L r dr \right)^2 + \left(\int_{r_1}^{r_2} \frac{\pi A_1}{2} \cdot \frac{\pi C_1}{Q} L r dr \right)^2 \right]^{1/2}$$

The problem now is to determine the nature of the integrals of Eq 11.9, which means first an evaluation of the coefficients. A_n is to come from solution of $\nabla^2 \psi_k = 0$ for a cylindrical geometry with no axial dependence.

$$\frac{1}{r}\left[\frac{\partial}{\partial r} r \frac{\partial}{\partial r} \psi_k + \frac{\partial}{\partial \theta} \frac{1}{r} \frac{\partial}{\partial \theta} \psi_k\right] = 0 .$$

It is assumed that a solution for ψ_k is a separable function, $X(\theta) \cdot B(R)$. Substitution of this gives

$$\frac{r^2}{B} \frac{d}{dr} r \frac{dB}{dr} = \gamma$$

$$\frac{1}{X} \frac{d^2X}{d\theta^2} = -\gamma .$$

The solution of the second is trigonometric, which with the conditions of single-valuedness, symmetry about $\theta = 0$, and periodicity gives the form $\cos n(N/2)\theta$, n being integral. The solution of the first is exponential. Thus, completely,

$$\psi_k = \sum_n \left(C_n r^{n(N/2)} + D_n r^{-n(N/2)}\right) \cos n \frac{N}{2} \theta ,$$

where the C's and D's are constants. However, since the induced current is to be found in the anode, ψ_k must vanish on the cathode, so that $D_n = -C_n r_c^{2n(N/2)}$. Let $R = r/r_c$ and $g_n = C_n r_c^{n(N/2)}$; then

$$\psi_k = \sum_n g_n \left(R^{n(N/2)} - R^{-n(N/2)}\right) \cos n \frac{N}{2} \theta . \qquad (11.11)$$

Now A_n is taken as $g_n \left(R^{n(N/2)} - R^{-n(N/2)}\right)$. g_n can be determined if the form for ψ_k is known at some value of R.

One either must know the actual form of ψ_k at some value of R or must make further approximation. The latter is done with sufficient accuracy for the purposes of this report.

Approximation for ψ_k. It can be seen from field maps that the potential function is close to being linear at the anode radius of the magnetron.* So, assume such a linear variation for ψ_k between anode elements at the anode radius. $\psi_k(\theta, r_a)$ has the form shown in Fig. 11.2. From Eq 11.11

$$g_n \left(R_a^{n(N/2)} - R_a^{-n(N/2)} \right) = \frac{N}{2\pi} \int_{-2\pi/N}^{2\pi/N} \psi_k(\theta, R_a) \cos n \frac{N}{2} \theta \, d\theta \quad .$$

ψ_k is unity from $\theta = 0$ to $\pi/N - \alpha$ and is $(1/2\alpha)(\pi/N + \alpha - \theta)$ from $\pi/N - \alpha$ to $\pi/N + \alpha$. Then the integral has the form

$$\frac{N}{\pi} \left[\int_0^{\frac{\pi}{N} - \alpha} \cos n \frac{N}{2} \theta \, d\theta + \int_{\frac{\pi}{N} - \alpha}^{\frac{\pi}{N} + \alpha} \frac{1}{2\alpha} \left(\frac{\pi}{N} + \alpha - \theta \right) \cos n \frac{N}{2} \theta \, d\theta \right],$$

which gives

$$g_n \left(R_a^{n(N/2)} - R_a^{-n(N/2)} \right) = \frac{\sin n(\pi/2)}{n(\pi/2)} \cdot \frac{\sin n(N/2)\alpha}{n(N/2)\alpha} \quad .$$

Therefore,

$$A_n = \frac{R^{n(N/2)} - R^{-n(N/2)}}{R_a^{n(N/2)} - R_a^{-n(N/2)}} \cdot \frac{\sin n(\pi/2)}{n(\pi/2)} \cdot \frac{\sin n(N/2)\alpha}{n(N/2)\alpha} \quad . \qquad (11.12)$$

---

* Technical Report No. 6, Fig. 7.2a.

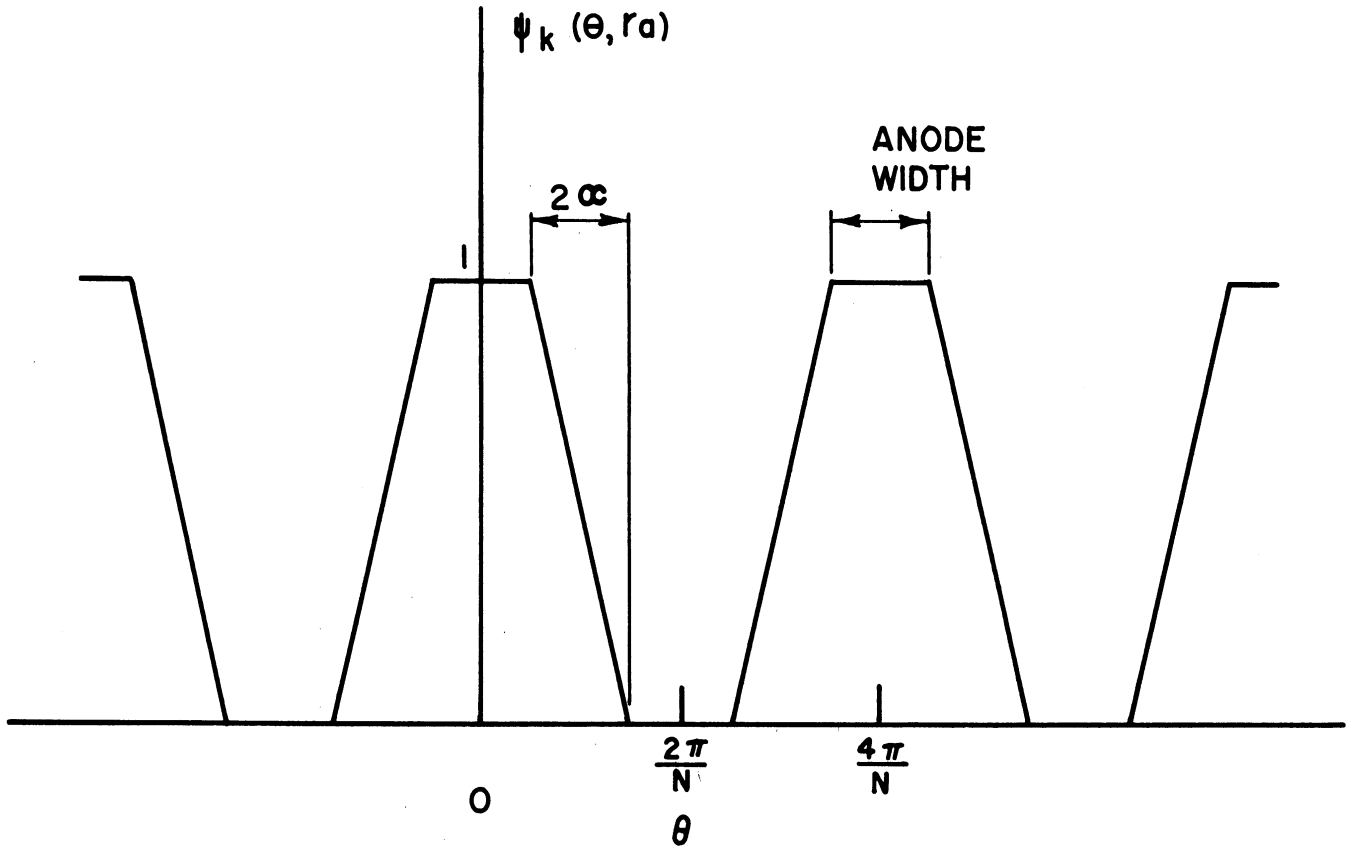

FIG. II.2
ANGULAR VARIATION OF Ψ_k AT ANODE RADIUS

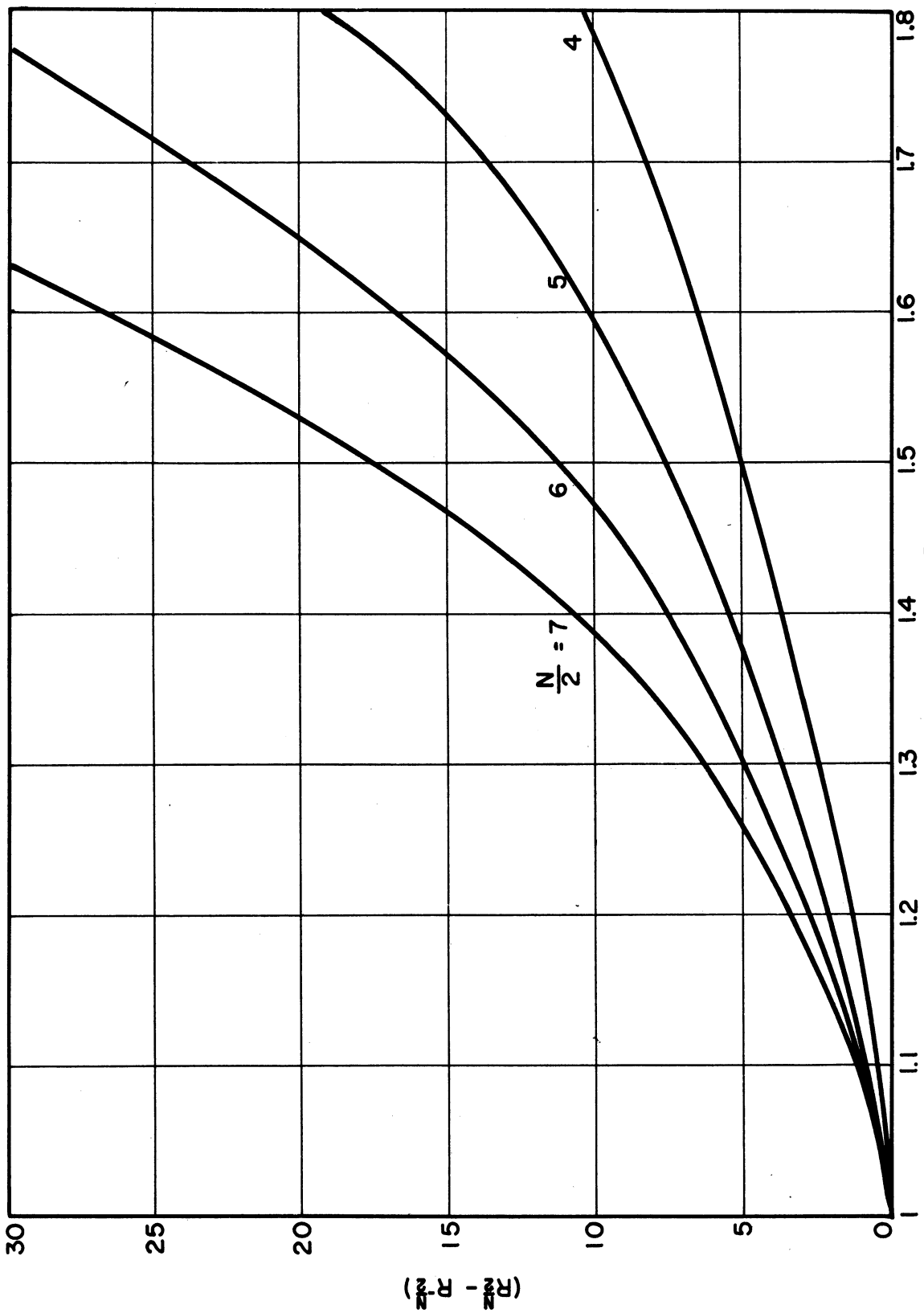

FIG. 11.3
FACTOR PRESENT IN EQUATION (11.12)

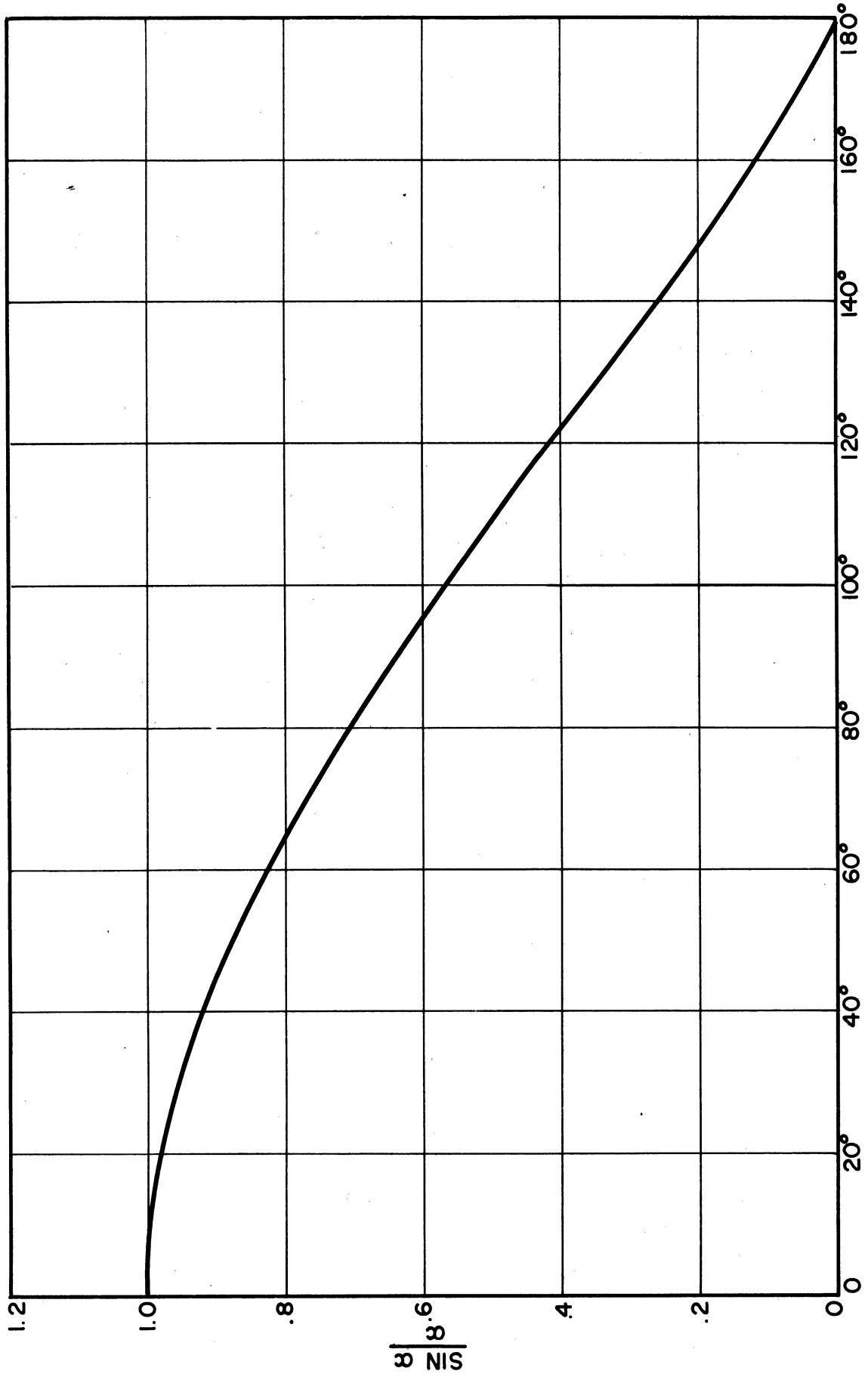

FIG. 11.4
FACTOR PRESENT IN EQUATION (11.12)

The earlier observations concerning the factor $\pi A_n/2$ can easily be verified from this. Graphs of $(R^{N/2} - R^{-N/2})$ and $(\sin\alpha/\alpha)$ are given in Figs. 11.3 and 11.4.

The determination of the B's and C's is not so easily carried through. In general, the angular limits of the spoke vary with r, e.g., Fig. 11.1. Thus, rewriting Eq 11.6,

$$B_n = \frac{N}{2\pi} \int_{\beta(r)}^{\gamma(r)} \rho(r,\theta') \cos n \frac{N}{2} \theta' \, d\theta' \quad , \tag{11.13}$$

where both integrand and limits depend upon r as parameter.

Trial Form for $\rho(R,\theta)$. Since the difficulty does exist that the distribution of ρ must be known in detail for Eq 11.13 to be evaluated, consider the simple case in which the spokes have the well differentiated shape shown in Fig. 11.5, and assume that within each spoke the space-charge density is a constant. Let them be symmetrically placed. Then the C_n's are zero.

$$B_n = \frac{N}{2\pi} \int_{-\beta}^{\beta} \rho \cos n \frac{N}{2} \theta' \, d\theta'$$

or

$$B_n = \frac{2\rho}{n\pi} \sin n \frac{N}{2} \beta \quad . \tag{11.14}$$

The total charge in the spokes is $(N/2)\, \rho\, r_c^2 (R_2^2 - R_1^2)\beta\, L$. Thus,

$$\frac{B_n}{Q} = \frac{2}{\pi L r_c^2} \frac{1}{R_2^2 - R_1^2} \frac{\sin n(N/2)\beta}{n(N/2)\beta} \quad . \tag{11.15}$$

Note that

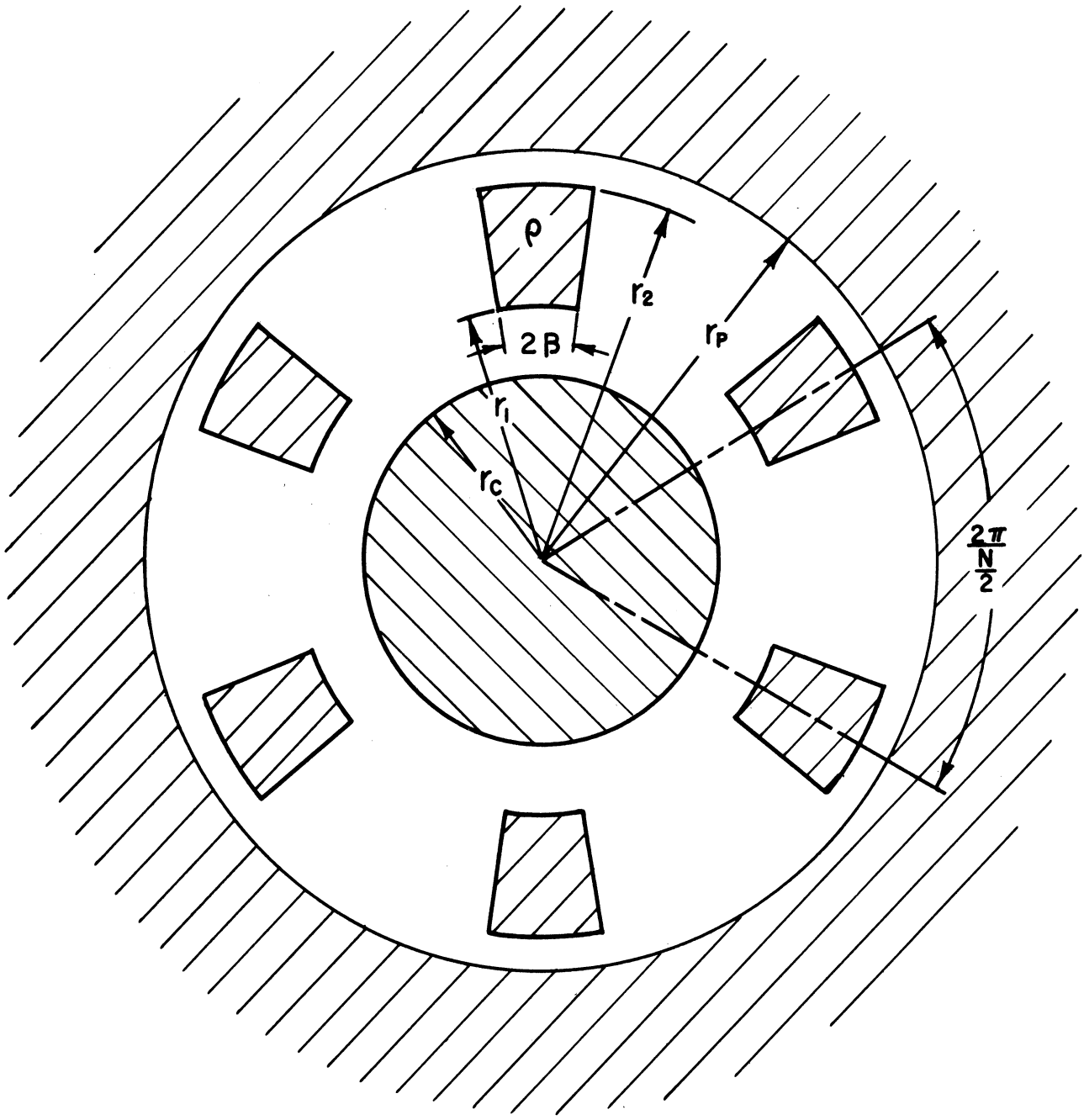

FIG. 11.5
SPACE CHARGE CONFIGURATION ASSUMED

$$\int_{r_1}^{r_2} \pi \frac{B_n}{Q} L\, r\, dr = \pi \frac{B_n}{Q} L \frac{r_2^2 - r_1^2}{2} = \frac{\sin n(N/2)\beta}{n(N/2)\beta} \leq 1 ,$$

as indicated previously.

The fundamental is found from Eq 11.9,

$$I_{kl} = L \pi r_c^2 \omega \int A_1 B_1 R\, dR$$

$$= 8Lr_c^2 f\rho \frac{1}{R_a^{N/2} - R_a^{-N/2}} \frac{\sin (N/2)\alpha}{(N/2)\alpha} \sin \frac{N}{2}\beta \left[\frac{R_2^{(N/2)+2}}{(N/2)+2} + \frac{R_2^{2-(N/2)}}{(N/2)-2} - \frac{R_1^{(N/2)+2}}{(N/2)+2} - \frac{R_1^{2-(N/2)}}{(N/2)-2} \right] \qquad (11.16)$$

The value of ρ entering is taken as the synchronous charge density.*

$$\rho = -2 \epsilon_o \frac{m}{e} \omega_n (\omega_c - \omega_n) . \qquad (11.17)$$

Calculations have been made for two different magnetrons based on this distribution. The results are given in the following section.

Induced Current for Point Charges. The form for B_n given in Eq 11.14 for the well differentiated spoke of constant space-charge density can be used to extend the analysis to the induced current due to point charges rotating in synchronism with the r-f wave. Each spoke is collapsed into a point charge at a chosen radius and angle. Choose the

---

* See Ref. 1, page 40, Eq 5.30. The question arises as to whether this density should be the average density in the region swept out by the spokes, in which case the density given by 11.17 should be multiplied by approximately 2 to give the density in the spoke, or the average density in the spoke itself, or some intermediate value. For the present the second assumption is made, to be corrected later if found to be in error.

angular position of the point charge so that it lies on the line of symmetry of its parent spoke. It is not necessary to choose this distribution to extend the previous equations for induced current, but since the method is to shrink each spoke to a given point, anyway, it is convenient to choose this simple distribution. Thus, the induced current is being found for N/2 point charges, each $4\pi/N$ radians from the next, and all located at the same radius. So, by Eq 11.5,

$$i_k = \sum_{n=1}^{\infty} \left[L \pi r_c^2 n\omega \int A_n B_n R \, dR \right] \sin n \frac{N}{2} \theta_1 \quad . \qquad (11.18)$$

A_n is taken from Eq 11.12; B_n, from 11.14. The factor of $A_n B_n R dR$ becomes

$$\frac{\sin n\pi/2}{n\pi/2} \frac{\sin n(N/2)\alpha}{n(N/2)\alpha} \frac{1}{R_a^{nN/2} - R_a^{-nN/2}} \int_{R_1}^{R_2} \int_{-\beta}^{\beta} \left[R^{nN/2} - R^{-nN/2} \right] \rho R \cos n \frac{N}{2} \theta' d\theta' dR$$

Collapse the spoke to an angle θ_o' and radius R, taking lim $\rho R \, d\theta' \, dR$ as q for $\Delta\beta$ and $\Delta R \to 0$. This gives

$$\frac{\sin n\pi/2}{n\pi/2} \cdot \frac{\sin n(N/2)\alpha}{n(N/2)\alpha} \cdot \frac{R^{nN/2} - R^{-nN/2}}{R_a^{nN/2} - R_a^{-nN/2}} \cos n \frac{N}{2} \theta_o' \quad .$$

θ_o' is given the values of the mid-line of each spoke, i.e., 0, $4\pi/N$, $2 \cdot 4\pi/N$, . . ., so that the cosine term becomes unity. Hence

$$i_k = \sum_{n=1}^{\infty} \frac{N}{2} 4 L r_c^2 q f \sin \frac{n\pi}{2} \frac{\sin n(N/2)\alpha}{n(N/2)\alpha} \frac{R^{nN/2} - R^{-nN/2}}{R_a^{nN/2} - R_a^{-nN/2}} \sin n \frac{N}{2} \theta_1 \quad .$$

But, the sin $n\pi/2$ is nonzero for odd values of n; therefore, this is put into the form

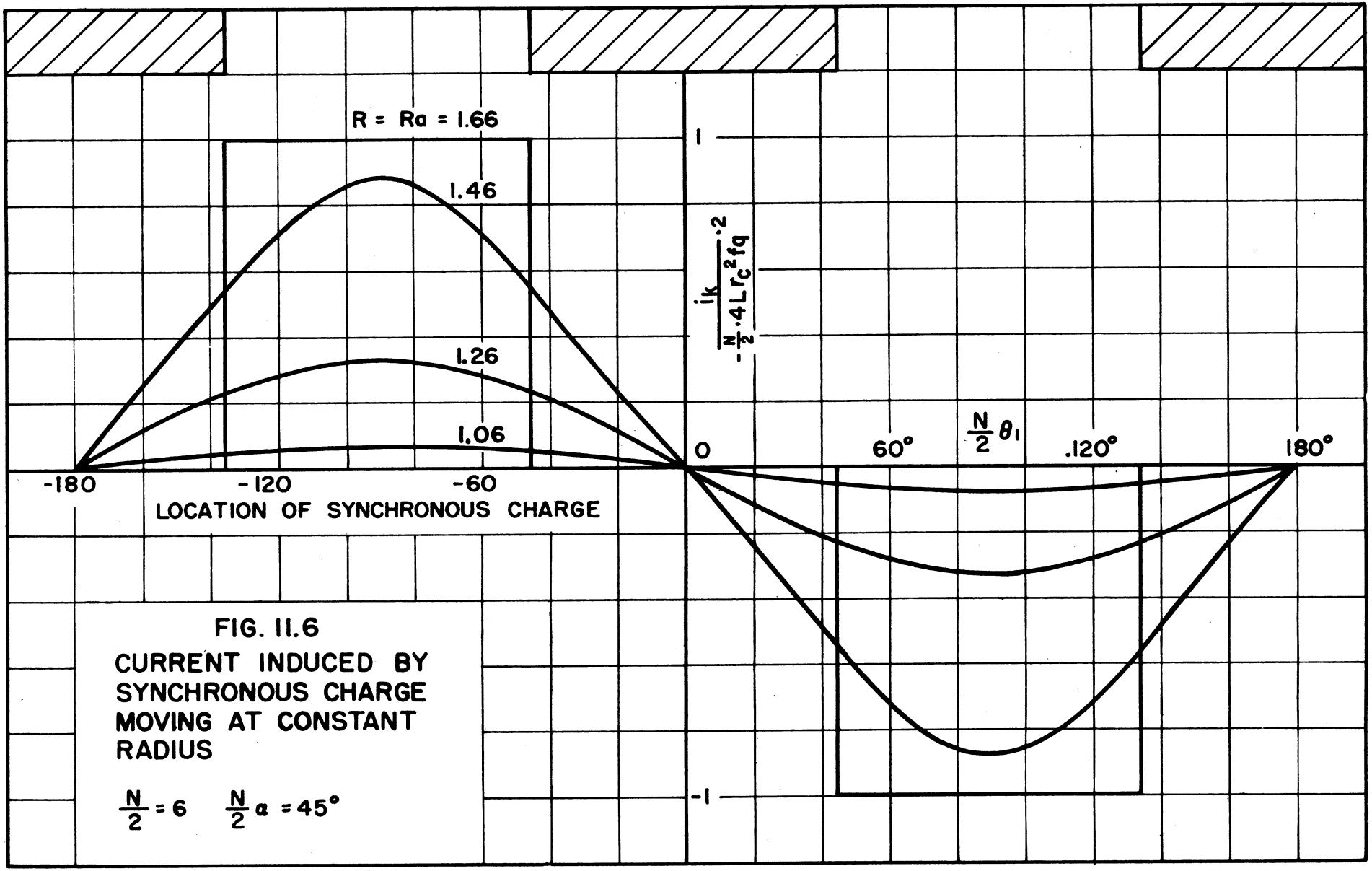

FIG. 11.6
CURRENT INDUCED BY SYNCHRONOUS CHARGE MOVING AT CONSTANT RADIUS

$\frac{N}{2} = 6 \quad \frac{N}{2}\alpha = 45°$

$$\frac{i_k}{\frac{N}{2}4Lr_c{}^2fq} = \sum_{n=0}^{\infty} (-1)^n \frac{\sin(2n+1)(N/2)\alpha}{(2n+1)(N/2)\alpha} \frac{R^{(2n+1)N/2} - R^{-(2n+1)N/2}}{R_a^{(2n+1)N/2} - R_a^{-(2n+1)N/2}} \sin(2n+1)\frac{N}{2}\theta_1 \tag{11.19}$$

Representative results are given in Fig. 11.6. Note the maximum value is obtained for $\alpha = 0$ and $R = R_a$, as pointed out previously.

Approximation Method of Calculation. A further step is to use the results obtained for rotating point charges for an approximation method of calculation of current due to any type of spoke. Given any arbitrarily shaped spoke, one may partition this into squares. Each square is then replaced by a point charge of equal value. The instantaneous current is the arithmetic sum formed from each contribution of Eq 11.19, but any harmonic amplitude is the vector sum to account for the angular difference of the point locations (phase shift). Since a harmonic is proportional to $R^{nN/2}$, the location of the equivalent point charge within a square must be weighted. If R_o represents the location of the charge q, it is found as

$$R_o{}^{nN/2}\, q = \int_\theta \int_R \rho\, R^{nN/2}\, R\, dR\, d\theta ,$$

where q is $\int_\theta \int_R \rho R\, dR\, d\theta$. For ρ constant and an angle subtended of θ,

$$R_o{}^{nN/2}\, \theta \frac{\left(R_2{}^2 - R_1{}^2\right)}{2} = \theta \frac{R_2{}^{n(N/2)+2} - R_1{}^{n(N/2)+2}}{n(N/2) + 2}$$

so that

$$R_o{}^{nN/2} = \frac{R_2{}^{n(N/2)+2} - R_1{}^{n(N/2)+2}}{\left(n(N/4) + 1\right)\left(R_2{}^2 - R_1{}^2\right)} . \tag{11.20}$$

Note that R_o is different for each harmonic. Figs. 11.7a and 11.7b are representative applications. Results are given in the following section.

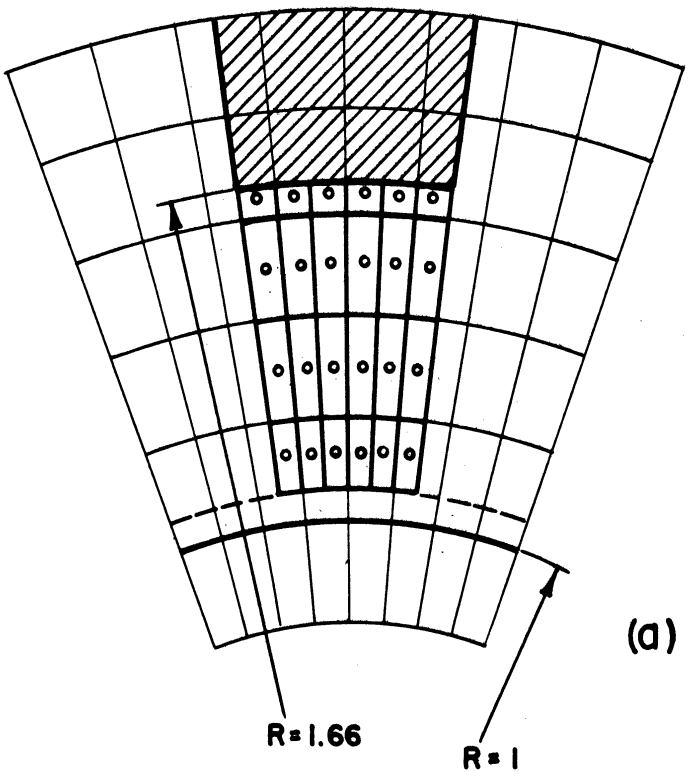

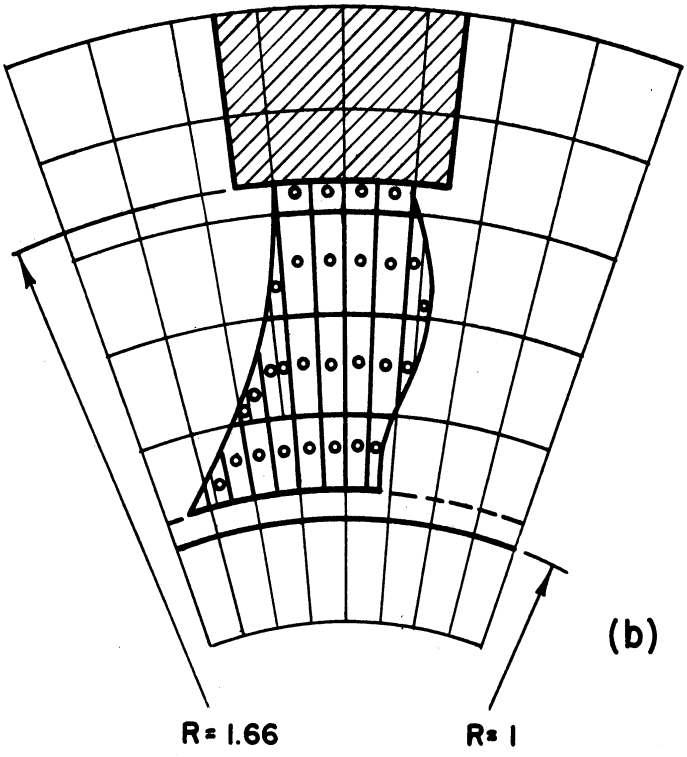

FIG. 11.7

APPROXIMATION METHOD FOR CALCULATION OF INDUCED CURRENT

Another scheme is to use the distribution of Fig. 11.5 directly by cutting the spoke into sectors and getting the contribution of each sector. This eliminates the calculation of R_o; but, on the other hand, it needs a longer calculation for each amplitude.

12. Calculation of Induced Current for Some Special Cases (S. Ruthberg, H. W. Batten)

Now the formulae of the preceding section are applied to some actually existent magnetrons. Numerical results are given. A comparison with experimental values and the discussion of these are made in Section 14.

a) The relations found for symmetrical spokes of constant charge density are applied to the Model 3 magnetron of this laboratory. See the appendix for tube parameters and Fig. 11.5, again, for this distribution.

Assume that a spoke subtends the same angle as an anode segment and that the spoke extends from the space-charge-swarm boundary to the anode. Thus, the spoke lies between the radius at which the charge comes up to synchronism with the r-f field and the anode. Then, the factors in Eq 11.16 are

$$(N/2)\,\alpha = (N/2)\,\beta = 45^\circ$$

$$r_2 = r_a$$

$$r_1 = r_n = \text{synchronous radius} = 1.06\, r_c \ .$$

This last is found from the relation

$$\omega_n = \omega_L \left(1 - \frac{r_c^2}{r_n^2} \right),$$

where ω_L is the Larmor angular velocity.* That is, $r_1 = r_c\sqrt{\frac{N}{2}\omega_L/(\frac{N}{2}\omega_L - 2\pi f)}$

From Eq 11.17

$$\rho = -6.03 \times 10^{-3} \text{ coulombs/m}^3 .$$

Also,

$$\frac{\sin (N/2)\alpha}{(N/2)\alpha} = 0.90$$

$$\sin (N/2)\beta = 0.707$$

$$\frac{1}{R_a^{N/2} - R_a^{-N/2}} = \frac{1}{21}$$

$$\frac{R_2^{(N/2)+2}}{(N/2)+2} + \frac{R_2^{2-(N/2)}}{(N/2)-2} - \frac{R_1^{(N/2)+2}}{(N/2)+2} - \frac{R_1^{2-(N/2)}}{(N/2)-2} = 6.69 .$$

Therefore, by Eq 11.16,

$$I_{k1} = 0.866 \text{ amp} .$$

This gives 0.612 amp rms for the fundamental component.

b) This same constant-charge-density distribution is tried on magnetron Model 7. The parameters and drawing are given in the appendix.

The vanes and bars, as wlll as the spacing between, subtend angles of arc $\pi/16$radians, since there are 16 anode segments. Then

$$R_a = 1.75$$

$$R_1 = R_n = 1.078$$

$$\rho = -3.84 \times 10^{-3} \text{ coulombs/m}^3$$

$$(N/2)\alpha = (N/2)\beta = \pi/4 \text{ radians}$$

$$\frac{\sin (N/2)\alpha}{(N/2)\alpha} = 0.9$$

$$\sin (N/2)\beta = 0.707 .$$

---

* See Ref. 1, page 28, Eq 6.5.

The amplitude of the fundamental component of the induced current is 1.384 amps, giving the rms value of 0.97 amps.

For the current for point charges, Eq 11.19 has been applied to Model 3 magnetrons. The results for a number of values of radius are given in Fig. 11.6 as functions of the location of the charges.

The Approximation Method.

I. As the first trial the fundamental is computed for the symmetrical-spoke, constant-charge-density case for Model 3 and compared to the exact result. This is given in Fig. 11.7a, where the spoke has been partitioned appropriately. The next step is to calculate the area of each section and hence the charge. The equivalent charge is located by Eq 11.20, where R_2 and R_1 are the bounding radii of the section. After this the amplitude of the fundamental can be had by Eq 11.19. The contributions of all the charges at the same angle are added arithmetically. The contributions for different angles are added vectorily with the phase difference in angles of $(N/2)\theta_1$.

The degree of approximation taken in Fig. 11.7a results in 0.91 amp peak value. This compares to 0.866 for the direct calculation of 12a.

II. The distribution of Fig. 11.7b for the same constant charge density gives 0.586 amp, peak. Note that the amount of charge near the anode is less for this case than for Fig. 11.7a. The greatest contributions come from those charges near the anode, since the fundamental drops off as R^6 or, in general, as $R^{N/2}$.

13. Methods for Calculation of R-F Currents from Experimental Observations and Estimation of Frequency Pushing (H. W. Welch, Jr.)

In Section 5, the mechanism of frequency pushing was described from the point of view of the space-charge behavior. In Sections 11 and 12, we have introduced methods for the calculation of the magnitude of the current induced by a rotating space-charge swarm with spokes. In this section, we will present a method for calculation of the r-f current from experimental observations and the estimation of frequency-pushing curves. It will then be possible to check the accuracy of the space-charge picture by direct comparison of results.

If we hold to the assumption that the only effect of raising the anode voltage is to increase the velocity of the spokes and advance the phase of the r-f current relative to the r-f voltage, we are making the assumption that the magnetron space-charge swarm is a constant-current generator. This has frequently been assumed to be approximately true in the discussion of the magnetron. We will find, however, that in the cases discussed here it is not true and, if one considers carefully the mechanism of the spoke formation, it does not appear to be a correct assumption. Nevertheless, it is convenient to use a current generator in discussing the magnetron equivalent circuit. This will be done and we will find that in a particular case the current-generator output is approximately proportional to the 2/3 power of the r-f voltage.

In Fig. 13.1 is given a simplified equivalent circuit of a magnetron.* The input admittance of this circuit near resonance seen from the terminals T - T' is given by the following:

---

* See Ref. 2 for further discussion of this circuit.

$$Y_T = \frac{I_g}{E_T} \angle\phi = \frac{Y_{oc}}{Q_L} \sqrt{1 + 4\delta^2 Q_L^2} \angle\tan^{-1} 2\delta Q_L . \quad (13.1)$$

This notation implies that the magnitude of the current delivered is not necessarily a function of the phase angle between the current and the voltage, ϕ, or the r-f voltage E_T. This will be shown to be untrue in experimental observations. The other symbols used in the expression are defined as follows:

$$Y_{oc} = \omega_o C \qquad \text{where} \qquad \omega_o = 1/\sqrt{LC}$$

$$\delta = \frac{\omega - \omega_o}{\omega_o} = \frac{\lambda_o - \lambda}{\lambda_o}$$

$$Q_L = \frac{Y_{oc}}{G_T + G_L} .$$

The various factors in this equation are plotted in Fig. 13.2. The r-f voltage at T - T', i.e., between anode sets in the magnetron, is given by

$$E_T = \frac{I_g}{(Y_{oc}/Q_L)\sqrt{1 + 4\delta^2 Q_L^2}} .$$

The power delivered to the load is given by

$$P_L = E_T^2 G_L$$

or

$$P_L = \frac{I_g^2}{(Y_{oc}/Q_L)^2 (1 + 4\delta^2 Q_L^2)} G_L . \quad (13.2)$$

G_L may be written in terms of external Q for matched load:

$$G_L = \frac{Y_{oc}}{Q_e} . \quad (13.3)$$

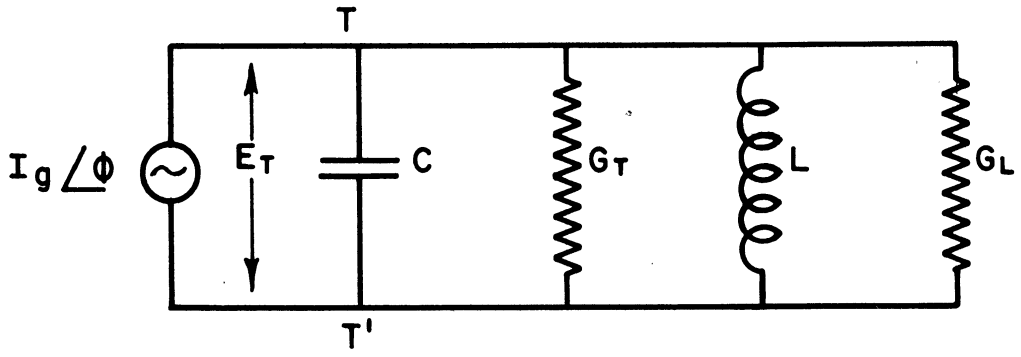

FIG. 13.1
EQUIVALENT CIRCUIT FOR OSCILLATING MAGNETRON

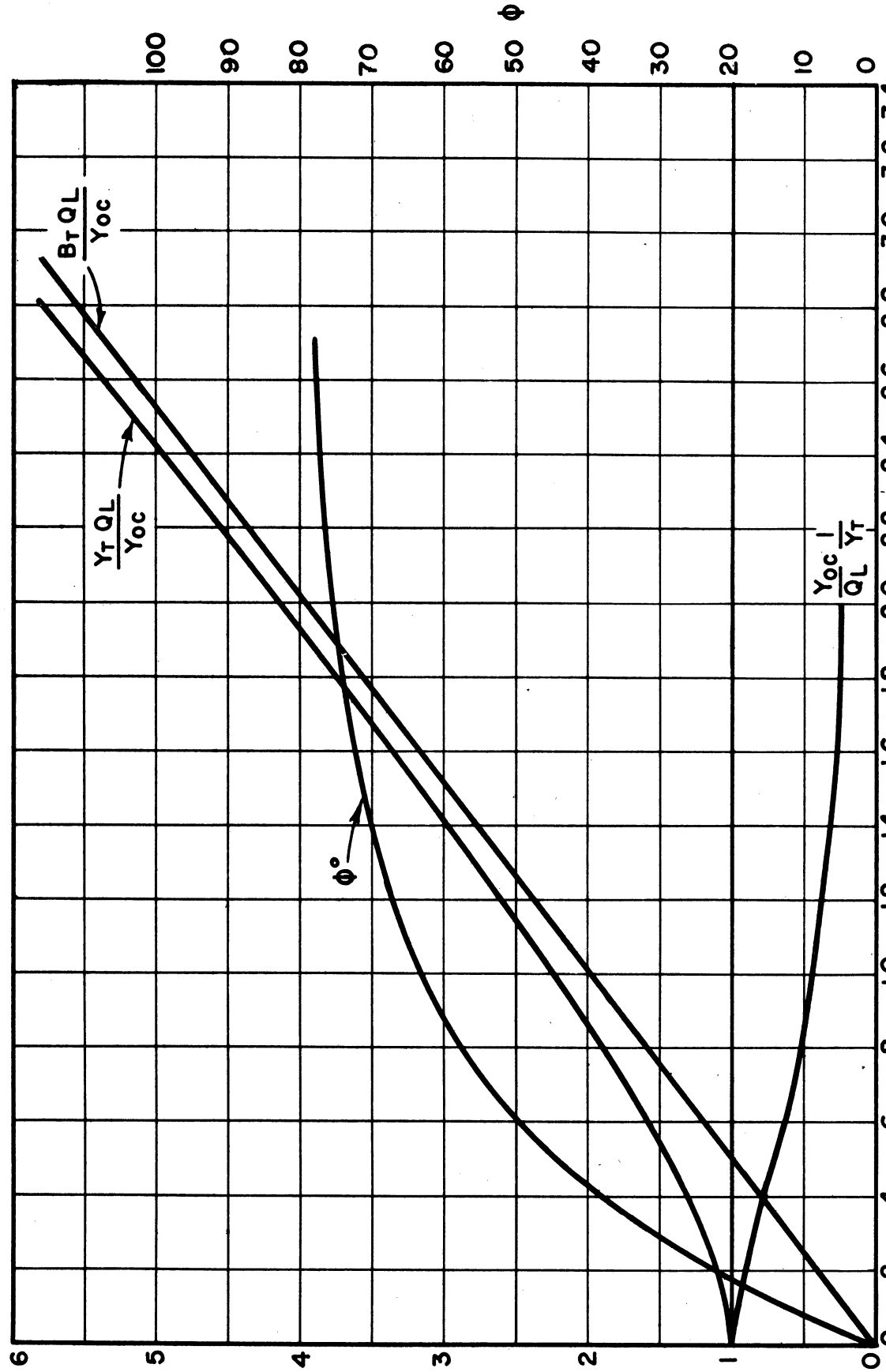

FIG. 13.2 PARAMETERS INVOLVED IN EQUATION 13.1 APPLYING TO CIRCUIT OF FIG. 13.1

Q_e can be determined from the measurable Q's, unloaded and loaded, by the following:

$$\frac{1}{Q_e} = \frac{1}{Q_L} - \frac{1}{Q_o} \quad . \tag{13.4}$$

Eq 13.2 can be written

$$P_L = \eta E_b I_b = \frac{I_g^2}{(Y_{oc}/Q_L)^2(1 + 4\delta^2 Q_L^2)} \frac{Y_{oc}}{Q_e} \quad . \tag{13.5}$$

The efficiency, η, may be further subdivided if desired.

$$\eta = \eta_e \eta_c \tag{13.6}$$

η_e = electronic efficiency

η_c = circuit efficiency, given by

$$\eta_c = \frac{Q_o - Q_L}{Q_o} \quad .$$

Eq 13.5 contains all measurable parameters except I_g. Thus the r-f current can be computed if the proper measurements are made and if the equivalent circuit is correct. This equivalent circuit has been found to be a very good approximation for the interdigital magnetron operating in the zero-order mode. The reason for this is that the characteristic admittance (Y_{oc}) of the resonant circuit is calculable to a very good approximation by using the lumped capacitance between anode sets. This capacitance is not difficult to determine.* In tubes where the electrical energy storage is distributed more evenly throughout the cavity (i.e., anode capacitance cannot be considered lumped), formula 13.5 would not necessarily be

---

* H. W. Welch, Jr., and G. R. Brewer, Technical Report No. 2, pages 9-13. Also, graphical techniques may be used; see J. S. Needle and G. Hok, Technical Report No. 6, Appendix A.

correct. It is always possible to derive some similar relationship, but usually transcendental equations will result.*

Eq 13.5 is a complete circuital relationship as it stands. If it could be made complete electronically, it could be used to calculate frequency pushing for a given electrode system and circuit. In order for the equation to be made complete electronically, it is necessary to relate the electronic efficiency, η_e, the anode voltage, E_b, and the current-generator output, I_g, to the anode current, I_b. A very rough approximation can be made by assuming the anode voltage and electronic efficiency to be constants given by Eqs 3.1 and 3.2 and using the induced-current calculations of the last section as an estimate of the current-generator output. Since we expect the spoke configuration to change as the r-f voltage changes, it will be necessary to establish a relationship between I_g and the r-f voltage E_T or the power output P_L. In the next section we will show that, in a particular case, a relationship of the following form can be used:

$$(I_g)^2 = K(P_L)^b \quad . \tag{13.7}$$

If this is substituted in Eq 13.5 and rewritten in logarithmic form, we have the following:

$$\log\left(\frac{Q_L^2}{Y_{oc}^2}\,\frac{G_L}{1+4\delta^2 Q_L^2}\right) = (1-b)\log P_L - \log K \quad . \tag{13.8}$$

In this relationship all the quantities except b and k are readily measurable. Thus, by plotting 13.8 on log-log paper and determining

---

* For example, see the equations for the coaxial-cavity resonator magnetron used in calculations of case b in the last section. These are given on pages 12 and 16 of the report by Needle and Hok, Technical Report No. 6.

the slope and intercept, a numerical relationship for the current-generator output in terms of power is obtained. By making this calculation on several magnetrons, it may be possible to obtain empirically some quantitative idea of the behavior of the current generator and therefore of the spoke pattern.

In order to estimate the amount of pushing possible for a given magnetron, it is convenient to use the form given in Eq 13.1. For oscillation to be supported, the ratio I_g/E_T must be supplied by the electron swarm at the phase angle ϕ. If we define this ratio in the electron swarm as $|Y_e|$, we may write

$$|Y_e| \angle \phi = \frac{I_g}{E_T} \angle \phi = \frac{Y_{oc}}{Q_L} \sqrt{1 + 4(\delta Q_L)^2} \angle \tan^{-1} 2\delta Q_L \quad . \quad (13.9)$$

We are certainly justified in the assumption that I_g is determined primarily by the following:

a) interaction-space geometry

b) r-f voltage between anode segments

c) space phase angle of spoke relative to the r-f voltage maximum (θ in Fig. 5.2)

d) applied magnetic field

e) applied d-c voltage

f) condition of cathode (this is included to take care of effects of emission limitation, initial velocities, back heating, etc.).

The right-hand side of Eq 13.9 can be kept constant if Y_{oc}/Q_L and δQ_L are kept constant. If this constancy is maintained, a given favorable relationship between I_g and E_T can be maintained. We know that, in any magnetron, the ratio I_g/E_T is satisfactory over a small frequency range, δ, given by the observed frequency pushing. If we wish to multiply δ by a

factor, say 10, we should reduce Q_L by the same factor to keep δQ_L constant, so that the quantities $\sqrt{1 + 4(\delta Q_L)^2}$ and $\angle \tan^{-1} 2\delta Q_L$ will go through the same range of values. If the value at resonance is to be the same, it is then necessary to change Y_{oc} in proportion to Q_L. This means essentially that if Q_L is to be reduced it must be done by decreasing the energy storage (since $Q_L = Y_{oc}/G_L$). If very large frequency pushing is desired, therefore, the energy storage in the circuit should be very low. This immediately imposes complications, since any attempt to reduce anode capacitance beyond certain limits will either alter interaction-space design or reduce the heat-dissipative possibilities of the anode structure. A little consideration of almost any type of magnetron will show that this is quite a restrictive limit. A decrease in anode capacitance by a factor of 10, for example, is almost inconceivable without alteration of interaction-space geometry or an almost proportional reduction of the heat-dissipative qualities.

If very wide voltage tuning (or frequency pushing) is desired, the anode voltage must necessarily change over a wide range, roughly proportional to the frequency change. The magnetic field is necessarily held constant (if the voltage change is at any frequency other than very low audio frequencies). This is another restriction on the amount of tuning possible, since the range of frequencies over which I_g/E_T can have a favorable value is related to the magnetic field.

The most important conclusion to be drawn from this brief discussion of Eq 13.9 is that the approach to wide voltage tuning must include new features in interaction-space design, since changes in the circuit alone cannot be made without appreciably affecting tube operation.

14. Comparison of Theoretical and Experimental Results (H. W. Welch, Jr.)

The experimental data which are sufficiently complete to be used to check theories given in this report are not plentiful. A most important factor, which is customarily omitted when performance data on a magnetron are given, is the resonant frequency of the magnetron under the exact physical conditions imposed during oscillation. The data given here should not be considered a complete check of the theory but as a demonstration of the method. When more data are available on different magnetrons under various operating conditions, one may be able to draw firm conclusions.

A pushing curve for the Model 3 magnetron which was used in the calculation of Section 12 is shown in Fig. 14.1. The percentage frequency deviation from resonance is plotted against power output for direct comparison with Eq 13.5. Actually, power was measured at only one current in this set of measurements and efficiency was assumed constant in plotting curve no. 1 of Fig. 14.1.* The data for this curve are given in Table 14.1. The measured valueeof power output is indicated in this table. The last column gives calculated values assuming a constant current-generator output. For the tube on which these pushing measurements were made,

Y_{oc} = 0.00555 mhos

Q_L = 100

Q_o = 600

Q_e = 120

λ_o = 16.770, resonant wavelength with hot cathode, space-charge effects not accounted for,

η = 58 per cent = overall efficiency at I_b = 200 ma (P_L = 220 watts)

---

* Previous data on this tube show that this assumption is sufficiently accurate for the comparison which is to be made here. (See Technical Report No. 2, page 48)

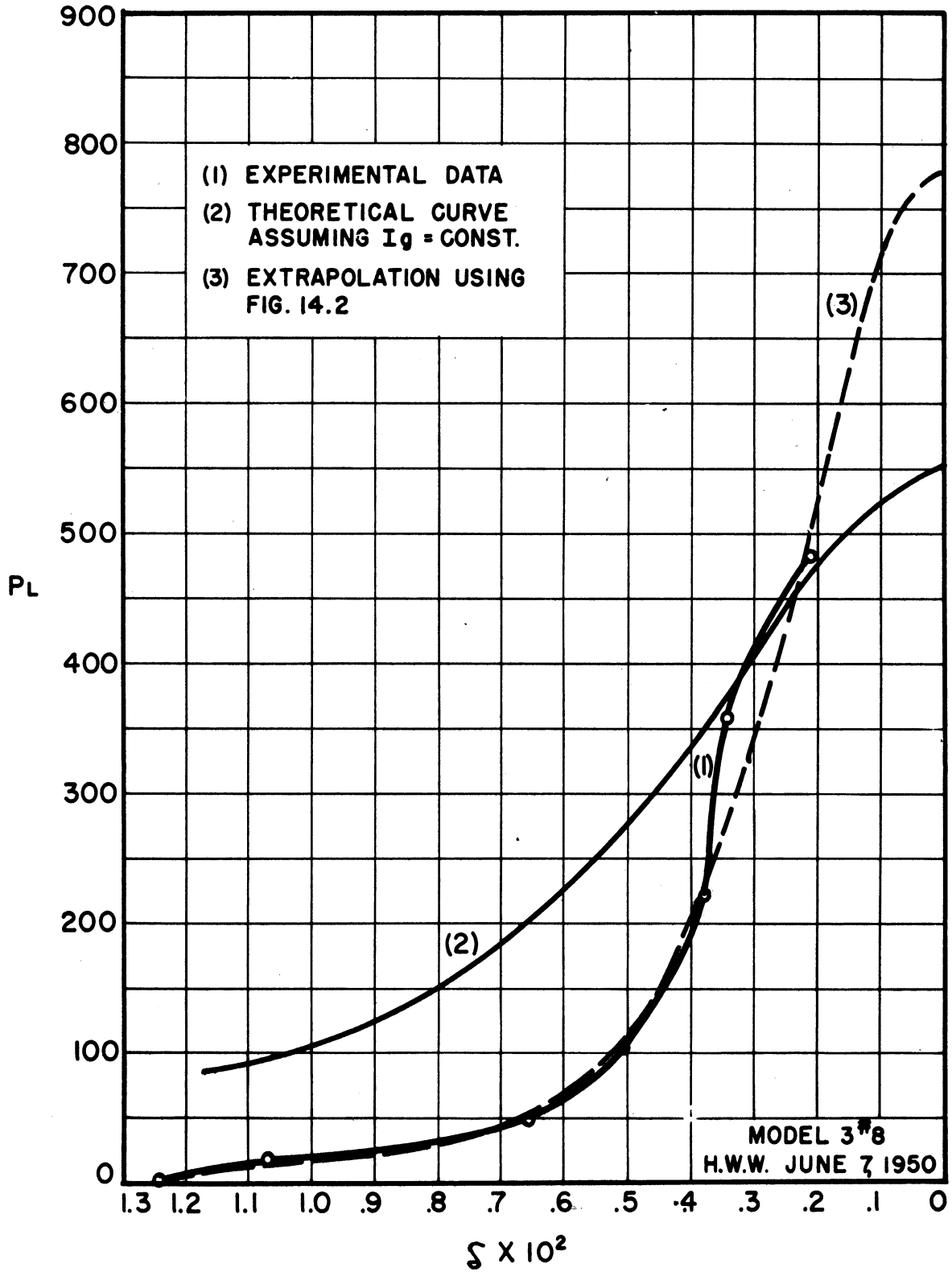

FIG. 14.1 COMPARISON OF PUSHING DATA WITH THEORY OF SECTION 13

$$Q_L/Y_{oc} = 1800 \text{ ohms}$$

$$Q_e/Y_{oc} = 2160 \text{ ohms}$$

$$I_g^2 = 0.37 \text{ (amp)}^2$$ (using the value from Section 12a).

Using these values, we have the formula at the top of the last column in Table 14.1. These data are plotted as curve no. 2 in Fig. 14.1 for comparison with the experimental data. It is quite encouraging to observe that, in spite of the simplifying assumptions which were made, the comparison shows both a rough quantitative agreement and similarly shaped curves. Quite obviously, however, the assumption of a constant-current generator is not valid.

In Fig. 14.2, the data from Table 14.1 are plotted on log-log paper. This plot is used with Eq 13.8 to determine a more exact idea of the current-generator output. Evaluation of b and k from this curve gives

$$I_g^2 = .00765\ P_L^{.64}$$

or

$$I_g = .0874\ P_L^{.32} \qquad (14.1)$$

The current in this particular case is approximately proportional to the 2/3 power of the r-f voltage between segments. The straight line of Fig. 14.2 is replotted on the coordinates of Fig. 14.1 as curve no. 3 and indicates the expected extrapolation of curve no. 1.

As is indicated on the extrapolated curves in Figs. 14.1 and 14.2, a maximum power output of about 775 watts would be expected in this tube at the particular voltage and magnetic field used if the phase angle could be reduced to zero. Experimentally, we observe that the current dropout point is reached before this power is reached. The observed d-c current, r-f

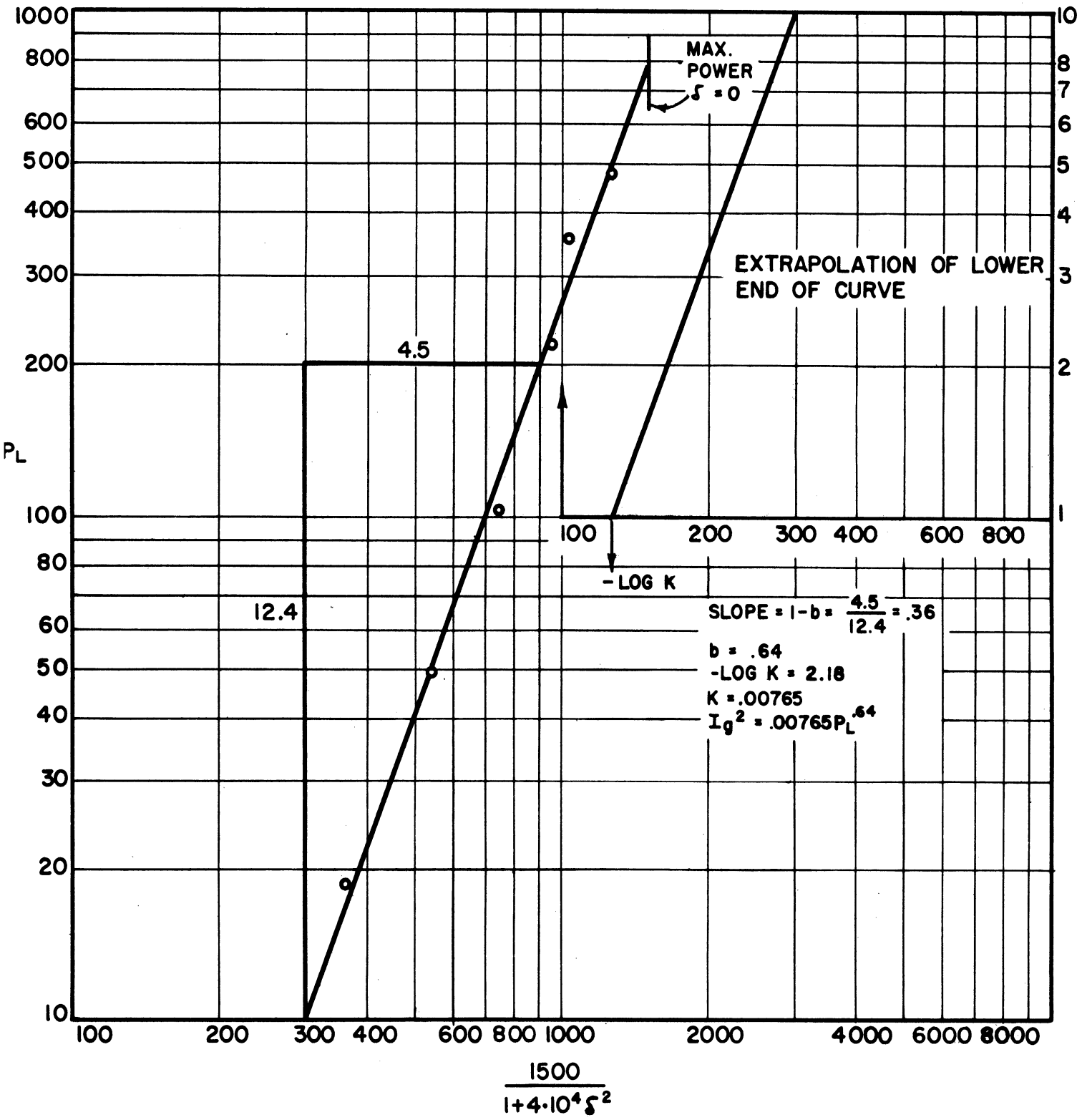

FIG. 14.2 LOGARITHMIC PLOT OF DATA FROM TABLE 14.1

current, and the theoretically predicted induced current are plotted for comparison in Fig. 14.3. Note that the phase angle is almost 25 degrees when the tube stops operating. The agreement between the intersection of the induced-current line with the r-f current curve and the observed maximum-current boundary is believed to be coincidental for several reasons: the space-charge density used here is probably questionable (particularly in the factor of 2 mentioned on page 86); the effect of collection current on r-f current has been ignored in the theory; the form of the spokes has been guessed. It should be emphasized, however, that this last estimate is not very critical in determination of the final result. One would definitely expect that the spoke formation used, with the correct space-charge density, would represent an upper limit on the amount of current which could be induced into the circuit. Thus, it can be used as an estimate on the upper limit of power output for a given interaction-space geometry.

The r-f current is seen to be a factor of 2 or more greater than the d-c current. This is possible only in a generator which induces current into the load. It would, as a matter of fact, be conceivable to have zero average current and finite induced current 90 degrees out of phase with the voltage if the voltage were supplied from an external source.

A number of measurements have been made on the Model 7 magnetron used in the calculations of Section 12b. Unfortunately, the magnetron used was found to have a poorly aligned cathode after the measurements were made, and it was not felt worthwhile to make comparisons with theory.* The procedure in the future will be to get the type of data needed as a routine measurement on tubes as they are tested for other purposes.

---

* These data were in Quarterly Report No. 3 on this project.

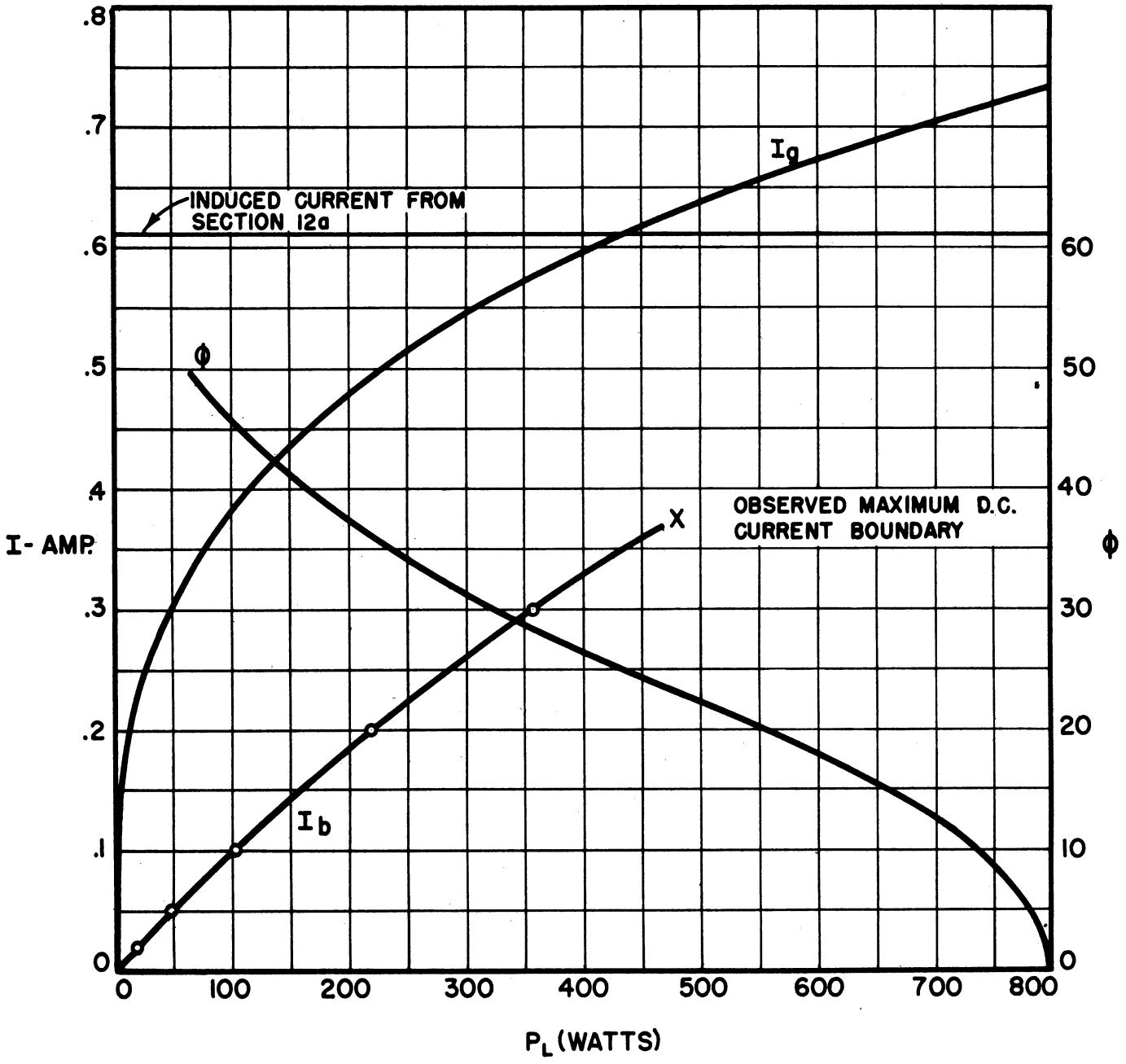

FIG. 14.3 GENERATOR CURRENT (Ig) CALCULATED FROM EQUATION 14.1 COMPARED WITH I_b AND PHASE ANGLE φ AS A FUNCTION OF LOAD POWER.

TABLE 14.1

COMPLETE PUSHING DATA FOR CURVE OF FIG. 14.1

E_b volts	I_b amps	λ cm	$\frac{\lambda - \lambda_o}{\lambda_o} \times 100$ ($\lambda_o = 16.77$) per cent	$\eta E_b I_b$ ($\eta = 58\%$) watts	$.37 \frac{1500}{1+4(10^2\delta^2)}$ watts
1600	.020	16.95	1.07	18.5	98
1670	.050	16.880	0.658	48.5	203
1750	.100	16.855	0.506	101	278
1900	.200	16.833	0.376	220 measured	358
2050	.300	16.827	0.340	357	386
2200	.375	16.805	0.208	480	470

15. Conclusions (H. W. Welch, Jr.)

In many respects this report must be considered preliminary, since the theoretical results are in some cases not substantiated by experimental evidence and the experimental results in some cases have no complete theoretical interpretation. It is hoped, nevertheless, that at least two purposes will be served by this report. It will serve as a summary of the factual and theoretical knowledge of dynamic magnetron space-charge characteristics available at this time, and it presents several new points of view and methods of analysis based on the more or less established picture of the magnetron space charge. It can thus serve as a guide for future work toward a quantitative understanding of magnetron space-charge behavior, both in this laboratory and elsewhere.

The following is a statement of the important conclusions.

a. Maximum-Current Boundary. Possible causes of maximum-current boundary are enumerated. We believe this list to be complete although, admittedly, at least one cause (defocussing or overbunching) is not clearly defined. Methods for estimating upper limits placed by the space-charge-current limitation and the induced-current limitation are presented. They compare favorably with experimentally observed values. Effects of transit time, temperature, and phase focussing are discussed, but no quantitative results can be claimed.

b. Voltage Tuning, Low-Q Operation, and Frequency Pushing. The relationship between frequency and voltage in voltage tuning is shown to be approximately that given by the Hartree equation. This equation is based on the assumption that all electrons in the interaction space, except those in the subsynchronous swarm, are travelling in synchronism with the r-f wave. The synchronous velocity, and therefore the fundamental

frequency of operation, are thus determined by the anode voltage. For high B/B_o, anode voltage and frequency are directly proportional to each other.

The magnetron space charge in a given interaction space acts as a current generator which will work satisfactorily into a given range of load impedances. If a low-Q circuit is used, this range of impedance may be covered over a very large frequency range, thus making possible operation at a wide range of frequencies determined by the anode voltage. In order to lower the Q in a given circuit without changing the value of the circuit shunt impedance at resonance, it is necessary to decrease the energy storage by decreasing the circuit capacitance. The steps which can be taken in this direction are limited by interaction-space design and necessary heat dissipation of the anode. It is therefore necessary, if one is to achieve very wide voltage tuning, to redesign the interaction space.

If the Q is extremely low (i.e., 1 to 5), the circuit obviously has little or nothing to do with the determination of the oscillatory frequency. This frequency is determined by the synchronous velocity of the space charge, which is dependent on the anode voltage. The impedance of the circuit must be high enough to develop r-f voltage sufficient to provide bunching of the electrons into spokes. However, since the Q is so low, the impedance of the circuit will be high for a wide range of frequencies, so that the induced voltage would be expected to have high harmonic content and, possibly, noise content. The exact form of the output wave depends on the shape of the spoke. Reference to Fig. 11.6 will show that, except for electrons very close to the anode, the harmonic content for frequencies higher than the fundamental component of the induced current is very low. Measurements at General Electric Laboratories were reported to show a fairly clean signal.

In order to prevent r-f current and r-f voltage from continually increasing as anode voltage is raised, it is necessary to limit the current-generator output. This is done by operating at a reduced temperature, which limits the collection current and makes power input proportional to anode voltage. The mechanism by which the current-generator output stays relatively constant over a wide frequency range under these conditions is not clear. Presumably, if it did not, the r-f voltage would build up too high and cause the magnetron to stop oscillating because of the so-called "overbunching phenomenon".

Power output as a function of frequency can be predicted semiquantitatively on the basis of theories of frequency pushing and induced-current calculation if enough is known about the resonant circuit. The electronic efficiency must decrease as voltage is raised to produce constant power output at very-low-Q operation. For moderately-low-Q operation a peak in the power-output curve is to be expected at the resonance frequency of the circuit.

Frequency pushing is described as a change in the phase relationship of the spoke with the r-f voltage wave at the anode. It is similar to voltage tuning but should not be identified with it. It is, for example, conceivable that voltage tuning could be obtained without any change in the phase relationship of the current and voltage. This could be done if the center frequency of the resonant circuit were tuned as the voltage changed to maintain a constant phase, or if no resonant circuit were used. Frequency pushing does require an increase in angular velocity of the spokes, but the voltage change required to achieve this change is not proportional to the frequency change, as it is in voltage tuning. Also, in the conventional definition, which is not yet standardized, frequency pushing is

considered a variation in frequency with anode current. In temperature-limited operation, the anode current does not change, so that this definition could not be used for voltage tuning.

c. The Magnetron Space Charge as an R-F Current Generator. The method presented in this report for prediction of the approximate r-f current to be expected in a magnetron is based on an assumption of the space-charge distribution and the assumption that the current is primarily induced current. Other contributions to the r-f current would be expected from the induced current due to radial motion and from the collection current. Of these two the collection current is probably the more important. Actually, as is pointed out in Sections 5 and 9, it is probable that current is collected at all times during the cycle, with the maximum probably being collected when the spoke is under an anode segment roughly 90 degrees out of phase with the induced current. There is in this a very fundamental difference between a magnetron and a Class C oscillator operating at conventional frequencies. It is quite possible to get r-f currents induced which are much larger than the peak collection current. Electrons do not needed to be collected at an instant when the anode voltage is a minimum for good efficiency, since the potential on the anode at this instant is not necessarily representative of the energy of the electron. Part of the reason for the relatively continuous collection of current is that the magnetron is essentially a sort of "push-pull" device, with collection current arriving every half cycle.

The general treatment of induced-current calculation in Section 10 should be quite useful in any microwave-tube problem.

The comparison of experimental results with theory in Section 14 is representative of what can be done with this type of analysis. It is

hoped that the method can be applied to other tubes in the near future. The use of the current generator is believed to be more easily related to the theoretical analysis and the experimental results than the electronic-admittance ideas introduced by Rieke.* This remains to be seen in further application of the method.

16. Proposed Future Activity (H. W. Welch, Jr.)

There are several specific ideas suggested in this report which require further clarification. The following problems, in particular, will be investigated in this laboratory as quickly as time permits:

a. The calculation of the electronic impedance as seen from the anode sets of the magnetron for assumed space-charge distributions similar to the one used in this report. This involves evaluation of $|Y_e|$ or I_g/E_T as defined in Section 13.

b. The calculation of the effect of the circuit on the electrons. In this report the space-charge distribution was assumed without much attention to the effect of r-f fields on the shape and size of the spoke. It is hoped that methods of analysis can be developed to dispense with the necessity of this assumption.

c. The calculation of the effect of collection current on r-f current. It should be possible to use approximate methods similar to those used in this report for this analysis.

d. Study of the meaning of the slope of volt-ampere characteristics. This information is considered primarily as a way of increasing the understanding of space-charge behavior, and thus the ability to design magnetron-type structures.

---

* See Ref. 8, pages 329-338.

e. Gathering of further experimental information to substantiate and help the improvement of theories presented in this report. In particular, information on maximum-current boundary, voltage tuning, and frequency pushing is desired.

f. Clarification of the effect of the cathode on magnetron performance. Solution to this problem depends on very basic knowledge of magnetron space-charge behavior, including, probably, statistical methods of analysis. It is believed to be not entirely a problem of temperature effects but also a problem of the cathode surface and emitting properties. This comment is based in part on recent observations of performance charts on tubes identical except for the cathode surface. Because of its fundamental nature, this is expected to be a long-term problem, and may or may not receive immediate attention.

APPENDIX

DATA FOR MAGNETRONS USED IN CALCULATIONS OF THIS REPORT

a) Model 3 Magnetron, University of Michigan

This model has 12 anode segments; the anode-anode gaps subtend the same angle as an anode segment.

r_a = 0.45 cm

r_c = 0.27 cm

R_a = 1.66

N/2 = 6

L = 0.66 cm

f = 1790 mc

B = 0.1950 webers/m^2

$(N/2)\alpha$ = 45 degrees

ω_c = eB/m = 3.43×10^{10}

ω_f = 1.13×10^{10}

b) Model 7 Magnetron, University of Michigan

There are 16 anode segments; the anode-anode gaps subtend the same angle as an anode segment.

r_a = 0.666 cm

r_c = 0.381 cm

R_a = 1.75

N/2 = 8

L = 0.762 cm

λ = 14.05 or f = 2135 mc

B = 0.1390 webers/m^2

$(N/2)\alpha$ = 45 degrees

ω_c = 2.442×10^{10}

ω_f = 0.1678×10^{10}

REFERENCES

1. H. W. Welch, Jr., Space-Charge Effects and Frequency Characteristics of C-W Magnetrons Relative to the Problem of Frequency Modulation, Technical Report No. 1, Electron Tube Laboratory, Dept. of Electrical Engineering, University of Michigan, November 15, 1948.

2. H. W. Welch, Jr., "Effects of Space Charge on Frequency Characteristics of Magnetrons", Proc.I.R.E. 38, 1434-1449 (December, 1950). (This paper also appeared as Technical Report No. 4, Electron Tube Laboratory, Dept. of Electrical Engineering, University of Michigan, January, 1951.)

3. O. Doehler, "Sur les Propriétés des tubes á champ magnétique constant", Annales de Radioélectricité, 3, 29-39 (January, 1948).

4. O. Doehler, "Sur les Propriétés des tubes á champ magnétique constant: II^{e} partie, Les Oscillations de résonance dans le tube á champ magnétique constant", Annales de Radioélectricité, 3, 169-183 (July, 1948).

5. J. Brossart and O. Doehler, "Sur les Propriétés des tubes á champ magnétique constant: III^{e} partie, Les Tubes á propagation d'onde á champ magnétique", Annales de Radioélectricité, 3, 328-338 (October, 1948).

6. D. A. Wilbur, R. B. Nelson, P. H. Peters, A. J. King, and L. R. Koller, C-W Magnetron Research, Final Report, Contract No. W-36-039 sc-32279, Research Laboratory, General Electric Company, April 1, 1950.

7. J. C. Slater, Microwave Electronics, D. Van Nostrand Co., New York, 1950.

8. Radiation Laboratory Series, Microwave Magnetrons, McGraw-Hill Co., New York, 1948.

9. J. B. Fisk, H. D. Hagstrum, and P. L. Hartman, Bell System Technical Journal, 25 (1946).

10. R. Q. Twiss, On the Steady State and Noise Properties of Linear and Cylindrical Magnetrons, Doctoral Thesis, MIT, 1949.

11. E. Dench, R. Damon, R. Smith, and W. White "Study of Magnetron Performance with Emphasis on Factors Affecting Maximum-Current Boundary". (This unpublished information was provided by Mr. W. C. Brown and Mr. E. Dench of Raytheon Mfg. Co.)

12. L. Page and N. I. Adams, "Space Charge in Plane Magnetron", Physical Review, 69, 492-3 (May, 1946).

13. L. Page and N. I. Adams, "Space Charge in Cylindrical Magnetron", Physical Review, 69, 494-500 (May, 1948).

14. L. Brillouin, Electronic Theory of the Plane Magnetron, O.S.R.D. Report No. 4510, Applied Mathematics Panel, Columbia University, 1944.

15. L. Brillouin, Electronic Theory of the Cylindrical Magnetron, O.S. R.D. Report No. 4742, Applied Mathematics Panel, Columbia University, 1944.

16. L. Brillouin, Oscillations in a Plane One-Anode Magnetron, A.M.P. Report 1293R AMG-C400 for N.D.R.C., Applied Mathematics Panel, Columbia University, 1945.

17. Columbia Radiation Laboratory Staff, Quarterly Reports, Physics Dept., Columbia University, June, 1948, to March, 1950 (particularly the sections by R. L. Jepson).

18. R. R. Moats, Mode Stability in Resonant-Cavity Magnetrons, Master's Thesis, MIT, 1947.

19. W. Shockley, "Currents Induced by a Moving Charge", Journal of Applied Physics, 9, 635-636 (1938).

20. S. Ramo, "Currents Induced by Electronic Motion", Proc. I.R.E., 27, 584-585 (September, 1939).

21. D. Gabor, "Energy Conversion in Electronic Devices", Journal I.E.E.. 91, 128-145 (June, 1944).

22. C. K. Jen, "On the Induced Current and Energy Balance in Electronics", Proc. I.R.E., 29, 345-348 (June, 1941).

23. Chao-Chen Wang, "Large-Signal High-Frequency Electronics of Thermionic Vacuum Tubes", Proc. I.R.E., 29, 200-214 (April, 1941).

DISTRIBUTION LIST

22 copies - Director, Evans Signal Laboratory
Belmar, New Jersey
FOR - Chief, Thermionics Branch

12 copies - Chief, Bureau of Ships
Navy Department
Washington 25, D. C.
ATTENTION: Code 930A

12 copies - Director, Air Materiel Command
Wright Field
Dayton, Ohio
ATTENTION: Electron Tube Section

4 copies - Chief, Engineering and Technical Service
Office of the Chief Signal Officer
Washington 25, D. C.

2 copies - H. W. Welch, Jr., Research Physicist
Electron Tube Laboratory
Engineering Research Institute
University of Michigan
Ann Arbor, Michigan

1 copy - Engineering Research Institute File
University of Michigan
Ann Arbor, Michigan

W. E. Quinsey, Assistant to the Director
Engineering Research Institute
University of Michigan
Ann Arbor, Michigan

W. G. Dow, Professor
Department of Electrical Engineering
University of Michigan
Ann Arbor, Michigan

Gunnar Hok, Research Engineer
Engineering Research Institute
University of Michigan
Ann Arbor, Michigan

J. R. Black, Research Engineer
Engineering Research Institute
University of Michigan
Ann Arbor, Michigan

Bell Telephone Laboratories
Murray Hill, New Jersey
ATTENTION: S. Millman

Special Development Group
Lancaster Engineering Section
Radio Corporation of America
RCA Victor Division
Lancaster, Pennsylvania
ATTENTION: Hans K. Jenny

Magnetron Development Laboratory
Power Tube Division
Raytheon Manufacturing Company
Waltham 54, Massachusetts
ATTENTION: Edward C. Dench

Vacuum Tube Department
Federal Telecommunication Laboratories, Inc.
500 Washington Avenue
Nutley 10, New Jersey
ATTENTION: A. K. Wing, Jr.

Microwave Research Laboratory
University of California
Berkeley, California
ATTENTION: Professor L. C. Marshall

General Electric Research Laboratory
Schenectady, New York
ATTENTION: P. H. Peters

Cruft Laboratory
Harvard University
Cambridge, Massachusetts
ATTENTION: Professor E. L. Chaffee

Research Laboratory of Electronics
Massachusetts Institute of Technology
Cambridge, Massachusetts
ATTENTION: Professor S. T. Martin

Collins Radio Company
Cedar Rapids, Iowa
ATTENTION: Robert M. Mitchell

Department of Electrical Engineering
University of Kentucky
Lexington, Kentucky
ATTENTION: Professor H. Alexander Romanowitz

G. R. Brewer, Research Associate
Engineering Research Institute
University of Michigan
Ann Arbor, Michigan

J. S. Needle, Instructor
Department of Electrical Engineering
University of Michigan
Ann Arbor, Michigan

Department of Electrical Engineering
University of Minnesota
Minneapolis, Minnesota
ATTENTION: Professor W. G. Shepherd

Westinghouse Engineering Laboratories
Bloomfield, New Jersey
ATTENTION: Dr. J. H. Findlay

Columbia Radiation Laboratory
Columbia University
Department of Physics
New York 27, New York

Electron Tube Laboratory
Department of Electrical Engineering
University of Illinois
Urbana, Illinois

Department of Electrical Engineering
Stanford University
Stanford, California
ATTENTION: Dr. Karl Spangenberg

National Bureau of Standards Library
Room 203, Northwest Building
Washington 25, D. C.

Radio Corporation of America
RCA Laboratories Division
Princeton, New Jersey
ATTENTION: Mr. J. S. Donal, Jr.

Department of Electrical Engineering
The Pennsylvania State College
State College, Pennsylvania
ATTENTION: Professor A. H. Waynick

Document Office - Room 20B-221
Research Laboratory of Electronics
Massachusetts Institute of Technology
Cambridge 39, Massachusetts
ATTENTION: John H. Hewitt

Department of Electrical Engineering
Yale University
New Haven, Connecticut
ATTENTION: Dr. H. J. Reich

Department of Physics
Cornell University
Ithaca, New York
ATTENTION: Dr. L. P. Smith

Document Office for Government Research Contracts
Harvard University
Cambridge, Massachusetts
ATTENTION: Mrs. Marjorie L. Cox

Mr. R. E. Harrell
West Engineering Library
University of Michigan
Ann Arbor, Michigan

Mr. C. L. Cuccia
RCA Laboratories Division
Radio Corporation of America
Princeton, New Jersey

Dr. O. S. Duffendack, Director
Phillips Laboratories, Inc.
Irvington-on-Hudson, New York

Air Force Cambridge Research Laboratories
Library of Radiophysics Directorate
230 Albany Street
Cambridge, Massachusetts

Air Force Cambridge Research Laboratories
Library of Geophysics Directorate
230 Albany Street
Cambridge, Massachusetts
ATTENTION: Dr. E. W. Beth

Raytheon Manufacturing Company
Research Division
Waltham 54, Massachusetts
ATTENTION: W. M. Gottschalk

General Electric Research Laboratory
Schenectady, New York
ATTENTION: Dr. A. W. Hull